

**Scientific and Technological Alliance for
Guaranteeing the European Excellence in
Concentrating Solar Thermal Energy**



FP7 Grant Agreement number: 609837
Start date of project: 01/02/2014
Duration of project: 48 months

Project Deliverable 11.2

**Report on suitable Process heat
and/or CHP systems for specific
industries and integration guidelines**

WP11 – Task 11.1	Deliverable 11.2
Due date:	01/2016
Submitted	07/2016
Partner responsible	FBK
Person responsible	Luigi Crema
Author(s):	Luigi Crema (FBK), Pedro Horta (FISE)
Document version:	1
Reviewed/supervised by:	Inigo Iparagirre (Tecnalia)
Dissemination Level	PU

Table of contents

PREAMBLE.....	7
1. INTRODUCTION.....	7
2. SYSTEM COMPONENTS, ENGINEERING AND RELATED TECHNOLOGIES.....	13
2.1. SYSTEM COMPONENTS	13
2.2. SYSTEM ENGINEERING	15
2.3. COOLING TECHNOLOGIES.....	16
3. SOLAR HEAT FOR INDUSTRIAL PROCESSES AND OTHER RELEVANT MEDIUM TEMPERATURE APPLICATIONS FOR CSP SYSTEMS.....	22
3.1. INTRODUCTION TO INDUSTRIAL PROCESS HEAT.....	22
3.2. SUITABLE PROCESSES AND SECTORS.....	24
3.3. STEAM GENERATION AND SYSTEM INTERFACES	25
3.3.1. System Components and Hydraulic Concepts	26
3.3.2. Steam generation and integration concepts.....	27
3.4. EXAMPLES AND RELEVANT PROCESSES	30
3.4.1. Cooling.....	30
3.4.2. Drying.....	34
3.4.3. Solar Desalination	40
3.4.4. Sterilization	43
3.4.5. Waste Processing.....	44
3.4.6. Applications in the cork processing industry	47
4. COGENERATION (POWER CYCLE).....	48
4.1. INTRODUCTION TO COGENERATION	48
4.2. INTRODUCTION TO SMALL SOLAR PLANTS	54
4.2.1. Case study: REELCOOP project.....	54
4.2.2. Case study: ORC coupling with storage and absorption systems	61
4.3. TEMPERATURE LEVEL vs POWER CYCLE TECHNOLOGIES	68
4.3.1. Analysed fluids for ORC: Selecting criteria	68
4.3.2. Operating conditions	72
4.3.3. Preliminary Conclusions	75
4.4. CASE STUDIES: a short introduction	77
5. MARKET ANALYSIS AND BUSINESS MODELS	81
5.1. INDUSTRIAL FUEL PRICING IN EUROPEAN COUNTRIES.	81
5.1.1. Fuels employed at industrial processes.	81
5.1.2. Natural Gas and Electricity price survey methodology.	82

5.1.3.	Natural gas and electricity prices for industrial end-users.	83
5.1.4.	Petroleum derivative prices.	87
6.	CONCLUSIONS	89
7.	REFERENCES	90
8.	APPENDIX	97

Figures

Figure 1. Impact/Probability matrix for CSP technological development	9
Figure 2. Final energy use of the EU industry	10
Figure 3. Direct flow receiver developed within DIGESPO project (left) and integration layout (right) between solar module with heat pipe receiver and the secondary fluid of the industrial process	14
Figure 4. Concept of the solar technology modularity and standardization.....	16
Figure 5. Comparison of mechanical and thermal vapour compression system	17
Figure 6. Thermal vapour compression circulation process	17
Figure 7. Principle of thermally driven cooling process	18
Figure 8. COP values of thermal reversible process	19
Figure 9. Performances of thermally driven chillers in function of COP and quality number ζ_{PQ}	20
Figure 10. Adsorption chiller system principle	21
Figure 11. Market – Industrial Process Heat (Source The Technology Roadmap • RHC-Platform 2012).....	24
Figure 12. Temperature Ranges for Different Industrial Applications (GESA Research Group)	25
Figure 13. Important symbols for integration concepts	27
Figure 14. Integration concept for direct solar steam generation.....	28
Figure 15. Integration concept for indirect solar steam generation.....	29
Figure 16. Integration concept for direct parallel integration at supply level with liquid heat transfer media.....	29
Figure 17. Solar cooling system (ESTIF 2015).....	31
Figure 18. Cooling process (Guía del Frío Solar, Ahorro y eficiencia energética con refrigeración solar, 2011)	31
Figure 19. Identification of the most suitable STE technology for integration in a drying process	36
Figure 20. Possible configurations for desalination powered by CSP. Left panel: Dedicated water production scheme using thermal desalination systems (MED presented as an example). Central panel: Power generation for reverse osmosis. Right panel: Co-generation of electricity and water using thermal desalination systems (MED presented as an example).[76]	40
Figure 21. Integration scheme for a low temperature MED plant powered by parabolic troughs in a co-generation scheme [81].	41
Figure 22. Integration scheme for a low temperature MED plant powered by parabolic troughs in a co-generation scheme including an extra condenser enabling the decoupling of electricity and water production [77].	42
Figure 23. Integration scheme for a TVC- MED plant powered by parabolic troughs in a co-generation scheme [81].	42
Figure 24. Generic schematic diagram of a CSP-RO system [83].....	43
Figure 25. Overview of possible options for wastewater sludge treatment and disposal [86].	45
Figure 26. Example of cogeneration valid for systems like gas turbines (Brayton cycle), Internal combustion engines, etc. [43,44].....	48
Figure 27. Cogeneration scheme representative of a Steam turbine (Rankine cycle). [43,44]	49

Figure 28. Cogeneration types [29].	51
Figure 29. Example of microgeneration system [29].	52
Figure 30. RORC system (a) and its typical Ts diagram (b) [32].	53
Figure 31. RORC system	54
Figure 32. Ts diagram of the RORC (a) $T_{cond} = 45$.(b) $T_{cond} = 90$ °C.	55
Figure 33. Schematic diagram of a single effect absorption refrigeration system [33].	58
Figure 34. Climatic conditions (monthly mean values at Benguerir, Morocco) (a) Horizontal Irradiation (kWh/m ²) (b) Ambient Temperature (°C).	58
Figure 35. Incident irradiation (monthly mean values) (MWh)	59
Figure 36. Heat provided to the RORC (monthly mean values) for the case of $T_{cond} = 45$ °C.(a) Auxiliar heat from the boiler Q_{aux} (MWh) (b) Usefull heat provided by the solar field Q_{usef} (MWh)	59
Figure 37. Solar fraction f (monthly mean values) for the case of $T_{cond} = 45$ °C.	60
Figure 38. Heat provided to the RORC (monthly mean values) for the case of $T_{cond} = 90$ °C.(a) Auxiliar heat from the boiler Q_{aux} (MWh) (b) Usefull heat provided by the solar field Q_{usef} (MWh)	60
Figure 39. Solar fraction f (monthly mean values) for the case of $T_{cond} = 90$ °C.	61
Figure 40. Temperature power diagram for different thermodynamic technologies.	61
Figure 41. Schematic principle of the technology used in the case study.	62
Figure 42. Monthly cumulated DNI in Larache (Morocco).	63
Figure 43. Monthly net electrical production in Larache (Morocco)	64
Figure 44. Monthly net electrical production coupling the studied system with absorption system.	65
Figure 45. Normalized LCOE for different cases studied.	66
Figure 46. Adjusted LCOE for different cases studied.	67
Figure 47. Saturation pressure as a function of saturation temperature for the fluids considered (except water).	71
Figure 48. Ts diagram for saturated fluids considered.	71
Figure 49. Process diagram for ICB manufacturing.	77
Figure 50. Actual process diagram for superheated steam production in cork industry.	78
Figure 51. The complete small scale m-CHP system developed in DIGESPO project.	79
Figure 52. Industrial use of energy by source in 2013 [87].	82

Tables

Table 1. Classification of different drying methods.....	35
Table 2. Typically required conditions of heat supply for flash dryer designs and identified most suitable STE technologies	36
Table 3. Typically required conditions of heat supply for spray dryer designs and identified most suitable STE technologies	37
Table 4. Typically required conditions of heat supply for rotary drum dryer designs and identified most suitable STE technologies	37
Table 5: Typically required conditions of heat supply for fluidized bed dryer designs and identified most suitable STE technologies	37
Table 6: Typically required conditions of heat supply for impingement dryer designs and identified most suitable STE technologies	38
Table 7. Typically required conditions of heat supply for through dryer designs and identified most suitable STE technologies	38
Table 8. Typically required conditions of heat supply for conveyor dryer designs and identified most suitable STE technologies	39
Table 9. Typically required conditions of heat supply for tray dryer designs and identified most suitable STE technologies	39
Table 10. Technical characteristics of different drying systems for wastewater sludge[86]. ..	46
Table 11. Definition of the inputs for each component.....	54
Table 12. RORC results for $T_{cond} = 45\text{ C}$ and $T_{cond} = 90\text{ °C}$	55
Table 13. Monthly and annual performance results for $T_{cond} = 45\text{ °C}$	56
Table 14. Monthly and annual performance results for $T_{cond} = 90\text{ °C}$	56
Table 15. Annual boiler input energy ($Q_{boiler\ annual}$), annual average solar electrical efficiency ($\eta_{sol,electr}$) and the annual global electrical efficiency (η_{electr}) for $T_{cond} = 45\text{°C}$	57
Table 16. Annual boiler input energy ($Q_{boiler\ annual}$), annual average solar electrical efficiency ($\eta_{sol,electr}$) and the annual global electrical efficiency (η_{electr}) for $T_{cond} = 90\text{°C}$	57
Table 17. Electrical consumption for different cases studied.	67
Table 18. Thermal cycles and maximum temperatures that can be reached with them.....	68
Table 19. Considered fluids (ordered according to their critical temperature)	70
Table 20. Fluids represented in the "Results" section	74
Table 21. Fluids represented in the Appendix.....	74
Table 22. Gas price categories for industrial end-users [88].....	83
Table 23. Electricity price categories for industrial end-users [88].	83
Table 24. Natural Gas prices for industrial end-users - annual consumptions [89].	83
Table 25. Price estimation for natural gas in industries in Spain – 2015/2035. Source: Solarconcentra.....	85
Table 26. Electricity prices for industrial end-users - annual consumptions [89]	86
Table 27. Price estimation for electricity in industries in Spain – 2015/2035 [90].....	87
Table 28. Prices in force on 14/12/2015 inclusive of duties and taxes. Source: https://ec.europa.eu/energy/en/statistics/weekly-oil-bulletin	87
Table 29. Price and its expected evolution for Fuel Oil. Source: Solarconcentra.....	89
Table 30. Price and its expected evolution for heating Gas Oil. Source: Solarconcentra.....	89

PREAMBLE

The present document is a comprehensive summary and guide to the integration schemes for concentrated solar power technologies in thermal applications and power cycles. The deliverable is focused on small scale systems. The document will provide an analysis of different solar layouts that are relevant for proposed application sectors.

The document is based on the objectives of Sub-Task 11.1.2 “Schemes of integration in thermal application and power cycle for small scale systems” of WP11, as reported in *Annex I – Description of Work* of the Stage STE project Grant Agreement No. 609837. CIEMAT - PSA is responsible for WP11. FBK is the leader of Sub-Task 11.2.1. FISE is responsible for the D11.2 hereby presented. The objective of this task is to define the integration schemes between CSP solar thermal or cogeneration technologies and related industrial applications, including industrial process heat.

The contact details for FBK and FISE with respect to this document are:

Luigi Crema (FBK)

Tel +39 (0)461 314922

Email: crema@fbk.eu

Pedro Horta (FISE)

Tel : +49 (0)761 45882126

email: pedro.horta@ise.fraunhofer.de

The document has been write with the contributions of different partners:

Loreto Valenzuela (CIEMAT)

Iñigo Iparraguirre (TECNALIA)

Pedro Horta (UEVORA)

Benoit Senechal (CEA)

João Cardoso (LNEG)

Mattia Roccabruna (FBK)

Fabienne Salaberry (CENER)

Miguel Frassetto Herraiz (CTAER)

1. INTRODUCTION

Industry is responsible for around one third of our total primary energy consumption, 60% of the energy used coming from process heat¹ ; and in the EU, 2/3 of these consists of thermal energy rather than electrical² (as shown in Figure 2).

Whereas the development of solar concentrating technologies was driven from the early 1980's by Solar Thermal Energy (STE) applications, their ability to operate in the medium temperature range ($100^{\circ}\text{C} < T < 400^{\circ}\text{C}$) renders them particularly suitable to applications in industry:

¹ Christian Zahler and Oliver Iglauer, “Solar process heat for sustainable automobile manufacturing” - Energy Procedia 30 (2012) 775 – 782, presented at SHC Congress 2012

² Source: ESTIF, “key issue for renewable heat development in Europe – K4RES-H”, http://www.estif.org/fileadmin/estif/content/policies/STAP/Madrid_SolarRegulation_FullStudyIDAE_English.pdf

producing heat for industrial processes or to cogeneration purposes. Several industrial processes require operating temperatures on that range, either due to process temperature or to the common use of steam as heat carrier in industrial networks.

Withstanding operating temperatures below 150 to 200 °C, conventional (stationary, non-concentrating) solar collectors can only supply a limited share of this demand. The use of Solar Concentrating technologies (CSP technologies) in this venue presents not only the ability to tackle the needs of processes occurring at higher temperature levels but also to enable integration at supply level, avoiding direct interaction with the processes.

Despite its promising potential, SHIP is facing a number of barriers, low competitiveness, low awareness and training. Application of solar concentrating technologies in the production of heat for industrial processes - also referred to as Solar Heat for Industrial Processes (SHIP) applications, is still at an early stage of development considering the full market application. New low carbon technological solutions and systems for energy supply to industry are highly requested at reasonable efficiency and costs³. To make industry more sustainable, new technologies, optimized integration layouts, simplified and modular technologies should be identified.

Solar energy can enter into a manufacturing process giving a viable contribution if its developers will be able to design improved integration layouts, maybe through hybridization of solar technology with demand side management via conventional energy sources. Design of CSP systems has to properly manage the temperature level and power supply in the distribution of energy, feeding properly the industrial process all day long. There are several challenges around this target, such as minimize the thermal dissipation, calibrate an efficient in-plant design, transfer the heat from solar circuit to industrial process efficiently.

A commercial system based on the use of Solar Concentrating technologies involves always a complex integration of active sub-systems. Yet, as recognized by the industry, the use of these technologies still faces multiple challenges (e.g. improving the optical efficiency of collectors, researching new heat transfer fluids or procuring higher efficiency components) as illustrated in Figure 1⁴., providing a Matrix on the *Impact on Levelized Cost of Energy (LCOE) / Probability of commercial deployment* for the different technologies.

This matrix confirms that several of the research objectives of the WP11 of STAGE STE project are indeed strategic and within a prioritization strategy. Improvements in process integration (for hybridization) in fact lay in the high impact/highest probability matrix for commercial deployment; on the other hand, Direct Steam Generation and Broader range of Receivers rest in the highest impact/low-medium probability of commercial deployment. Mirrors and receiver tubes are considered to be critical components in parabolic-trough plants, and provide an opportunity for innovation and improvements.

³ Nicolas Cottret and Emanuela Menichetti, "Technical Study Report: Solar Heat for Industrial Processes" - United Nations Development Programme (UNDP) and United Nations Environment Programme (UNEP). Available online at <http://www.b2match.eu/system/stworkshop2013/files/SHIP.pdf?1357835481>

⁴ <http://www.renewableenergyworld.com/> (2015)



Figure 1. Impact/Probability matrix for CSP technological development

Besides a direct use of these technologies in the production of heat for industrial processes (following either a supply or process level integration approach), one other possible use of Solar Concentrating technologies in industry related applications is solar-driven (or assisted) Cogeneration.

Traditionally used as a means to exploit waste heat potential of conventional heat production systems enabling the simultaneous production of electricity and thermal energy at suitable temperatures for the use in industrial processes. Use of Solar Concentrating technologies on this context might be especially suitable in stand-alone applications, in locations where electricity supply is not available. On conventional systems can only be regarded as a way to integrate a solar fraction in waste heat recovery driven systems, including also the possibility of different hybridization concepts. The most suitable solar integration layout in this case relates not only to the combination of heat sources but also to the suitable thermodynamic cycle temperatures.

In brief, application of Solar Concentrating technologies for industrial purposes relies on:

- the potential of industry related energy consumption, amounting to around one third of the total primary energy consumption, 2/3 of which related to process heat⁵; (as shown in Figure 2);

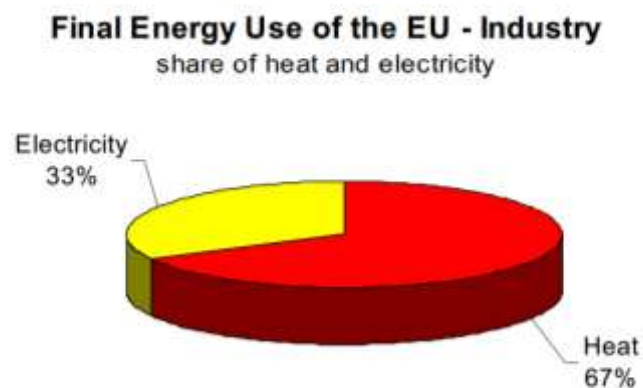


Figure 2. Final energy use of the EU industry

- industrial process requirements for medium-high temperatures (200 – 400°C) or steam as a heat transfer fluid. However, conventional, non-concentrating solar collectors can only provide solar process heat for a limited fraction of this demand. Consequently, concentrating solar collectors, like parabolic-trough collectors (PTC), can generate higher temperatures and meet this target;
- There is a clear gap between “solar thermal technologies” and industrial utilization of solar thermal power in terms of industrial processes. Despite its promising potential, SHIP is facing a number of barriers, including low competitiveness, low awareness and training.

⁵ Christian Zahler and Oliver Iglauer, “Solar process heat for sustainable automobile manufacturing” - Energy Procedia 30 (2012) 775 – 782, presented at SHC Congress 2012

The present report addresses some of the most relevant issues related to the use of Solar Concentrating technologies in industry:

Issue 1. optimization of the integration layout

The integration layout optimization lays down on the best design for the solar technology integrated with the industrial process. A standardization effort is hereby necessary, to create classes of integration design categorized in class of applications (e.g. based on direct steam generation process, in thermal oil based fluid, in superheated pressurized water). The integration layout can be optimized starting from heat exchangers, thermal storage and/or insulating materials. All these elements can bring to a significant improvement of performances, when optimized. Each component layout is an important element affecting the overall integration layout. Other elements are sensors and actuators, valves, transducers, flow meters, oil degradation: all involved in the optimization of an integration layout. The dynamic behaviour of a solar plant with respect to the integration layout and to necessary degrees of freedom has to be considered.

Considering the industrial application, small to medium CSP technologies at medium temperatures between 150 and 300 - 350°C) are the best candidates to be integrated in industrial processes due to the high demand of thermal energy for lot of them.

Issue 2. Classification by temperature level, heat transfer and dynamic behaviour

There are several layouts and integration design classified by temperature level, by heat transfer potential, by necessary dynamic behaviour of the solar plant and/or hybrid technology. The working temperature necessary to the industrial plant will affect the design of heat exchangers, the choice of the thermal fluid, the use of storage media or hybrid configuration, the insulating materials and several other components and parts. Overall energy efficiency can be maximized only balancing properly the fluid dynamic versus the heat transfer. The dynamic behaviours are therefore constrained by energy and mass balance of the system and by demand side management.

Issue 3. Combination with thermodynamic cycles and distributed cogeneration

The second use of thermal energy directly produced from the solar system is for energy conversion into electricity through a thermodynamic power cycle. This process, coupled with thermal power in a cogeneration layout, allow for high-energy efficiency production. Available technologies will be analysed, matching the double advantage of decentralized power generation and heat utilization.

Issue 4. Relevant International activities on Solar Heating and Cooling (IEA Task 49)

A similar work based on solar application and integration in industries has been studied inside the IEA SHC Task 33 and IEA SHC Task 49 [5]. The Technical University of Graz has presented the wiki-web “Matrix of indicators”, a database on unit operations in industry, providing information on solar process heat used now in industry and showing possible integration schemes.

Issue 5. Case studies

Within the subtask of Stage STE 11.1.2, three case study will analyse the integration of specific solar systems inside industrial processes. The three case studies proposed will be introduced in the present deliverable and fully described in further documents to be realized within M36 of Stage Ste project.

2. SYSTEM COMPONENTS, ENGINEERING AND RELATED TECHNOLOGIES

The present chapter will describe some of the main CSP technology components, highlighting the related system engineering aspects and providing information on related cooling technologies, considering their potential for supplying process cooling requirements from medium temperature heat sources.

2.1. SYSTEM COMPONENTS

MIRRORS: design and realization of new supports for lightweight and low-visual-impact optical systems, one-axis tracking (only for specific cases will two-axis tracking be applied) and standard hydraulic connections (rapidity in installation) are the main aspects to take into account in the design and development of efficient mirrors. Improvement of the overall integration design involving chemically treated thin glass mirrors, manufacture tailoring and integration process, are necessary to realize robust and reliable mirrors.

RECEIVERS: there are several technologies used in design and development of receiver tubes, like vacuum or glass encapsulation. Some of the most diffused layouts are based on two main different approach (as shown in Figure 3):

- direct flow receiver (as realized in the DIGESPO project⁶);
- medium temperature innovative heat pipe receiver.

Specifically, the solution based on the heat pipe receiver paves the way in solving several integration problems of solar energy in industrial processes such as: (a) avoidance of high temperature fluids in form of mineral oils, (b) costs reduction through simplification of the system design, (c) easy adaptation and integration of the solar system to different existing industrial processes.

⁶ <http://www.digespo.eu/default.aspx>

The integration design has to be optimal solution for what concerns customization, dimensions, optimized heat transfer and fluid dynamics, optimized materials and sizes.

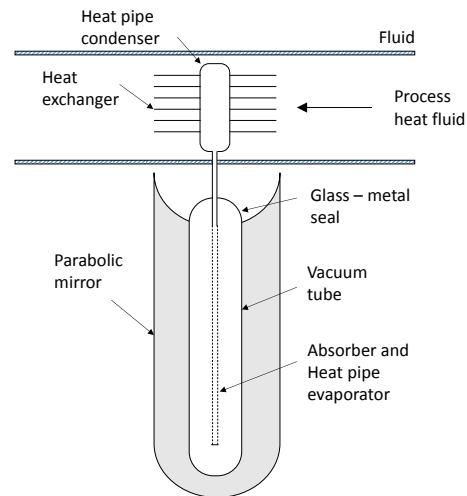
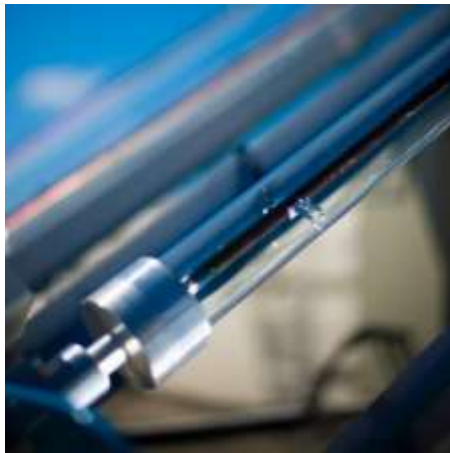


Figure 3. Direct flow receiver developed within DIGESPO project (left) and integration layout (right) between solar module with heat pipe receiver and the secondary fluid of the industrial process

DIAGNOSTIC TOOLS: Current diagnostic tools are important for the characterization of concentrated solar flux distribution on the receiver (e.g. radiometers and CCD camera imaging), and to evaluate optical errors related to the concentrating optics. The different component configurations will be evaluated to maximize the performance of the optical system. Experimental data will be used for validating the numerical radiation model, which is the main tool in optimizing the optical components and analyse the influence of mirror quality, structure deformation or tracking errors.

THERMAL FLUIDS: use of the heat pipe receiver can define a solution where only the heat process fluid is maintained and required. This allows an easier and direct integration of the solar system within the overall layout. Thermal fluids are mainly used in industrial processes, except the case of a direct flow receiver, where a primary circuit maintains a thermal fluid in the form of mineral oil, connected through a heat exchanger with a secondary circuit with the proper thermal fluid used in the industrial process. Innovative solutions will consider direct steam generation (DSG), low condensation point molten salts or super critical fluids coupled with heat pipes.

THERMAL STORAGE SYSTEM: In addition to hybridization using biomass and/or conventional fossil fuels, the integration layout can include a latent heat thermal storage system (TES) to manage in a flexible way the demand of thermal energy of the industrial plant. TES will be mainly designed as an energy buffer, whose purpose is to improve the assembly between the solar and the boiler and guarantee a fine control on energy and temperature delivered by the heat transfer fluid. This capability would make possible the integration of traditional boilers, already available on the installation site, with the TES. Latent heat storage allows maintaining a desired constant temperature during long periods and small-size storage reservoir. The TES will be capable to provide an output of an hour at a full capacity level. The charging process of the TES will take advantage of solar heat overproduction, biomass or fossil fuels as well as exceeding renewable electricity obtained from the grid, thus increasing the industrial facilities reliability and reducing CO₂ emission.

HEAT EXCHANGERS: heat exchangers are the basic element for heat transfer in energy systems. In the specific context of CSP systems applied to the industrial heat process [to industrial process heat], they represent one of the most important components, being at the interface between the solar plant and the industrial process itself. There are several potential ways for their improvement, which take in consideration aspects like: energy conversion, the heat transfer medium, the temperature levels or the time constant involved in the process. In general, one optimization element for the design of heat exchangers is the minimization of the entropy generation. In this context of integration, a thermal heater exchanger is classifiable as either an external or an internal component.

Internal heater exchangers (IHX) are mainly used to directly heat up tanks or baths. These types of heaters exchanger are cheaper and easier to install. The heater exchangers in this case are heating jackets, heating coils and tube bundles.

The external ones (EHX) are chosen accordingly to the applied temperature, pressure, space availability and other specific constrains such as corrosion or viscosity. The main type is characterized by tubular design like shall tubes. Other types are more compact and present extended surface design.

2.2. SYSTEM ENGINEERING

Overall engineering activities regarding the integration of system components are required, aiming the achievement of the following targets:

- Designing standardized components for *plug-and-play connections* of the different elements (like optics, tubes, hardware for tracking and fluid circulation) and to guarantee affordability and sufficient precision for components matching during the system installation;
- Improving system modularity to extend the *dimensions* of the CSP module (in width and length for all of its components) in order to achieve different working ranges (with respect to the basic module). In this way, with the addition of standardized plug-and-play modules to the basic configuration of the collector (mono or bi-axial), it will be possible to scale up the output (temperature, power and energy) of the system without significant modification at the existing circulating system, allowing sensible reduction in terms of time spent in maintenance services and costs; (see Figure 4)
- Industrial process integration design, showing a detailed view of the overall flowsheet of the CSP plant must be developed and evaluated under various operating modes, taking also into account different working conditions within different scenarios, representing the real industrial applications. The analysis will provide a preliminary assessment of the system performances on renewable energy/fuel contribution, thermal storage sizing and potential market niches.

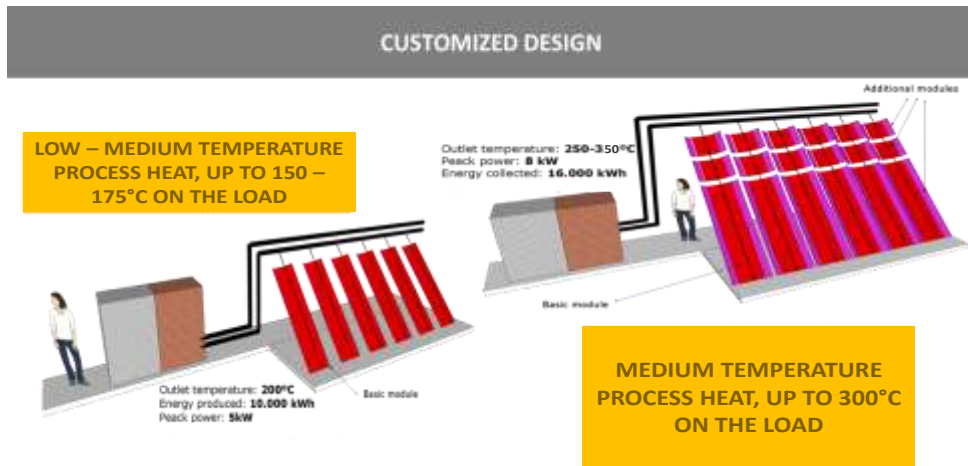


Figure 4. Concept of the solar technology modularity and standardization

2.3. COOLING TECHNOLOGIES

ABSORPTION SYSTEMS: Absorption chillers are the most distributed thermally driven chillers worldwide. A thermal compression of the refrigerant is achieved by using a liquid refrigerant/sorbent solution and a heat source, which is replacing the electric power consumption of a mechanical compressor. For chilled water above 6 °C, as it is used in air conditioning, typically a liquid H₂O/LiBr solution is applied with water as the refrigerant. Nevertheless, other liquid solutions can be used like NH₃/H₂O, which enables producing chilled water at temperatures below 0 °C.

The main components of an absorption chiller are: generator, condenser, evaporator and absorber. The mechanical vapour compressor (used in conventional compression chillers) is replaced by a thermal compressor (see Figure 5), that consists of an absorber, a generator, a pump, and a throttling device. A solution mixture (in the absorber) absorbs the refrigerant vapour from the evaporator, in this way releasing heat. This solution is then pumped into the generator where the refrigerant is re-vaporized by adding heat using, as an example, a waste steam heat source as shown in Figure 5. The refrigerant-poor solution is then returned to the absorber via a throttling device.

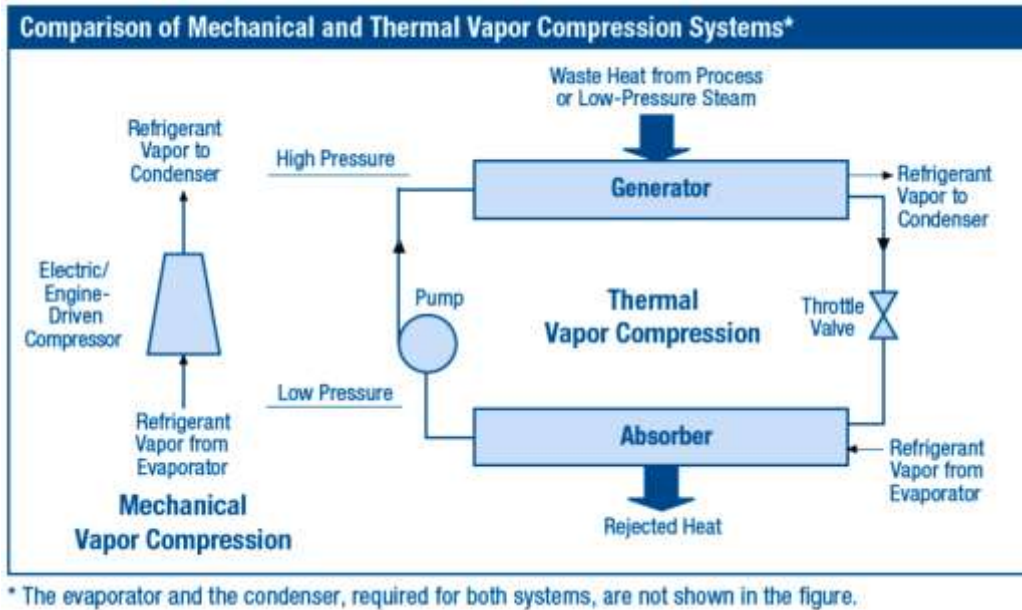


Figure 5. Comparison of mechanical and thermal vapour compression system

As for mechanical compression systems, the cooling effect is based on the evaporation of the refrigerant in the evaporator at very low pressure. The solution is continuously pumped into the generator, where the regeneration of the solution is achieved by applying the driving heat, such as that from hot water supplied by a solar collector. The refrigerant moves from the generator to the evaporator by the described process, condenses through the application of cooling water in the condenser and circulates by means of an expansion valve again into the evaporator and follows to the absorber where it is absorbed by the refrigerant poor solution (as shown in Figure 6). The absorption process releases heat that must be removed in order to keep the efficiency of the process. This is usually done using water from cooling towers, although some prototypes exist using air cooling both in the absorber as in the condenser.

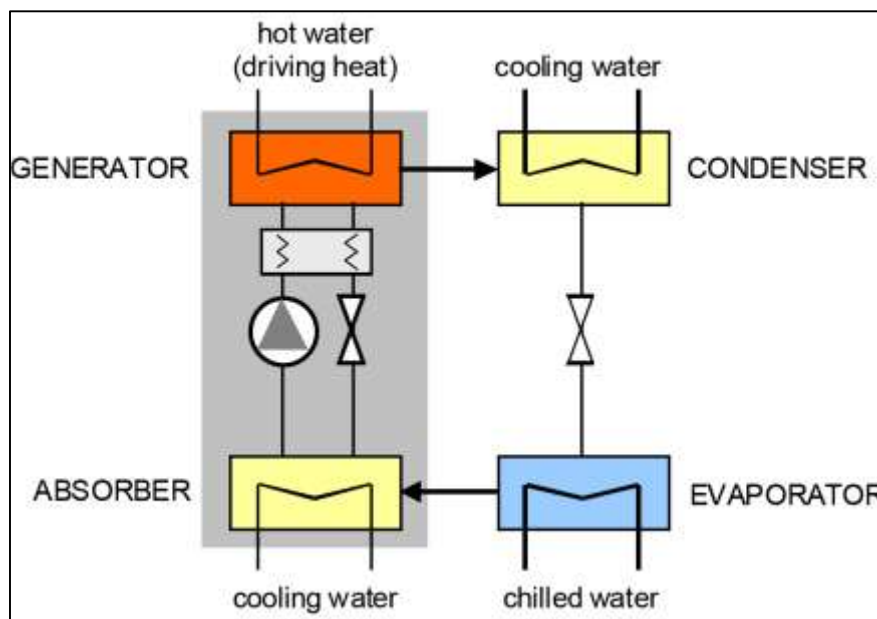


Figure 6. Thermal vapour compression circulation process

Figure 7 shows that any thermally driven cooling process operates at three different temperature levels: with driving heat Q_{heat} supplied to the process at a temperature level T_H , heat is removed

from the cold side thereby producing the useful cold Q_{cold} at a temperature T_C . Both amounts of heat are to be rejected (Q_{reject}) at a medium temperature level T_M . The driving heat Q_{heat} may be provided by an appropriate designed solar thermal collector system, either alone or in combination with auxiliary heat sources.

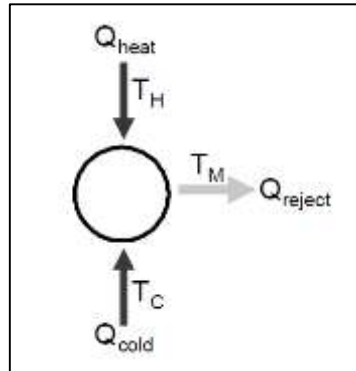


Figure 7. Principle of thermally driven cooling process

Closed chilled water processes require an external heat rejection, e.g., a cooling tower. The type of the system heat rejection is one of the main components to be optimized, as it usually is responsible for a considerable fraction of the remaining energy consumption of solar cooling systems. A basic number to quantify the thermal process quality in thermally driven chilled water systems is the coefficient of performance COP, defined as:

$$COP = Q_{\text{cold}} / Q_{\text{heat}}$$

Thus indicating the amount of required heat per unit of “produced cold” (more accurately: per unit removed heat). The COP and the chilling capacity depend strongly on the temperature levels of T_H , T_C and T_M . On chilled water systems, a maximum process performance COP_{ideal} for each temperature level can be derived from thermodynamic laws:

$$COP_{\text{ideal}} = \frac{T_C}{T_H} \frac{T_H - T_M}{T_M - T_C}$$

As shown in Figure 8, the ideal performance of a reversible process is far above the performance obtained in thermally driven chillers today available on the market. In fact, the estimated COP value ranges from 0.5 to 0.8 in single effects chillers (absorption and adsorption) and may range to 1.4 in double effect chillers.

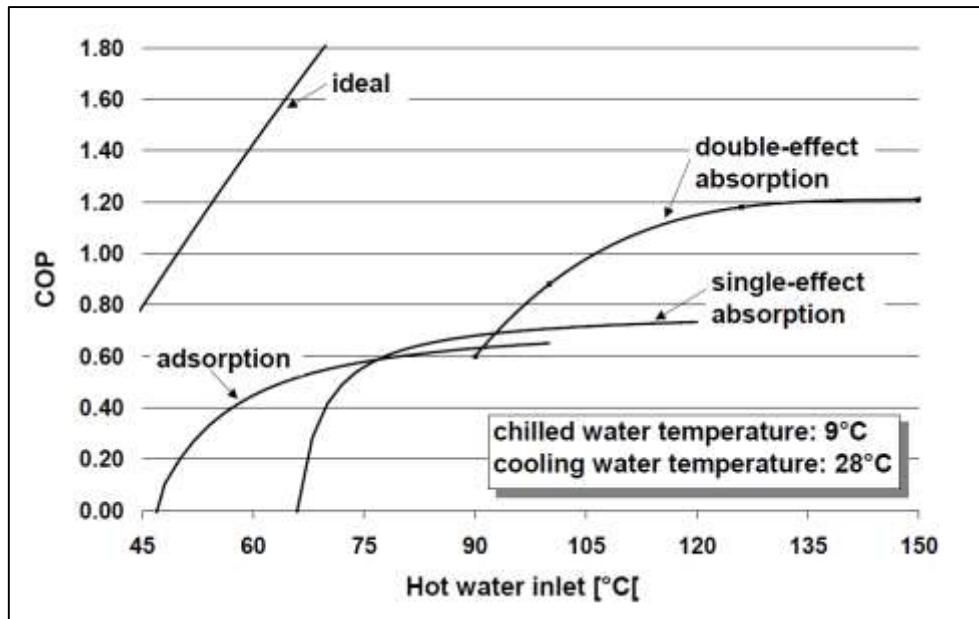


Figure 8. COP values of thermal reversible process

The difference between real and ideal performance of the thermally driven chillers can be expressed with a process quality number ζ_{PQ} :

$$\zeta_{PQ} = \text{COP}_{\text{real}} / \text{COP}_{\text{ideal}}$$

The process quality number allows assessing the advantages of an improved process quality with respect to the required driving temperature. Typical values of ζ_{PQ} , got from market available products, amount to a value of 0.3 as is shown in Figure 9. The graph represents the driving temperature as a function of the “temperature lift” ΔT , which is defined as the temperature between the heat rejection temperature T_M and the chilled water temperature T_C :

$$\Delta T = T_M - T_C$$

As an example, the temperature lift is low in case of high chilled water temperature and wet heat rejection (low cooling water temperatures) and high in case of low required chilled water temperatures and dry cooling. Driving temperatures for two different COP values (1.1 and 0.7) are reported. For each COP-curve, the driving temperature shows a dependency on the process quality: therefore, two different quality numbers are assumed (0.3 and 0.4) as realistic. The operation areas of different collector technologies are indicated as well. As an example, a single-effect chiller with a COP of 0.7, working as $\Delta T = 35^\circ\text{C}$, may be still driven with vacuum tube collectors, if the process requires driving temperatures of approximately 100°C (process quality number of 0.4). In case of a lower process quality, the required driving temperature is higher and tracked concentrating collectors are necessary.

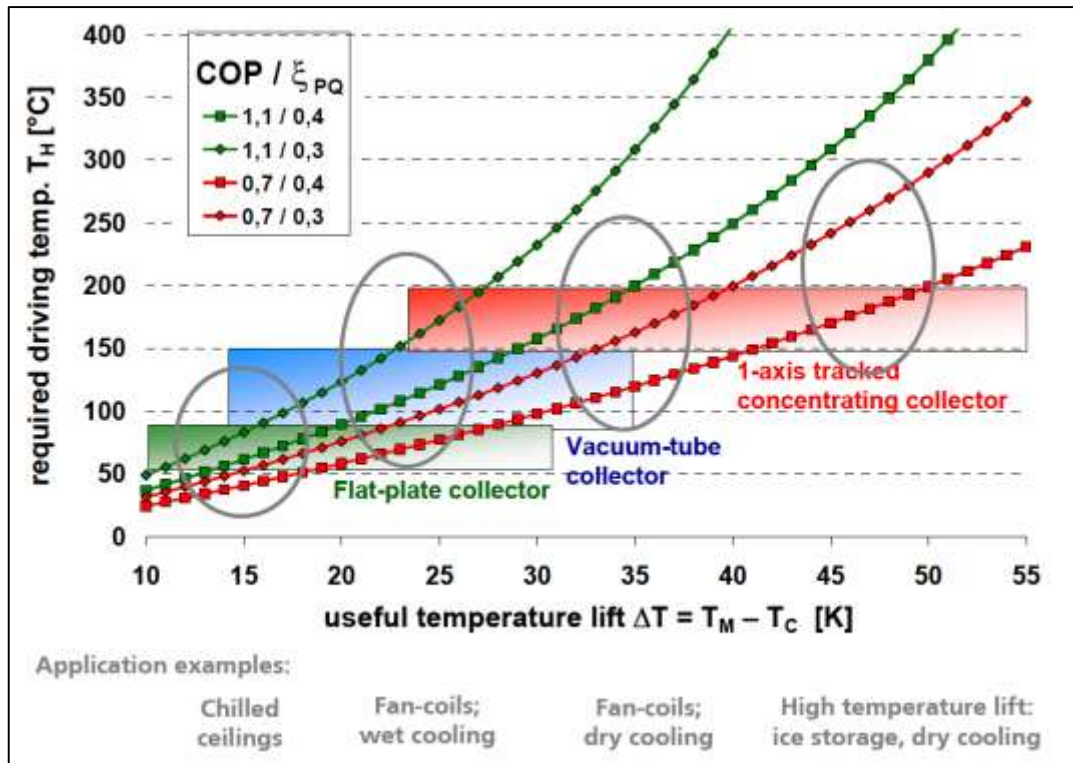


Figure 9. Performances of thermally driven chillers in function of COP and quality number ζ_{PQ}

Many products are available in the market, however typical chilling capacities of absorption chillers are several hundred of kW, mainly used when district heat, waste heat or heat from co-generation is available. The required heat source temperature is usually above 80°C for single-effect machines and the COP is in the range from 0.6 to 0.8. Double-effect machines with two generator stages require driving temperature of around 140°C, but the COP's may achieve values up to 1.2. Triple effect chillers are now available in the market, with a COP around 1.7 or 1.8 for driving temperatures in the range 195°C-225°C and capacities between 350kW to 3500kW.

Since many years, several single-effect absorption chillers with capacities below 50 kW are available. For a long time, the smallest machine available was a Japanese product with a capacity of 35 kW. Currently, chillers with capacities as small as 3kW can be found in the market. In systems with absorption chillers, these small units are now often implemented. A chiller model, newly developed for small capacities, enables part-load operation with reduced chilling power at a heat source temperature of 65°C and a COP with still a value of approximately 0.7, which is very promising in combination with a solar heat source. That leaves open doors for performance improvements of absorption chillers. In fact, new medium/small size developments have been designed recently by European and Asian manufacturers, which are convenient for covering the cooling loads of small areas with extensions from 200 m² to 500 m². The European manufacturers are located in Germany, Austria, Spain, Sweden, Italy and Portugal. Developments are still being tested in pilot installations.

ADSORPTION SYSTEMS: Adsorption chillers use solid sorption materials instead of liquid solutions. Market available systems use water as refrigerant and silica gel as sorbent. Recently, an alternative to silica gel is represented by zeolites, which are used by some manufacturers. By this way, two technologies are now available: Silica gel/H₂O and Zeolites/H₂O.

The physical machines used in adsorption chillers, as shown in Figure 10, consist of mainly two sorbent compartments: one evaporator and one condenser. While the sorbent in the first compartment is regenerated using hot water from the external heat source (e.g. the solar collector), the sorbent in the second compartment adsorbs the water vapour entering from the evaporator. Compartment 2 has to be cooled in order to enable a continuous adsorption. Due to the low-pressure conditions in the evaporator, the refrigerant in the evaporator is transferred into the gas phase by taking up the evaporation heat from the chilled water loop and thereby producing useful "cold". If the sorption material in the adsorption compartment is saturated with water vapour to a certain degree, the chambers are switched over in their function.

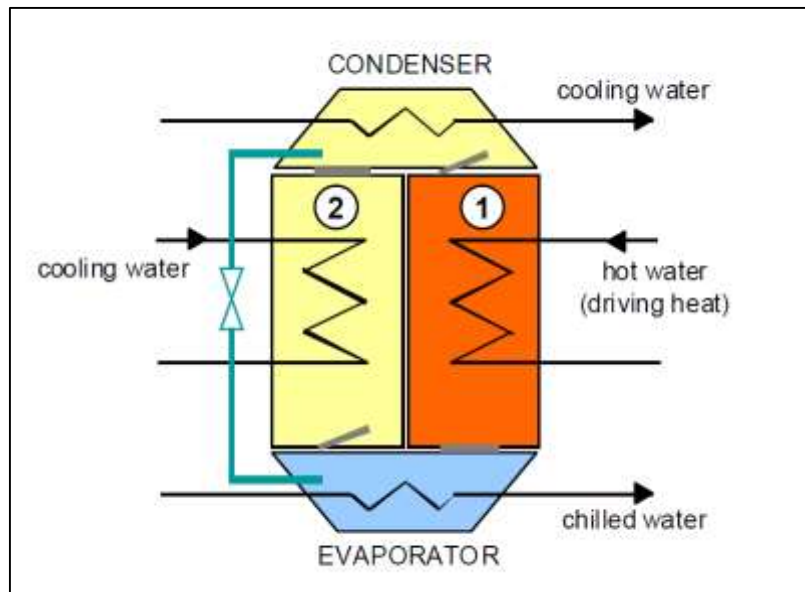


Figure 10. Adsorption chiller system principle

Since today, only a few Asian and European manufacturers produce adsorption chillers. The two historical actors are Japanese, but now a German manufacturer has entered the market. Under typical operating conditions with a driving temperature of 80°C, the systems achieve a COP of about 0.6, but operation is possible even with temperatures of approximately 60 °C. The capacity of the chillers ranges from 5.5 kW to 500 kW chilling power.

The simple mechanical construction of adsorption chillers and their expected robustness is an advantage. There is no matter about adsorbing material crystallization and thus no limitation in temperature ranges. There is no internal solution pump and electricity consumption is thus reduced to a minimum. A disadvantage is the comparatively large volume and weight. Furthermore, due to the small number of produced items, the price of adsorption chillers is currently still high. A large potential for improvements is expected in the construction of the heat exchangers in the adsorber compartments, which would reduce volume and weight considerably in future generations of adsorption chillers.

3. SOLAR HEAT FOR INDUSTRIAL PROCESSES AND OTHER RELEVANT MEDIUM TEMPERATURE APPLICATIONS FOR CSP SYSTEMS

3.1. INTRODUCTION TO INDUSTRIAL PROCESS HEAT

Thermal energy demand in industry fields accounts worldwide for more than two thirds of the total global energy demand. The industrial primary energy consumption nowadays is covered approximately for 40% by natural gas and for 41% by heavy fuel. Half of this demand is requested in low to medium temperatures ranges (<400°C). Looking in detail at the energy demand, 75% of the full industry heat demand is requested by energy-intensive industries, which account for the 5% of all enterprises. The remaining 95% of all industry plants are small or middle-sized enterprises, which account for only the remaining 25%. Solar process heat has high application potential in the industry sectors with high thermal energy demand below 250°C, as in food and beverage sector, as well as in textiles and paper industry [17]. (see also Figure 11)

By this way, according to current studies, solar thermal applications can satisfy up to 33% of the industrial energy demand [15], replacing the actual energy generation system based on gas and heavy fuel with renewable energy solutions, especially if system regeneration is addressed on energy-intensive industry fields.

Due to individual production schedules, process temperatures (even among plants within the same industrial sector) and different integration options of solar thermal energy systems in low or medium temperatures, the design of feasible solutions tailored for specific application and energy demand require a high effort from the planner side. Furthermore, lack of expertise on solar thermal technology among industry enterprises and the actual high investment costs (especially for small enterprises) increase the implementation barrier and the market penetration of solar process heat. However, with high temperatures supplied by solar thermal plants and increasing costs for fossil fuels, solar process heat becomes more and more economically competitive.

In IEA Task 49 [5], an integration guideline is outlined to simplify the feasibility and design process regarding usage of CSP system for industrial applications, including the methodology to identify the best integration parameters for solar thermal energy generation, correlated to solar thermal system designs [16].

The suitability of industrial processes is directly related to their temperature level. As the decision for installing a solar heating system is mainly based on its economic feasibility, the solar heat generation costs have to be considered. The feasibility for a selected solar process heat application is assessed by combining simulation results with a cost analysis of solar heating systems using different collector types and conventional heat generation costs in industry.

The analysis of industrial sectors shows that many processes seem to be promising for the integration of solar heat in several sectors. Additionally, similar processes across all industrial sectors can be categorized into typical applications for solar process heat. The processes listed

below can be found in nearly all industrial sectors and are the three major application of solar process heat:

- **Heating of fluid system** - Processes where a cold (or in some cases a preheated) fluid stream has to be heated up to a certain temperature are classified in this application. Application of heat for make-up or to boiler feed water, material preheating, wash, cleaning and sterilization belong to this category;
- **Heating of baths/vessels** - The processes classified in this application have in common that a bath or vessel filled with a liquid has to be heated to a certain temperature and/or kept at this temperature during a production period. Processes like cooking, blanching, pasteurization, degreasing, bleaching and surface treatment in the machinery and equipment sector belong to this application;
- **Drying** - Drying is the process of thermally removing moisture from a wet material to obtain a solid product. Through the application of heat, a liquid (in most of the cases water) is separated from a solid, semisolid or liquid feedstock by evaporation of the liquid. Hence, a drying operation consists of energy transfer from the surrounding environment to the material and simultaneous mass transfer of moisture from the interior of the material to the surface and from there to the environment. Most commonly, energy is transferred to the surface of the material in form of heat by convection, conduction, radiation or a combination of these. Nevertheless, in other methods like microwave, radiofrequency or dielectric drying, the energy of an electromagnetic field directly generates heat internally within the material. The external mass transfer consists of the evaporation of the moisture at the material's surface to the surrounding environment, from where it is carried away by a carrier gas flow or by the application of vacuum. The process of evaporation depends on the conditions in the drying vessel like temperature, pressure, air humidity and flow, area of exposed surface and the method of supporting the solid during the drying operation. [65]

Heterogeneous industrial processes look for different temperatures and working conditions. The industrial world is so wide that it is quite impossible to give a standard conclusion of the level and amount based on the industry needs. A classification of thermal energy demands can be made considering the temperature level of the industrial processes found in different industrial branches.

The trends of energy demand and of its amount are basilar in developing the right integration strategy. The thermal energy can be supplied by different techniques, the use of energy for drying in respect of the simple heating of a bath require different interface components.

Furthermore, other technical specification like characteristics of the buildings, roof orientation, height of facilities, roof capability to support weight are, at this level, not well quantifiable for the analysis.

Only a specific investigation inside the selected industrial case, made on the field by a person with a good technical knowledge and experience will yield a proposal of a system easily amortizable and efficient.

Based on experience and expertise in design and deployment of medium-temperature solar thermal application, research efforts should be focused on reducing both technological and final

user barriers, which are currently undermining the market penetration. Addressed technological barriers are related to efficient conversion, ease of integration, operational requirements and durability performance. These key targets will be dealt with by focusing the research contribution toward cost reduction, and by selecting and pushing forward improvements on the major technical factors needed.

Efficiency improvements, thanks to the proposed new solutions, are expected to be in the order of 10%, leading to a reduction of cost in the order of 50% compared at the current state of the art (800 €/m²). Previous experience and results in this specific field will provide the initial guidelines and support, for instance by preferring optical efficiency improvements instead of coating materials research efforts. Innovation in the approach is thus related to a wider view of the design-to-user chain, encompassing the technical limitations and explicitly including in the research chain, from the beginning, any specific needs and preference of the final industrial users. By moving the design toward a system installed outside any controlled research environment, the challenges include the preparation of guidelines for the final operator and the adoption from the early stage of simple and reliable installation procedures.

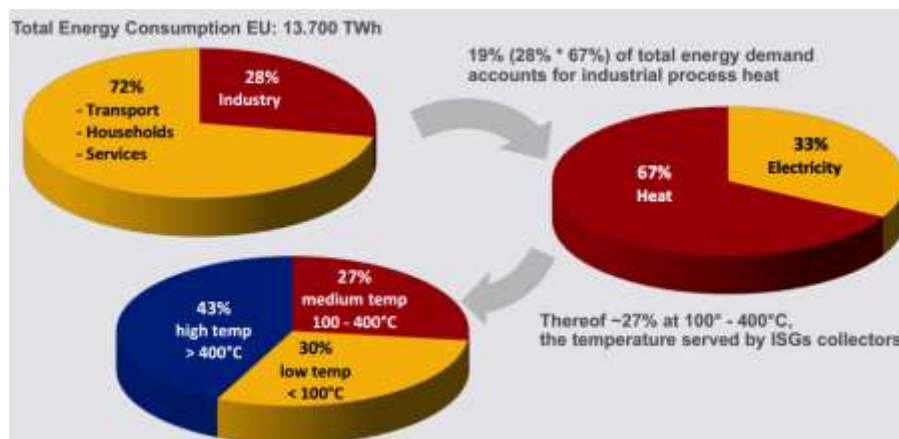


Figure 11. Market – Industrial Process Heat (Source The Technology Roadmap • RHC-Platform 2012)

3.2. SUITABLE PROCESSES AND SECTORS

Among the renewable energy sources, the solar one is the most interesting for application to industrial process heat. Industries are looking at commercial solutions for peculiar needs, targeting fuel savings in heat process applications at competitive cost (400 €/m², 5-9 c€/kWh), when compared to conventional energy sources.

The potential industrial applications included for the temperature level are wide (Figure 12), and the aggregated demand at European level is massive. There is great potential for market developments based on innovations, as 28% of the overall energy demand in the EU27 countries originates in the industrial sector and the majority of this heat demand is in the temperature range below 250°C [53].

TEMPERATURE RANGES FOR DIFFERENT INDUSTRIAL APPLICATIONS

INDUSTRY	PROCESS	TEMPERATURE										
		80	100	120	140	160	180	200	220	240	260	
DAIRY	PRESSURIZATION											
	STERILIZATION											
	DRYING											
	CONCENTRATES											
	BOILER FEED WATER											
TINNED FOOD	STERILIZATION											
	PASTEURIZATION											
	COOKING											
	BLEACHING											
TEXTILE	BLEACHING, DYEING											
	DRYING, DEGREASING											
	DYEING											
	FIXING											
	PRESSING											
PAPER	COCKING, DRYING											
	BOILER FEED WATER											
	BLEACHING											
CHEMICAL	SOAPS											
	SYNTHETIC RUBBER											
	PROCESSING HEAT											
	PRE-HEATING WATER											
MEAT	WASH., STERIL., CLEANING											
	COOKING											
TINNED FOOD	STERILIZATION											
	COOKING											
BEVERAGES	WASHING, STERILIZATION											
	PASTEURIZATION											
FLOURS & BY-PROD.	STERILIZATION											
TIMBER BY-PRODUCTS	THERMODIFFUSION BEAMS											
	DRYING											
	PRE-HEATING WATER											
	PREPARATION PULP											
AUTOMOBILE	PAINTING											
	DRYING											
	COOKING											
BRICKS & BLOCKS	CURING											
PLASTER	CALCINATING											
	CURING PLASTERBOARD											
GLASS	SHEETS											
	DRYING FIBRE-GLASS											
PLASTICS	PREPARATION											
	DISTILLATION											
	SAPARATION											
	EXTENSION											
	DRYING											
	BLENDING											

Source: GESA Research Group, 1988

Figure 12. Temperature Ranges for Different Industrial Applications (GESA Research Group)

3.3. STEAM GENERATION AND SYSTEM INTERFACES

The coupling of the industrial heat process with the proper industrial sector has its starting point in the industrial specific need. The most common system to deliver heat is by introducing a thermal gradient, using some heat exchangers. They can be placed inside or outside the process line. Different types of heat exchangers are used to supply heat. Pressures, temperature, available space, characteristic of fluids as well as cleanliness of the process are elements to be considered in the choice of the best candidate.

When it comes to integrate solar heat into an industrial plant, the point of integration can be either on the level of heat supply, such as steam or hot water networks, the so called “supply level”) or the heat can be directly integrated into a unit operation (heating, washing, drying processes etc.). Linear concentrating collectors can be applied in solar process heat generation to generate steam (direct steam generation) or heating a fluid to evaporate water in an evaporator (indirect steam generation). The solar steam is then integrated to a steam supply network or directly into a process. Considering this ability, the integration concepts herein presented are related to steam generation and rely on a supply level integration approach.

Within the IEA SHC Task 49 ‘Solar Process Heat for Production and Advanced Applications’ integration points and methods as well as system concepts for solar process heat with linear

concentrating collectors were developed. The content of the following sections was extracted from the integration guideline developed within the project work [16].

3.3.1. System Components and Hydraulic Concepts

The selection of a collector type depends on the integration temperature levels, the process medium and the local annual irradiation characteristics. For integration temperatures below 100 °C, generally non-tracked and usually non-concentrating or low-concentrating collectors are sufficient. For temperatures above 160 °C, usually concentrating collectors tracking the sun must be employed. Within the temperature range between 100 °C and 160 °C both collector types are technically suitable. For a specific site and application, the technology selection must be based on the lowest heat generation costs during service lifetime. Below it is reported a list of different concentrating collectors:

- Parabolic trough collectors;
- Linear Fresnel collectors;
- Collectors with tracked receiver;
- Parabolic dish;
- Heliostats with central tower receiver.

Currently, solar process heat is mostly supplied by linear concentrating solar collector fields (<http://ship-plants.info/>). However, there are also a couple of dish collectors in use. [14]

The collector **field size** depends mainly on the desired solar fraction (share of the energy supplied to the loads by the solar thermal) and on the available collector mounting area. Another important parameter is the system utilization ratio, which is influenced by the collector size and type, storage volume size and type, the required feed temperatures and heat transfer rates at the integration point(s). With defocussing of concentrating collectors, the maximum energy output can be controlled and stagnation can be avoided.

The **collector fluid** type depends on the collector type and on the risk of freezing, but can also be influenced by the heat transfer fluid (HTF) or by the process medium at the integration point. If this is air or steam, it is common to supply the heat directly via injection to the process, so the collector- and the heat transfer medium can be the same. Normally, the collector fluid and the HTF differ from each other and are separated by heat exchangers. If freezing protection is necessary, non-evacuated collectors usually use a mixture of about 60 % water and 40 % glycol in the collector loop. A charging heat exchanger transfers the heat to the storage medium, which is usually water. For indirect steam production with focussing collectors, water or thermal oil are used and the HTF evaporates at the integration point, which becomes an evaporator in this case. For direct steam generation within the collector's absorber tubes, a steam drum with a steam separator is needed. Summarizing, the media commonly used in collectors are water-glycol-mixture, (pressurized) water, steam, thermal oil and air.

The collector loop **control** manages the operation of the pumps and detects stagnation or malfunction. Depending on the collector type and system design, it can be necessary or beneficial to circulate the collector medium only through the collectors, thus bypassing the heat transfer unit (e.g. charging heat exchanger). By this way, the heat capacity of the collector loop can be increased, until a certain temperature level is reached and stabilized before starting the heat (mass) transfer to the storage (or HTF or process medium).

Steam generated directly within a collector or through hot fluid and an evaporator, can be supplied to a steam distribution network to supply several processes. Alternatively, it can be directly used for purposes like water desalination, enhanced oil recovery, polygeneration etc. Fluid heated within a concentrating collector field can be used to pre-heat oil for CSP plants or MED processes. In the following section solar heat generation for industrial steam and hot fluid distribution networks are explained in more detail.

3.3.2. Steam generation and integration concepts

The contents of this section are based on the integration guideline developed within the IEA SHC Task 49 ‘Solar Process Heat for Production and Advanced Applications’ (Muster et al. 2015) [16]. Some integrating concepts for linear concentrating collectors will be briefly introduced and illustrated, using a process flow sheet. Figure 13 shows the most important symbols used as legend in all the following flow sheets.

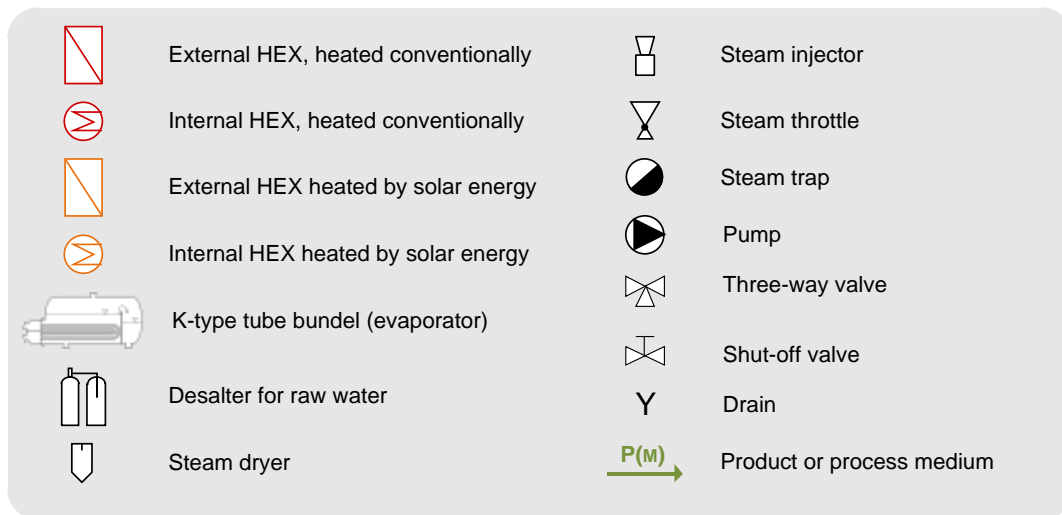


Figure 13. Important symbols for integration concepts

If high temperature levels are needed for the parallel integration of solar heat (solar steam generation), suitable collector concepts have to be applied. Due to the fact that the required temperature level for parallel integration of solar heat in conventional steam systems is usually above 150 °C, concentrating collectors should be applied. Therefore, irradiation data of the location have to be taken into account for the choice of the appropriate collector concept.

Solar Direct Steam Generation (DSG)

For the integration concept of direct solar steam generation a steam drum is required, fed by solar concentrating collectors. Boiler feed water is fed to the solar heating system and partially evaporated. The water-steam mixture is fed to the steam drum where it is separated. The accumulated water is fed back to the collector loop. In case of a sufficient pressure in the steam drum, the steam is fed into the conventional steam circuit. Figure 14 shows the schematic of this integration concept.

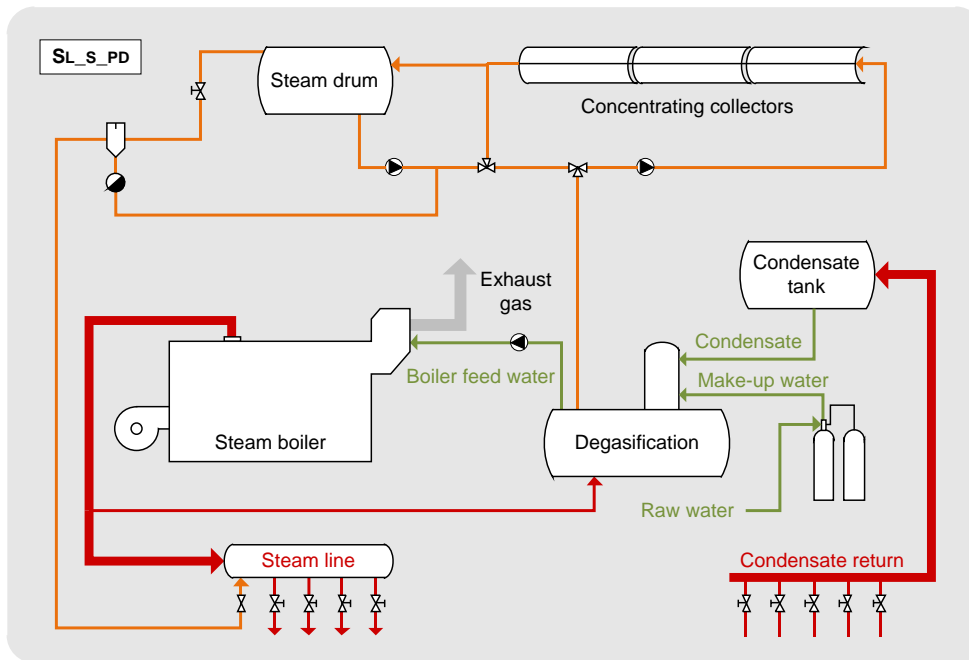


Figure 14. Integration concept for direct solar steam generation

While solar steam is fed into the existing circuit, the conventional steam boiler reduces its steam production similarly to operation periods with a reduced load. The actual loss of efficiency of the steam boiler caused by the solar heating system is influenced by the ratio of installed solar power to conventional capacity, the typical load, and by steam boiler performance (scope of modulation). This integration concept has been realized within several demonstration plants.

Sola Indirect Steam Generation (ISG)

Regarding the interaction of the solar heating system with the conventional steam supply system, this integration concept is similar to the previous one. As shown in Figure 15, for this concept, concentrating collectors with pressurized water or thermal oil as heat transfer medium are used to feed a special heat exchanger for evaporation (typically a kettle type reboiler). The heat exchanger operates at the same pressure as a conventional steam system.

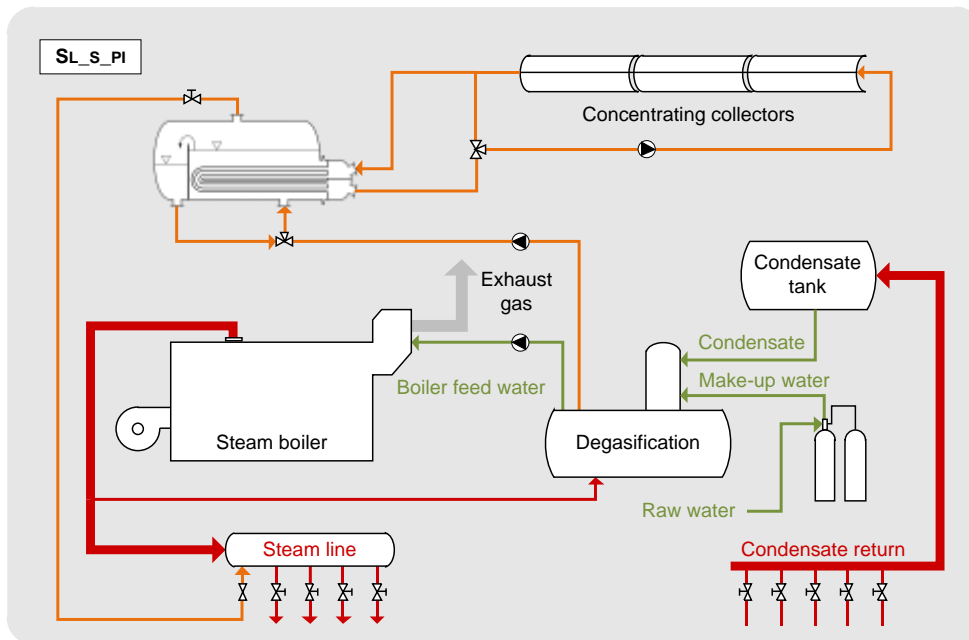


Figure 15. Integration concept for indirect solar steam generation

For liquid heat transfer media other integration concepts can be applied, as compared to the concepts for steam. Besides the parallel and serial integration of solar heat, it is also possible to heat storages or cascades that are integrated into the conventional heat supply system. Due to the relevance in industry, the main application of these integration concepts is for hot water circuits. However, they can also be applied to synthetic heat transfer media and thermal oils that are typically used for a temperature range of $250 \div 400$ °C.

For the parallel integration of solar heat into hot water circuits, the return flow is first divided to the conventional boiler and partially directed through the solar heating system and fed back into the flow. Therefore, the control of the solar heating system has to ensure the heating of the return to the required flow temperature. The integration can be realized directly or indirectly. For the direct integration, the water of the heating circuit flows directly through the collectors (cf. Figure 16), while a heat exchanger is used for the indirect integration.

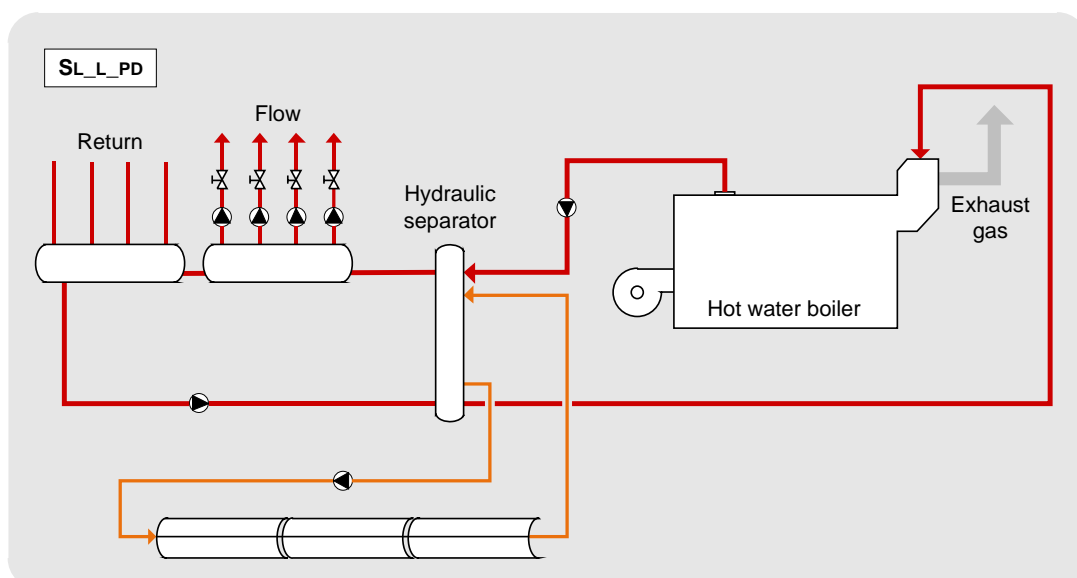


Figure 166. Integration concept for direct parallel integration at supply level with liquid heat transfer media

Sometimes also, combined heating circuits can be found in Industry, which use steam as the primary heat transfer medium to generate hot water as secondary heat transfer medium via heat exchangers or hot water cascades. This also can be vice versa in companies with little low-pressure steam demand. In this case, hot water is used as primary heat transfer medium and produces steam via hot water in a small steam drum.

3.4. EXAMPLES AND RELEVANT PROCESSES

3.4.1. Cooling

In 2014, about 50% of the energy demand is used for heating and cooling purposes. That is why the solar heating and cooling represent a great opportunity to cover this demand.

According to the IEA-SHC, 99% of solar heating and cooling technologies is used to provide warm water or space heating in residential homes [58].

The cooling demand has been growing worldwide, even in colder climates, and mainly for tertiary buildings. The air conditioning is the main process used for comfort cooling, and the solar cooling could therefore reduce considerably the electricity demand, particularly in summer when the electricity demand increases due to air-conditioning. However, some barriers exist for this technology: lack of awareness from the public, the limited number of demonstration projects, the system first installation cost and components' market availability.

In industry the cooling demand is generally continuous, so the solar cooling can hardly compete with the conventional electrical cooling, but in some applications this technology is fruitfully applicable and cost competitive. Solar assisted air conditioning systems are the ideal in industrial applications where dry air is permanently required, such as in the drying of agricultural crops and in livestock plants.

For commercial buildings, installing solar cooling systems requires an area of sufficient extension to install the cooling system's solar collectors. Therefore, not all commercial buildings are suitable for solar assisted air conditioning. The most suitable buildings to install solar cooling systems are commercial buildings with large roof areas, such as supermarkets, shopping centers, hotels, hospitals and convention centers. (See also Figure 17)

For the space heating and cooling, two different strategies are distinguishable: passive and active modes. In the passive solar house, all the elements are designed in order to absorb and store the solar energy, while rejecting solar heat during summer. In this design only the natural circulation of air by temperature gradient is used to move hot or cold air, without the need of mechanical and electrical devices. The natural processes that are used for the spontaneous loss of heat being: cooling by radiation, convection or evaporation, conduction by contact between two bodies with a lower temperature. Active solar cooling system implies the use of pumps, solar collectors and storage.

The artificial solar cooling is based on different processes: a chemical one with the dissolution of a solution in a solvent, another chemical one with phase change of some element, occurring

at low temperature; a mechanical one with expansion of gases previously compressed or, finally, a thermos-electrical one.

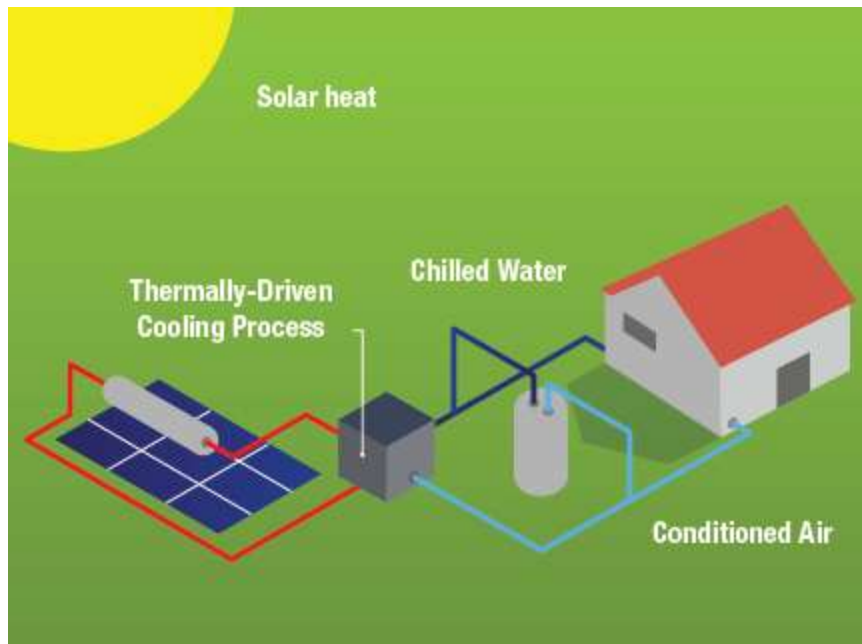


Figure 17. Solar cooling system (ESTIF 2015)

The temperature range for the cooling depends on the applications and will need different processes. For temperature from 24°C to 14°C the process is called simply cooling and can be managed in a natural way, but for temperature from 14°C to 0°C the process is called refrigeration and can be managed by water phase change.

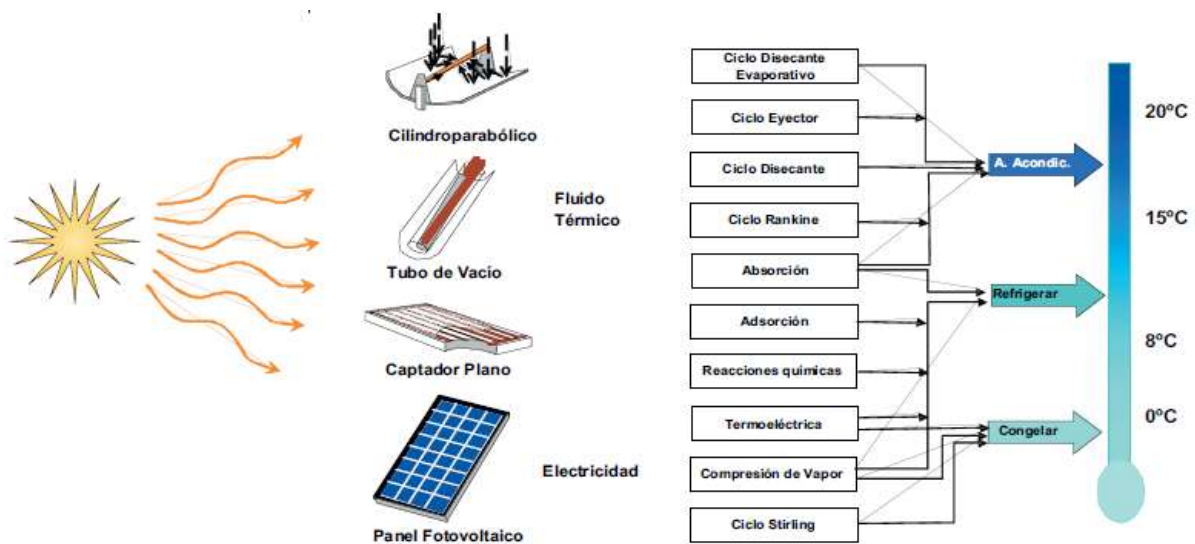


Figure 18. Cooling process (Guía del Frío Solar, Ahorro y eficiencia energética con refrigeración solar, 2011)

As shown in Figure 18, many processes are possible for cooling but not all of them can be used with solar energy and more particularly with solar thermal energy. To be used for cooling application, the solar thermal systems as to replace gas driven or electricity-driven absorption/adsorption chillers or to replace electricity driven, vapour-compressing air conditioning systems. For refrigeration, different processes are available, based on absorption, which depends on the capacity of some element of absorbing others.

Solar energy can be converted into cooling using two main principles: Electricity generated with photovoltaic modules is converted into cooling using well-known refrigeration and air-conditioning technologies, mainly based on vapour compression cycles. Heat generated with solar thermal collectors is converted into cooling using thermally driven refrigeration or air-conditioning technologies, which mainly use the physical phenomena of sorption in either an open or closed thermodynamic cycle. In the case of solar thermal cooling, the warmed fluid is used in a device called absorption/adsorption chiller, to drive the cooling of process fluids.

The first solar cooling system invented by Edmond Carré to produce ice from solar energy, presented in 1850 at the Exposition in Paris, used a sorption technology. Sorption processes are divided into two branches: periodical sorption processes (which use either a liquid refrigerant like ammonia or a suitable absorptive substance like water or calcium chloride, or water as a refrigerant and a solid adsorptive material, such as silica gel or zeolite) or continuous sorption processes.

Absorption and adsorption chiller systems use liquid or solid refrigerants to cool the environment.

Among the sorption processes, the most common system for solar cooling is the absorption chiller, used to regenerate the absorber fluid, which contains the refrigerant after it has been evaporated. The other chiller type is the adsorption chiller. The two common type of absorption chillers are: closed absorption chiller systems with ammonia-water ($\text{NH}_3/\text{H}_2\text{O}$) or water-lithium-bromide ($\text{H}_2\text{O}/\text{LiBr}$) as refrigerant/absorber fluids.

The ammonia-water chiller's COP is slightly lower than the $\text{H}_2\text{O}-\text{LiBr}$ machines (because of the need to rectify the ammonia vapour after generation). In both technologies cooling towers must be used to remove the heat released at the condenser and absorber. In the case of lithium bromide chillers this translates into the use of wet cooling towers in order to avoid crystallization of the water-lithium-bromide solution. Cooling at freezing temperatures demand the use of ammonia-water chillers and requires higher temperatures in the generator (~ 100-120°C for single effect units).

Other kind of cooling systems are the desiccant system, which uses a desiccant material to absorb or adsorb warm water from the air to get it cooled. In this case, the desiccant is regenerated with solar energy. The efficiency of the systems and the temperature range both depend on the technology used. For example, the single effect chillers, like desiccant cycles, have low efficiency but the temperatures required are between 70°C and 100°C. But the double- and triple-effect absorption chillers have higher efficiencies (COP above 1 and up to 1,8) but the temperature required is higher: 150–180°C and 200–250°C, respectively.

In the last years, the hot water/steam temperature required for the chillers' operation has decreased, with the creation of new companies which offer systems which could be integrated within hybrid systems. But this way, the solar air-conditioning system could supply lower temperatures (+20°C to -10°C) using low temperature collectors, such flat plates or evacuated tubes.

According to a survey from the IEA SHC [60] based on 276 installations studied worldwide, a measure of the most used technologies and applications can be envisaged. A first rough

classification shows that 113 are large scale solar cooling systems and 163 are small scale systems. By this way:

- For small-scale installations, the major percentage (38%) of the installations are dedicated to office buildings, then to private houses (28%), laboratories (9%), industry (8%), school and universities (7%), and finally sport centres (4%) or others (6%).
- For large-scale installations, the major percentage (53%) of the installations are dedicated to office buildings, then to laboratories (7%), industry (9%), school and universities (9%), and others (12%).

Within 269 installations, the most used technology of thermally driven chillers is based on absorption technology (71%) for large-scale installation and 90% for small-scale installations. In 2013 [15] more than 1000 solar cooling systems were installed worldwide, of which 135 were large installations. Several hundred solar thermal assisted cooling pilot systems are already installed in Europe, in the year 2012. According to Daniel Mugnier from TECSOL Company, in 2014 more than 1200 solar thermally driven cooling systems were installed worldwide, based on solar thermal collectors, among which more than 800 were installed in Europe. Really, they represent a small percentage of all the air-conditioning systems, as compared to the tens of millions compression air-conditioning systems sold annually.

The types of collector used for solar cooling can be conventional collectors and flat-plate or evacuated tube, when the operating temperature is below 110°C. However, solar cooling systems such as the one working with multi-stage absorption chillers needs an higher temperature, so typically use of single-axis tracking with optical concentration is required.

Regarding solar heating for domestic hot water and space heating, one of the solutions recently introduced is the combi-system. This solution is compact and can reduce installation con and space required. These systems are mainly used in central Europe, especially in Germany, Austria, Switzerland and France. In Germany, about 50% of newly installed systems are combi-systems with usually a 10 to 15 m² flat plate collector and a 600 to 1000 litres of hot water storage. In a well-insulated building, the solar fraction is about 25% of the overall building heat demand for DHW and space heating. In Austria combi-systems have a larger collector area of 20 to 30 m².

The cost of the solar cooling installations is between 2 and 5 times higher than a conventional cooling system, depending on local conditions, building requirements, system size, and technology used. In recent studies, first cost for total systems ranged from 2,000 €/kW to 5,000 €/kW_{cold}.

Some reasons for employing line-focus concentrating collectors in solar cooling systems are: thigh efficient air-conditioning by coupling with double-triple effect chillers, and solar refrigeration serving industrial end-users, possibly in combination with process heat and steam.

The choice of the best solar configuration for a given application (domestic air-conditioning, large-buildings air-conditioning, solar refrigeration in the industry, etc.) can be carried out targeting the highest primary energy saving achievable on a yearly base. The primary energy savings that could be reached with single stage absorption chillers are quite small. Thus, double and triple effect absorption chillers with higher COP are required for higher energy savings. Double and triple effect chillers require high driving temperatures, which can be achieved by

line-focus collectors working at these temperatures with reasonable efficiency. Besides, in many cases, space restriction on roofs or urban areas makes the utilization of single effect chillers with large flat plate or evacuated tube collectors not feasible.

3.4.2. Drying

The heat in conventional drying systems at a medium high or high temperature level is usually supplied by combustion of fossil fuels. In direct-fired heating systems the combustion gases are directly used as heat transfer medium for the drying process. In indirect fired heating systems, the heat of combustion is transferred to another fluid (e.g. air, steam or oil) [66]. Solar energy as a source of heat for evaporation, already has wide application in drying at low temperature levels [67]. In order to identify the most suitable concentrating solar power technology for the heat supply of conventional dryers, a classification of drying methods is first given, followed with an overview of the most common industrial dryer types.

Classification of drying methods

There are over 100 distinct well-trying dryer types available in different industries, not including a lot of new systems not yet applied in practice. Selection of the appropriate dryer type for a particular drying operation strongly depends on the nature of the product to be dried and the thereby required drying conditions. The principal classification criteria for industrial drying methods depends on the way in which heat is supplied to the material, temperature and pressure of the drying operation and the handling of the material in the dryer [65].

The possible methods of transferring heat to the material to be dried are based on the three different heat transfer principles: convection, conduction and radiation. In convective dryers, also called direct dryers, heat is supplied by a heated drying medium, which is flowing over the exposed surface of the solid and carries away the evaporated moisture. Over 85 % of the industrial dryers are convective types. The drying medium can be heated air (most common), inert gas (e.g. N₂), direct combustion gases or superheated steam. In contrast, in conductive dryers, also called indirect dryers, heat is supplied through heated surfaces, represented by either stationary or moving parts of the dryer that support, convey or confine the solids. Hence, the product being dried does not come into contact with the heating medium, which can be oil or hot water (fluid type) or steam (condensing type) [68]. In indirect dryers, either the application of vacuum or a stream of gas carries the evaporated moisture away. Additionally, there is the possibility of combined convective and conductive heat supply. Finally, heat can also be applied through radiative heat transfer. However, radiative heat transfer is insignificant at temperatures lower than 700°C and since most drying processes are carried out at temperatures lower than this, radiant heat transfer will be neglected in the following. [65]

Dryers are usually operated at either near atmospheric pressures or vacuum. Vacuum operation is expensive but permits drying at lower temperatures. In the case of superheated steam drying, the systems are operated at either low, near atmospheric or high pressure [69]. The temperature of the drying operation can be above or below the boiling temperature of the removed liquid. In most of the systems it is below. In a special case, freeze-drying, the temperature is below the freezing point, and as for vacuum operation below the triple point of water, the application of heat directly leads to the sublimation of ice into vapour [65].

Furthermore, a dryer can be operated in continuous or batch mode, the state of the material in the dryer can be either stationary, moving, agitated or dispersed. The residence time of the material in the dryer can be short (< 1 minute), medium (1 – 60 minutes) or long (> 60 minutes). Applying these and further possible characteristics, there exist a lot of different dryer types and designs, the principle of the most common ones are described in point 2. [65]

Table 1 shows a summary of the mentioned classification criteria and their possible types, which are shortly described in the sequel.

Table 1. Classification of different drying methods

Heating method	Convection (direct)	Drying medium: air, superheated steam, flue gases
	Conduction (indirect)	Heating medium: Steam (condensing type), Oil / water (fluid type)
	Radiation	
	Combined direct and indirect heat transfer	
Drying temperature	Below boiling temperature, above boiling temperature, below freezing point	
Operating pressure	Near atmospheric, vacuum, high pressure	
Handling of material in dryer	See examples in point 2	

Different industrial dryer types and most suitable STE technology

Below it is reported a short description of the most common conventional dryer types. According to the typically required conditions of heat supply, for each dryer type the most suitable concentrating solar power technology is identified. The basic information used for this purpose is the heat transfer fluid adopted in the dryer and its inlet temperature (see Figure 19).

For direct dryers with hot air as drying medium there is the possibility of using an air-based CSP collector (e.g. AIRLIGHT) for air inlet temperatures up to 650°C. For lower temperatures (<400°C) there is also the possibility of Parabolic Trough Collector (PTC) or Fresnel Collector using heat transfer fluids (HTF) different from air. In this case however, a heat exchanger (HEX HTF-air) would be needed. For very high air temperatures there is the option of a central receiver system (CRS, usually volumetric receivers). In addition, the use of hot air as HTF allows easy thermal energy storage in a packed rock bed. Direct and indirect dryers using (superheated) steam as heat transfer fluid can integrate either parabolic trough collectors with direct steam generation (DSG) for steam temperatures up to 450°C, or PTC/Fresnel systems with a steam generator (SG HTF-steam). For indirect dryer types using thermal oil, the suitable STE technology is parabolic trough or Fresnel collector.

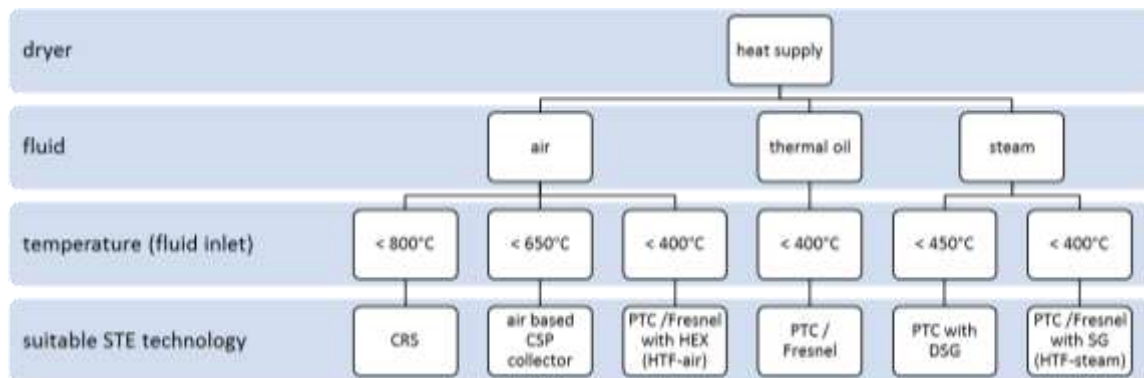


Figure 19. Identification of the most suitable STE technology for integration in a drying process

The thermal load or the size of the drying systems are further important information, especially when it comes to concrete integration schemes. In general, it ranges between several hundred kW up to several MW. However, since thermal power loads of particular drying processes mainly depend on the evaporation load for the amount of water to be removed and thus on the particular dryer design and scale, categorizing for the different dryer types is not reasonable. [66]

Below there is an overview of different dryer types, their typical heat supply requirements and the respectively identified most suitable STE technology for integration. Since this subtask is focused on linear focusing systems, CRS are not included in the following study.

Flash dryers

Flash drying, also called pneumatic drying, is a direct drying method. A flash dryer consists basically of a vertical drying tube in which the wet material is dispersed into a stream of the hot drying medium. The material dries as it is conveyed upward through the tube by the drying medium. The product of this process is a mixture of dried material and drying medium, which is separated usually by cyclones and/or bag filters. The temperature of the drying medium should be as high as possible, without exceeding limits imposed by the thermal sensitivity of the solids or safety considerations. Table 2 shows the identification of suitable STE technologies for heat supply of flash dryers. [65, 70]

Table 2. Typically required conditions of heat supply for flash dryer designs and identified most suitable STE technologies

Heat input type	Drying/heating medium	Inlet temperature of heat transfer medium	Pressure of heat transfer medium	Suitable STE technology
Direct drying	Air	400-600°C [65]	near atmospheric [65]	Air-based CSP coll.
	Superheated steam	> 230°C	high (25 bar) [69]	PTC/Fresnel + HEX DSG

Spray dryers

A spray dryer is another sort of direct dryer. Liquid feeds are atomized into small droplets and dispersed at the top of a large drying chamber. There the drying occurs by a stream of hot drying medium while the droplets fall to the bottom of the chamber. Afterwards the dried particles are separated from the drying medium by cyclones. Table 3 shows the identification of suitable STE technologies for the heat supply of spray dryers [65].

Table 3. Typically required conditions of heat supply for spray dryer designs and identified most suitable STE technologies

Heat input type	Drying/heating medium	Inlet temperature of heat transfer medium	Pressure of heat transfer medium	Suitable STE technology
Direct drying	Air	200-450°C [65]	near atmospheric [65]	Air-based CSP coll. PTC/Fresnel + HEX
	Superheated steam	< 700°C [7]	near atmospheric [69]	-

Rotary Drum Dryers

In a rotary drum dryer, the wet material is dried in a rotating cylindrical shell. The solids are moved through the shell by the combined effect of air flow, gravity, speed of rotation and the shell slope. The rotary drum system can be applied as direct or indirect dryer or as a combination of both. In direct rotary dryer models the hot drying medium passes through the shell while the material is moved through it. There are two principle designs of indirect rotary drum dryers: an indirect steam-tube dryer, in which steam passes through rows of metal tubes in the interior of the dryer, and an indirect rotary calciner, which consists of a metal cylinder surrounded by a fired or electrically heated furnace. There is also the possibility of a combined direct-indirect design [69]. Table 4 shows the identification of suitable STE technologies for heat supply of rotary drum dryers. [65].

Table 4. Typically required conditions of heat supply for rotary drum dryer designs and identified most suitable STE technologies

Heat input type	Drying/heating medium	Inlet temperature of heat transfer medium	Pressure of heat transfer medium	Suitable STE technology
Direct drying	Air	200-600°C [65]	near atmospheric [65]	Air-based CSP coll. PTC/Fresnel + HEX
	Superheated steam	< 300°C [69]	low or near atmospheric [65]	PTC/Fresnel + HEX DSG
Indirect drying	Steam (steam-tube)	< 300°C (surface temperature) [65]	not specified	PTC/Fresnel + HEX DSG
	Combustion gases (calciner)	up to 700-900°C [69]	not specified	-

Fluidized Bed Dryers

In Fluidized bed dryers a continuous feed of wet material is dried by contact with warm air that is blown from below to maintain the material in a fluidized state. The fluidized layer can be compared in its behaviour to that of boiling liquid: it assumes the shape of the containing vessel, heavy objects sink and light objects float. The material is dried while suspended in the upward-moving drying gas. Additionally, heat exchanger panels or tubes can be immersed in a fluidized bed making available a heat fraction for drying by conduction, which offers the possibility to deploy lower air/steam temperatures. Table 5 shows the identification of suitable STE technologies for heat supply of fluidized bed dryers. [65]

Table 5: Typically required conditions of heat supply for fluidized bed dryer designs and identified most suitable STE technologies

Heat input type	Drying/heating medium	Inlet temperature of heat transfer medium	Pressure of heat transfer medium	Suitable STE technology
Direct drying	Air	100-600°C [65]	near atmospheric [65]	Air-based CSP coll. PTC/Fresnel + HEX
	Superheated steam	50-360°C [69]	low, near atmospheric or high (< 5 bar) [69]	PTC/Fresnel + HEX DSG
Indirect drying	Steam	< 300°C (surface temperature) [65]	not specified	PTC/Fresnel + HEX DSG

Impingement Dryers

Impingement dryers are direct dryers, which are commonly employed for very fragile and wet crystals, paper or textiles. Through the incident flow of the drying medium in the normal direction against a moving loosely formed bed of wet feed, the hot gas is made to impinge on such bed. Moisture evaporates as the material traverses along the length of the ventilated bed so that the material at the discharge end is dry. Table 6 shows the identification of suitable STE technologies for heat supply of impingement dryers. [72]

Table 6: Typically required conditions of heat supply for impingement dryer designs and identified most suitable STE technologies

Heat input type	Drying/heating medium	Inlet temperature of heat transfer medium	Pressure of heat transfer medium	Suitable STE technology
Direct drying	Air	100-350°C [65]	near atmospheric [65]	Air-based CSP coll. PTC/Fresnel + HEX
	Superheated steam	>100°C	near atmospheric [69]	PTC/Fresnel + HEX DSG

Through Dryers

Through drying is a direct drying process, in which a pressure differential across a wet, porous material forces a stream of hot drying medium through the material. The design of through dryers can be similar to an impingement dryer or a rotary design with a porous cylinder. Table 7 shows the identification of suitable STE technologies for heat supply of rotary drum dryers [73].

Table 7. Typically required conditions of heat supply for through dryer designs and identified most suitable STE technologies

Heat input type	Drying/heating medium	Inlet temperature of heat transfer medium	Pressure of heat transfer medium	Suitable STE technology
Direct drying	Air	150-370°C [73]	near atmospheric [65]	Air-based CSP coll. PTC/Fresnel + HEX
	Superheated steam	>100-180°C [74]	near atmospheric [69]	PTC/Fresnel + HEX DSG

Conveyor Dryers

In conveyor dryers, the wet material is carried by either a steel belt, screwing or vibrating through a chamber, where a hot drying medium is forced through the product bed. This direct drying method can be applied for a wide range of different products. Table 8 shows the identification of suitable STE technologies for heat supply of conveyor dryers. [65]

Table 8. Typically required conditions of heat supply for conveyor dryer designs and identified most suitable STE technologies

Heat input type	Drying/heating medium	Inlet temperature of heat transfer medium	Pressure of heat transfer medium	Suitable STE technology
Direct drying	Air	50-175°C [65]	near atmospheric [65]	Air-based CSP coll. PTC/Fresnel + HEX
	Superheated steam	>160°C	high (< 5 bar) [69]	PTC/Fresnel + HEX DSG

Tray Dryers

Tray dryers (also truck or tunnel dryers) are usually direct dryer types. The material to be dried is placed in pans, trays or on trolleys, which are introduced at one end of a tunnel and discharged from the other end after having dried in the tunnel by a stream of hot air. However, there is also an indirect tray dryer type, in which heat is supplied to the material through the pans or trays, internally heated by oil or steam. Table 9 shows the identification of suitable STE technologies for heat supply of tray dryers [65].

Table 9. Typically required conditions of heat supply for tray dryer designs and identified most suitable STE technologies

Heat input type	Drying/heating medium	Inlet temperature of heat transfer medium	Pressure of heat transfer medium	Suitable STE technology
Direct drying	Air	100-200°C [65]	near atmospheric [65]	Air-based CSP coll. PTC/Fresnel + HEX
Indirect drying	Steam/ thermal oil	< 300°C (surface temperature) [65]	not specified	PTC/Fresnel + HEX DSG

Vittoriosi et al. [75] demonstrate the integration of heat supplied by a solar field into a drying process for a brick manufacturing process. The whole industrial process includes the mixing, drying and cooking of bricks. The drying is carried out by a direct dryer – not further specified, but similar to a tray dryer design – using hot air at temperatures between 200°C and 260°C with an average thermal load of 2,2 MW. Part of the heat is supplied by heat recovery from the downstream brick cooking process, carried out in a tunnel kiln at 900°C after drying. A Fresnel collector field with 2700 m² and a maximal thermal power of 1,2 MW is installed and integrated in the drying process, in order to replace the formally gas fired heater. Nevertheless, for times when the solar radiation doesn't suffice for heating the air up to the required temperature, a back-up natural gas burner is installed. Half of the Fresnel solar field is operated with direct steam generation and the other half with indirect steam generation (thermal oil – steam). At the entrance of the dryer, the heat from the solar field is integrated into the drying process by means of an air to steam radiant heat exchanger [75].

For drying processes a fluid stream has to be heated. However, it is considered separately since there is the possibility to use different components (e.g. air collectors) and system configurations for this application.

Inside the “IEA SHC Task 33/IV – Solar Heat for Industrial Process”, 71 solar heating systems built in industrial companies have been analyzed. 51% of them were used for applications related to “heating of fluid system”, 14% were integrated in processes of application or “heating of baths/vessels” and 6% for drying processes. The remaining 29% are spread on other processes.

The temperature level needed for an industrial processes is crucial for feasibility assessment, as the annual energy yield of a solar heating system strongly depends on the provided temperature.

3.4.3. Solar Desalination

Concentrating Solar Power (CSP) can perform well when integrated with energy intensive desalination processes [65] since CSP can provide both thermal and electrical power in large amount (including base-load production), being able to reliably and economically store energy to produce at a constant output (using thermal storage or hybridization with renewable or conventional fuels) even when solar energy is insufficient. CSP can power both thermal and membrane desalination systems in co-generation or dedicated water production schemes [77] (see Figure 20).

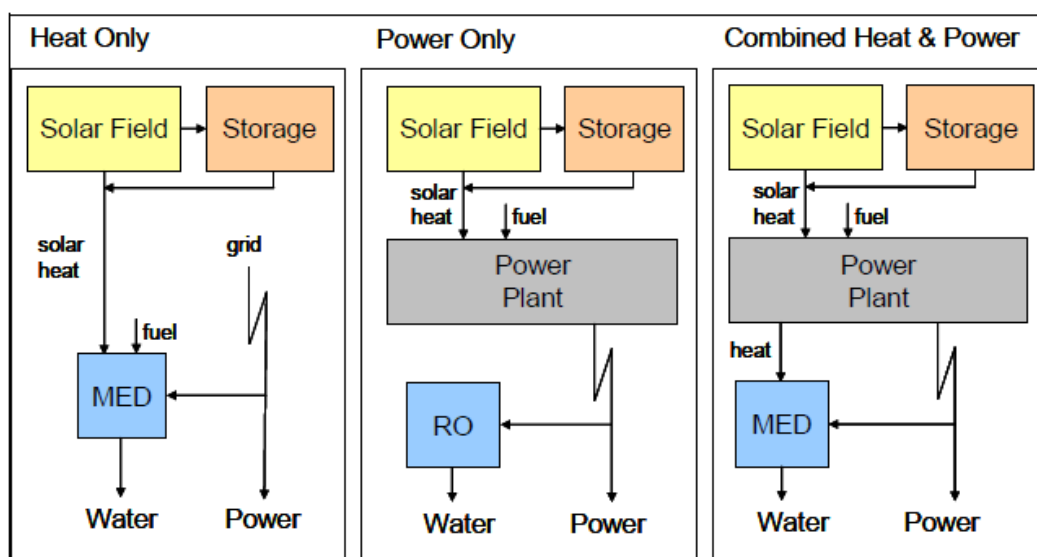


Figure 20. Possible configurations for desalination powered by CSP. Left panel: Dedicated water production scheme using thermal desalination systems (MED presented as an example). Central panel: Power generation for reverse osmosis. Right panel: Co-generation of electricity and water using thermal desalination systems (MED presented as an example).[76]

The cogeneration of water and electricity using commercial desalination units powered by fossil fuelled thermal power plants is not a novelty, particularly in the Middle East region [78], however there are yet no commercial CSP plants operating in direct cogeneration with desalination units, and very few experimental projects were actually built. Powering desalination plants using the CSP technologies represent a challenge regarding optimization of the installed power and energy storage, operating schedules, and technologies to be chosen.

Also, depending on the price of water and electricity in a determined region, it may be more profitable to favour water production instead of electricity or vice versa, depending on the time of the day and time of the year [79].

Thermal desalination systems use thermal energy to produce fresh water from the sea or from brackish water sources. Thermal desalination systems produce distillate using phase change (liquid to vapour). Only water molecules pass to the vapour phase, leaving all other constituents in the unevaporated liquid. Contamination of the distillate produced with dissolved salts is negligible (~ 100 ppm for total dissolved solids) [80]. Thermal desalination systems can be split into two main technologies: multi-stage flash (MSF), which accounts for 21% of the total installed desalination capacity worldwide [78], and multi effect distillation (MED) technologies, which accounts for 7% of total capacity [78].

MSF plants use steam at $90 - 120^\circ\text{C}$ at around 2.5 to 3 bar of pressure, as a minimum. A typical MSF plant has a heat requirement of 250 - 330 kJ/kg of water produced, and electricity consumption in the order of 3-5 kWh/m³. In a CSP+D co-generation scheme, steam is extracted from the turbine at the required temperature and pressure level. Considering the aforementioned figures, this steam extraction would imply a net electrical output reduction equivalent to 6-8 kWh/m³ of clean water produced. A typical performance ratio (ratio of the produced water to the input heat) of a MSF plant is in the range of 7 to 9 [79].

MED plants operate at top brine temperatures between 55°C and 70°C to limit scale formation and corrosion, allowing the use of low-grade waste heat if coupled to a steam cycle power plant, obtaining a better performance than MSF. Also, standard condensing turbines may be used instead of back-pressure turbines [76]. Low temperature MED plants can have a heat consumption of 190-390 kJ/kg in the form of process steam at less than 0.35 bar, withdrawn from the condensing steam turbine, with a specific electricity consumption of 1.5-2.5 kWh/m³ (for pumping and control) [76]. Figure 21 presents a typical integration scheme for a low temperature MED powered by parabolic troughs. In this case the production of water and electricity is coupled since the MED system is used as condenser of the steam cycle.

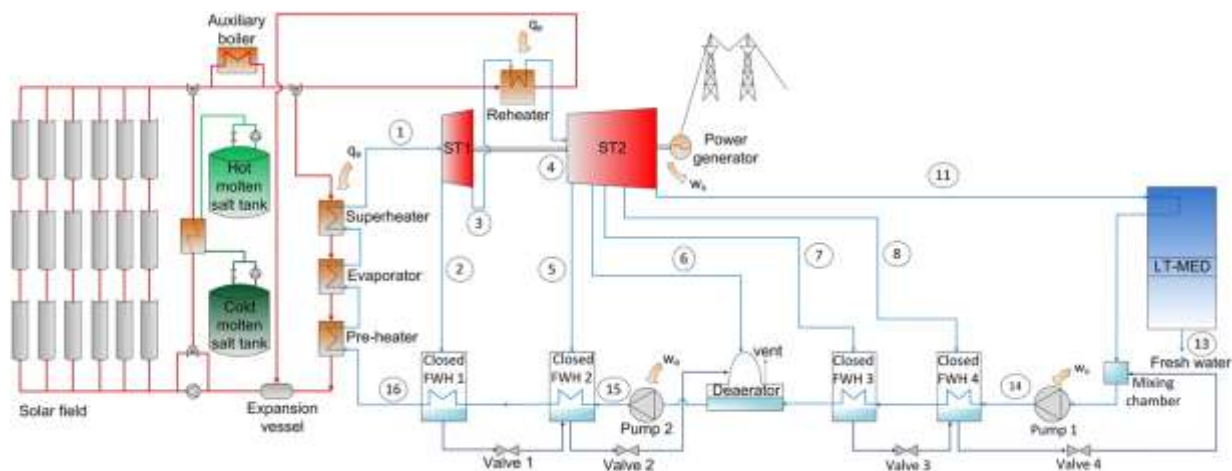


Figure 21. Integration scheme for a low temperature MED plant powered by parabolic troughs in a co-generation scheme [81].

It is also possible to consider a more flexible configuration that enables the decoupling of the water and electricity productions. Such configuration scheme considers the use of an additional

condenser, connected in parallel with the MED system, able to condense the steam exiting the low pressure turbine when the MED system is not operating. It is presented in Figure 22.

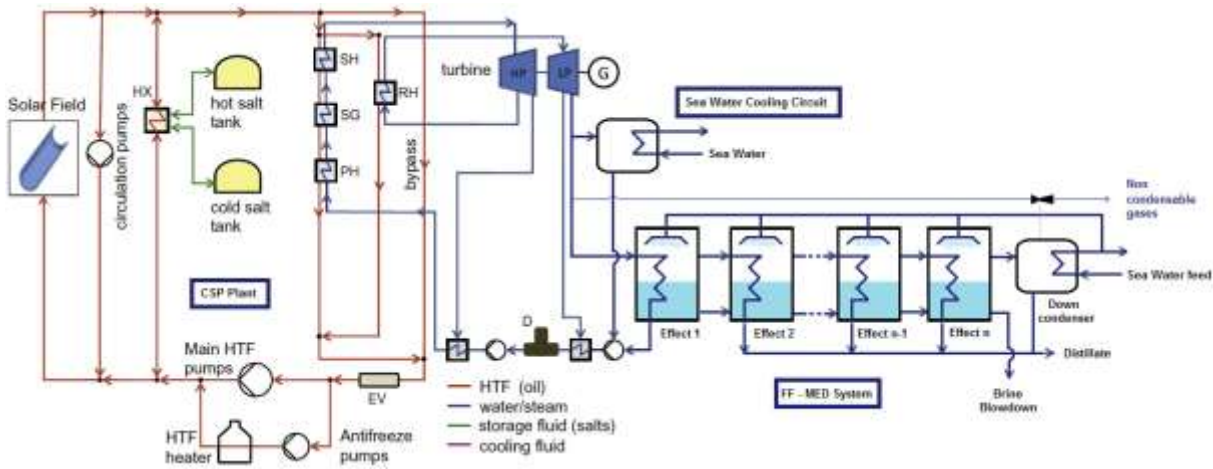


Figure 22. Integration scheme for a low temperature MED plant powered by parabolic troughs in a co-generation scheme including an extra condenser enabling the decoupling of electricity and water production [77].

MED systems can be combined with heat input between stages from several sources, including mechanical (MVC) or thermal vapour compression (TVC) ones. TVC-MED systems may have thermal performance ratios up to 17, while the combination of MED with a heat-absorption heat pump can reach a ratio of 21 [76]. TVC-MED systems use high pressure steam extracted from the low pressure turbine (see Figure 23). They have heat requirements similar to MSF, although presenting lower specific electric power requirements: between 1 to 1.5 kWh/m³ of clean water produced [79].

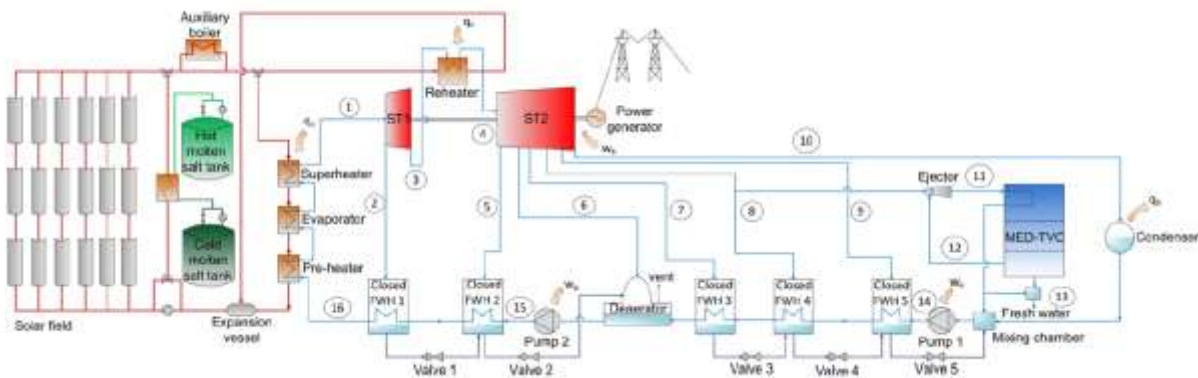


Figure 23. Integration scheme for a TVC- MED plant powered by parabolic troughs in a co-generation scheme [81].

Membrane processes use pressure to force water molecules through thin selective membranes. There are different types of membranes available with different characteristics. They differ in thickness, mechanical strength, pressurization capacity, working life, pH stability, and selectivity and efficiency in removing solutes [93]. Some are used for pre-treatments, like micro and ultra-filtration with larger pores, which help reducing processes' loads, as reverse osmosis (RO) ones that however have more restrictive membranes. The RO process uses high-pressure

water pumps to force saltwater against selective membranes. Other membrane processes use other techniques, for instance membrane distillation that only allows vapour to flow across hydrophobic membranes. However, RO clearly dominates the membrane desalination market accounting for 65% of the total installed desalination capacity worldwide [78]. To power the RO units, 4-7 kWh_e of electricity are required to produce every cubic meter of distilled water, depending on the plant size and the energy recovery systems used [82]. Since RO plants only consume electricity from CSP plants, their integration is straight-forward and a generic schematic diagram of a CSP-RO system can be seen in Figure 24.

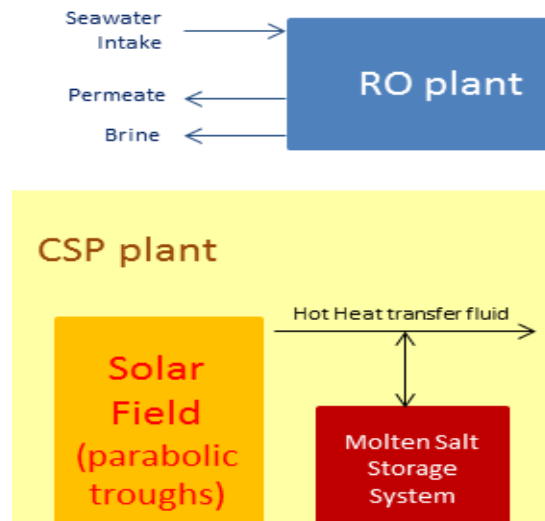


Figure 24. Generic schematic diagram of a CSP-RO system [83].

It is also possible to consider hybrid systems containing both thermal and membrane desalination processes. This combination is quite suitable for improving the matching requirements between water and power. A combination of desalination units that use both thermal energy (MSF or MED) and electricity (RO) can reduce the overall energy requirements and operating costs for water production and electricity generation [94].

3.4.4. Sterilization

Solar sterilization could help reducing diseases, which are in an amount of 80% caused by water quality, in developing countries. A simple device was presented by Hamed and Ahmad in 1997 based on the typical black box solar cooking system and could provide 15 litres per day, which represents half of the water needs for a family of four-six members. Moreover the minimum temperature to be reached to sterilize water was demonstrated to be 65°C without boiling need.

Within the applications of solar thermal energy, according to Hans Schweiger [17] and Kalogirou [35], the sterilization process demand is for different temperature ranges: dairy (120°C -180°C), canned food (110°C-120°C), beverages (60°C-80°C), flours and by-products (60°C-80°C). Sterilization is one of the most important industrial processes using heat at a mean temperature level [35]. Sterilization is used mainly for food processes in industry.

In the milk industry, thermal energy can be used for pasteurization (60–85°C) and for sterilization (130–150°C according to Kalogirou [35] and 110–135°C according to Hobeikaa et al.). In food preservation industries, the sterilization (vegetables, fish and meat) with hot water or direct steam, processes were identified where solar thermal energy could be used. In the fruit and vegetables industry, the temperature demand range are 120–125°C.

3.4.5. Waste Processing

Refused Derived Fuel

Refuse-derived fuel (RDF) is a solid fuel obtained from non-hazardous waste (mainly municipal solid waste) after a mechanical biological treatment (MBT). The waste input is treated and subjected to several mechanical sorting processes. One of the outputs of the MBT is the RDF (other outputs being recyclable materials, organic waste and rejected waste to be buried in landfills). RDF receives the designation of solid recovered fuel (SRF) when its production follows the requirements defined by EN15359 standard [92].

RDF is used as substitute fuel in cement kilns, coal-fired power plants, lime kilns, industrial boilers and CHP. However, the use of RDF as alternative fuel is limited by its humidity level (typically around 40 to 50%). Thermal drying is used in order to reduce the RDF humidity level (to values around 10%), increasing its low heating value and decreasing its weight (which is important to reduce costs of RDF transportation).

In order to achieve the required humidity levels, a drying step is included in the RDF production line. Usually hot air is used to dry the waste within rotating drums or belt dryers. In order to avoid melting of RDF plastic contents and potential ignition of the fuel, the air maximum temperature is within the range of 80 to 100°C. For a particular plant, specific consumption of energy for the drying process amounts to 1 390 MJ per ton of input material, representing the entire fuel consumption of a plant besides fuel consumed by forklift cars [91].

It is possible to conceive the use of solar thermal energy supplied by CST systems either in co-generation or in dedicated heat production schemes. In the first case the drying air could be heated by steam extracted from a back-pressure turbine powered by the solar field. This scheme would allow the use of the generated electricity to power the mechanical systems used in the MBT, besides the supply of thermal energy to the hot air used in the drying process, leading to a decrease of the conventional energy needs of the municipal solid waste treatment plant. In the second case the solar field would be dedicated to the production of hot heat transfer fluid that would be used in a liquid-air heat exchanger to heat the air used in the drying process. This case would not address the plant's power necessities, but would require a lower temperature level enabling the use of cheaper collectors, with low concentration ratios and a simplified installation, leading to low CAPEX and OPEX costs.

An estimated market outlook for the use of SRF in the EU27 by 2020 has a total of 24 to 43 Mt per year, 20 to 23% used in cement kilns, 17 to 19% used in coal-fired power plants and 58 to 63% in CHP plants [92]. This would represent a potential thermal market in excess of 9.3 TWh per year.

Sewage sludge treatment

The waste water treatment process produces waste activated sludge that need further processing, being one of the most significant challenges in wastewater management [84]. Several options are available to process the sludge (figure 25), some of which use thermal energy.

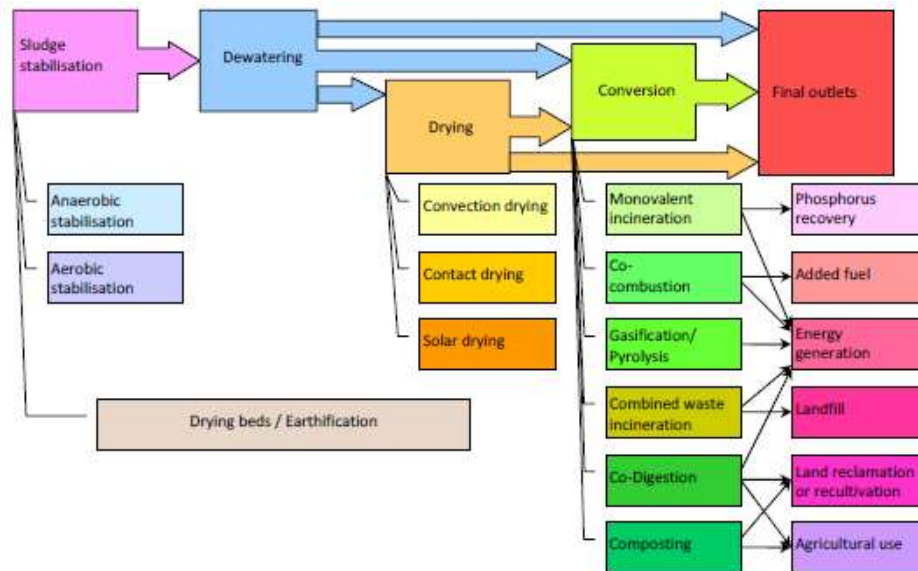


Figure 25. Overview of possible options for wastewater sludge treatment and disposal [86].

Thermal energy is used in sludge stabilisation processes [84,85] such as:

- sludge pre-treatment: sequence of processes to improve dewaterability of sludges, involving heating the sludge at temperatures ranging 60 to 200°C for time periods between 15 minutes to 5 hours, such as thermochemical pre-treatment and thermal hydrolysis;
- sludge pasteurization: sludge heating achieving 70°C for at least 20 minutes or 55°C for at least 4 hours;
- sludge digestion: sludge maintained for several days at minimum temperatures of 35°C (mesophilic anaerobic digestion), 55°C (thermophilic aerobic digestion) and 40°C (composting). It should be noted that some of these processes are exothermal thus producing part of the required heat.

Sludge drying appears as an interesting option, after the mechanical dewatering step, since it recovers more water, reducing the amount of sludge to be handled, facilitating its transportation and storage, as well as enhancing its stabilisation and hygienic safety and providing for an increase of the sludge calorific value, thus enabling its use as a secondary fuel. In fact, it is possible to economically dry wastewater sludge when there is heat available from other processes or where solar energy can be used and the dry sludge can be sold as a secondary fuel (for power plants, cement kilns, incineration for phosphorus recovery, etc.) [86].

Several drying processes are currently used such as contact drying, convection drying and direct solar drying. The drying of wastewater sludge from 25 to 90% of dry solid content (DS)

consumes approximately 70 to 80 kWh per kg of evaporated water, when using contact and convection drying techniques. Table 10 presents different drying systems for wastewater sludge whose heat source can be supplied by CST technologies.

Table 10. Technical characteristics of different drying systems for wastewater sludge[86].

Applied technology	Heating medium	DS sludge input [%]	DS sludge output [%]	Process temperature [°C]	Electric energy [Wh/kg H ₂ O]	Thermal energy [kJ/kg H ₂ O]
Rotary kiln (direct drying)	Air	22.5	90	100-130	63	4 250
Rotary kiln (indirect drying)	Saturated steam	30	95	95-130	50	3 060
Direct/indirect drying belt	Air Thermal oil	25	95	100-140	70	3 300
Fluidized bed dryer	Thermal oil	20	95	85-115	110	2 500
Linear thin film drying	Thermal oil	25	90	115	70	3 000
Rotadisc dryer	Saturated steam	27.5	95	115-120	125	2 900
Mobile disc dryer	Thermal oil Saturated steam	25	90	110-120	87	2 900
Mobile drum drying	Air	25	92.5	120	112	3 000
Mobile dryer	Air	20	95	110-130	31	3 560

3.4.6. Applications in the cork processing industry

As previously mentioned, different heat processes are required for specific industrial applications.

As an example, industrial heat processes are used in the cork industry. It is well known that cork is a natural product obtained from the outer bark of the cork oak tree (*Quercus suber*). It is native from the Mediterranean area, where most of its cultivation and industrial processing is located. Cork is used in a wide range of applications such as: stoppers for alcoholic beverages; thermal, acoustic and vibratory insulation; decoration and furniture; clothing; automotive industry; aeronautic industry; chemical and pharmaceutical industry. The industrial processing of cork presents a wide range of processes some of which require heat at medium and high temperatures. The most common thermal processes in the cork industry are:

- cork boiling: set of boiling stages where cork is placed in boilers with water heated to at least 100°C. A first boiling is performed for at least one hour and a second boiling usually occurs taking at least half an hour;
- cork drying: for some applications granulated cork is mixed with synthetic resins, and is submitted to a drying step where the mixture is placed in drying kilns where it is dried using air at temperatures around 130 to 150°C;
- expanded cork agglomerate production: its production involves a step where granules are placed in autoclaves where they undergo light compression and steam is injected at more than 300°C, usually between 17 to 30 minutes.

4. COGENERATION (POWER CYCLE)

4.1. INTRODUCTION TO COGENERATION

Cogeneration is a highly efficient way to produce electricity and thermal energy simultaneously. It is based on the fact that in order to satisfy a specific demand of electrical energy, different processes with relatively low efficiency are combined to transform different form of energy into electricity. If the need of energy is relatively small (< 50 kW) [11], the term used for this specific dimension is "micro-cogeneration".

The overall efficiency of the cogeneration system can be improved if the thermal energy normally wasted during the energy transformation process is used for other useful applications or processes (thermal desalination, refrigeration systems, domestic heat water, industrial applications, etc.). In addition, the implementation of cogeneration system is attractive because the energy produced, converted in electricity and used on site, avoids the investment and maintenance cost of transmission lines for grid distribution of electric energy.

Cogeneration is a highly efficient way to produce electricity and useful thermal energy simultaneously. It's based on the fact that many processes used to transform some form of energy into electricity have a relatively low efficiency due to the waste of heat generated in the conversion process. This efficiency can be improved if thermal energy, normally wasted by those devices, can be utilized for other useful application.

Two examples of simultaneous use of electricity and thermal energy are shown in the figures 26 and 27 below:

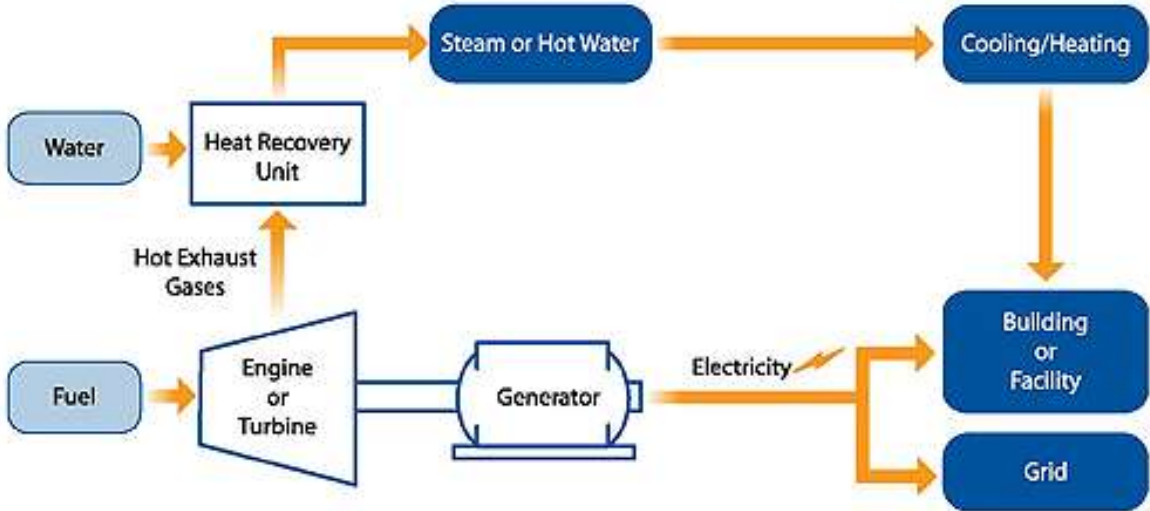


Figure 26. Example of cogeneration valid for systems like gas turbines (Brayton cycle), Internal combustion engines, etc. [43,44]

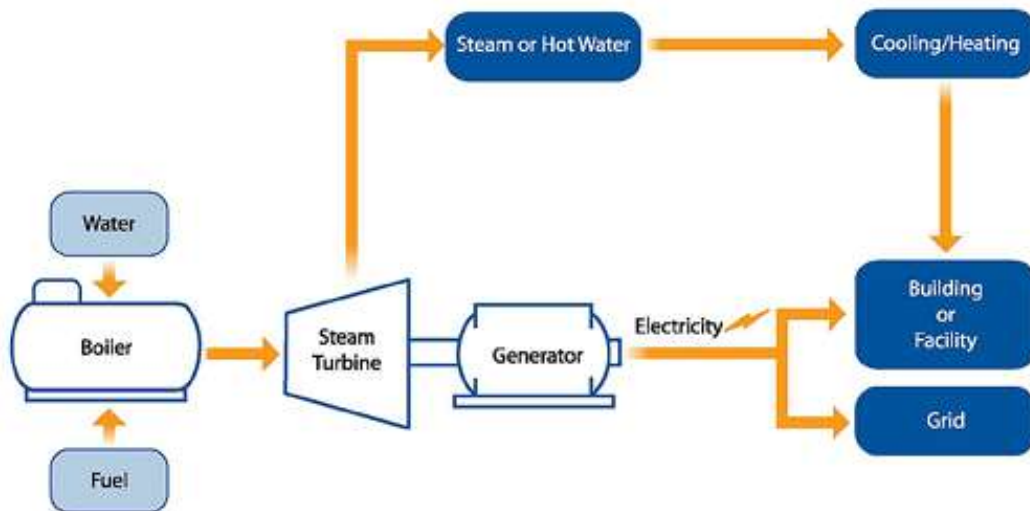


Figure 27. Cogeneration scheme representative of a Steam turbine (Rankine cycle). [43,44]

Although there are also other means to implement cogeneration (see Figure 28), the more obvious candidates to provide electricity and thermal energy at the same time are mainly thermal engines, such hot air engines (Stirling), Rankine cycles (with water or organic fluids), Brayton cycles, Internal combustion engines (Otto and Diesel cycles).

The main thermodynamic cycles relevant for conversion of heat to electricity are the following:

Rankine cycle plant (RC): This cycle is one of the most important way to transform thermal energy into power; main examples being nuclear and coal-fired power plants. The steam Rankine cycle is the fundamental operating cycle of all power plants where an operating fluid is continuously evaporated and condensed.

Steam engine (SE): The most familiar steam Rankine engine is the steam engine in which water is boiled by an external heat source, expands exerting pressure on a piston (instead of a turbine rotor) and hence producing useful work. This cycle has a great importance from a historical point of view. Nowadays it has been supplanted by Rankine cycle with a turbine (due to higher efficiency), but some applications still exists.

Organic Rankine Cycle plant (ORC): An organic Rankine cycle machine is similar to a conventional steam Rankine cycle energy conversion system, but uses an organic fluid, characterized by higher molecular mass and a lower ebullition/critical temperature than water.

Kalina cycle plant (KA): The Kalina cycle resembles the conventional Rankine cycle. The major difference being that a solution of two fluids with different boiling points is used as a working fluid. Thus, in Kalina cycle heat addition and heat rejection happen at varying temperature even during phase change, since the fluid is a mixture.

Gas turbine plant (GT) and Micro gas turbine (MGT): The Brayton cycle is the air standard model for gas turbine engines. Gas turbines were mainly used as internal combustion engines. However there is no conceptual difference to use such systems with an external heat source. From a technological point of view an external heat exchanger must be added to transfer heat from the source to the fluid, after compression. To be rigorous we should add the words “externally fired” to gas turbine in the name of the cycle. The ideal cycle is described by the

following (ideal) steps: (isentropic) compression, (isobaric) heat transfer in the heater, (isentropic) expansion through turbine, (isobaric) heat exchange in the cooler.

Closed cycle gas turbine plant (CICGT): In a closed cycle gas turbine, the gas turbine exhaust is recycled to the compressor after being cooled and thereby forms a closed working fluid circuit.

Ericsson engine (ER): If isothermal compression and expansion are used, in place of isentropic processes in the Brayton cycle, the Ericsson cycle is obtained. The corresponding engine is based on a reciprocating piston-cylinder machine. The cycle can be divided in the following (ideal) steps: (isothermal) compression, (isobaric) heating, (isothermal) expansion, (isobaric) cooling.

Stirling engine (ST): Stirling engine is also based on a reciprocating piston-cylinder machine. This heat engine operates by cyclic compression and expansion of air (or other gas). The cycle can be divided in the following (ideal) steps: (isothermal) compression in the compression stroke, (isochoric) heat transfer in the expansion stroke, (isothermal) expansion in power stroke, (isochoric) rejection of heat to the surroundings.

Thermogenerator (TE): The concept consists in a thermoelectric generator device, able to convert a portion of the heat flux traveling through the device directly into direct current (DC) electrical power. The general principle behind this direct energy conversion is the same as a thermocouple, but the materials used are semiconductors with improved thermoelectric performances as compared to metals. In fact, these devices are composed of units consisting of many 'thermocouples' arranged electrically in series and thermally in parallel to produce DC power at a reasonable voltage.

Thermoacoustic generator (TA): A thermoacoustic generator consists of a thermoacoustic device using a temperature difference to produce high-amplitude sound waves. The acoustic power can be used directly to generate electricity via a linear alternator or other electroacoustic power transducer. One of the main advantages is the absence of moving parts. Only few prototypes were developed to generate electricity. Additional references of such systems exist for acoustic refrigerators or pulse-tube refrigerators to provide heat-driven refrigeration.

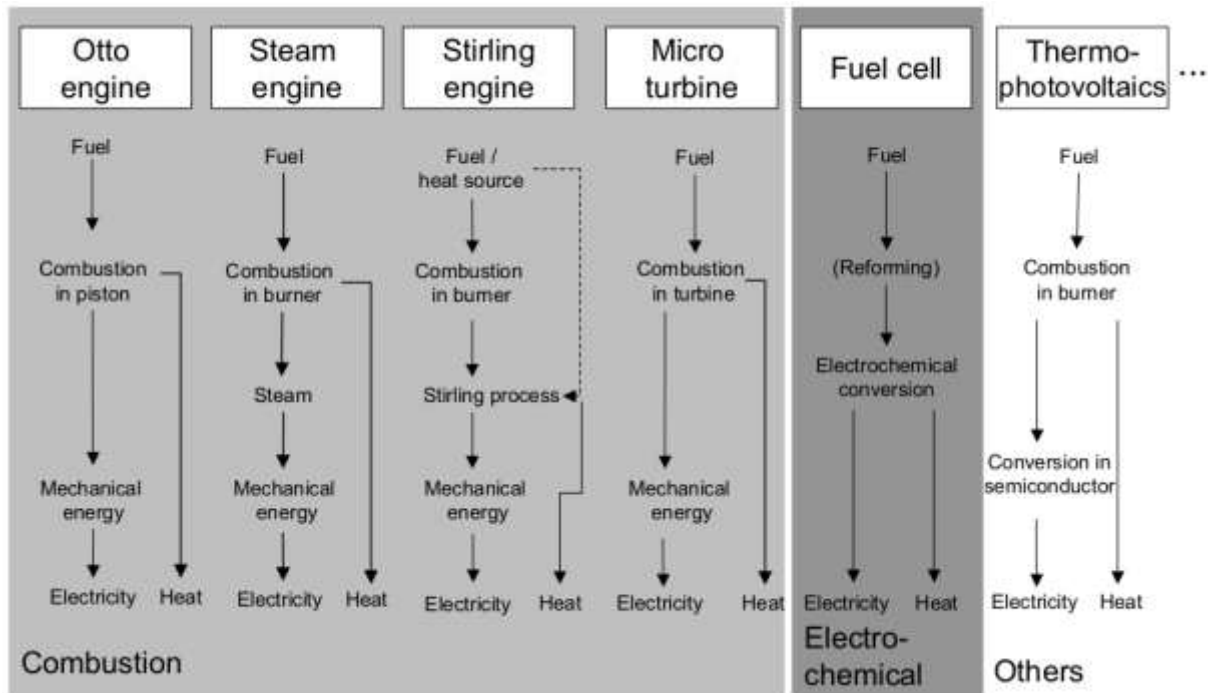


Figure 28. Cogeneration types [29].

This is true because thermal engines are limited by an efficiency that is below 30 % in most of practical applications (only very big engines can reach 50 % of thermal efficiency). Thermal engines need, at least, a heat source at high temperature and a heat sink at low temperature to work. Coupling a thermal application to the heat sink it's said to be a cogeneration. This thermal energy can be used for feeding processes like thermal desalination, refrigeration systems, domestic heat water, industrial applications, etc.

Another attractive implication in the use of cogeneration is that the energy produced can be consumed on site (without the use of transmission lines for the distribution of electric energy). If the need of energy is relatively small (< 50 kW, according to [11]), the term used is "micro-cogeneration".

Figure 29 below shows a schema where a micro-cogeneration system can be used to supply a large part of the energy needs of a house:

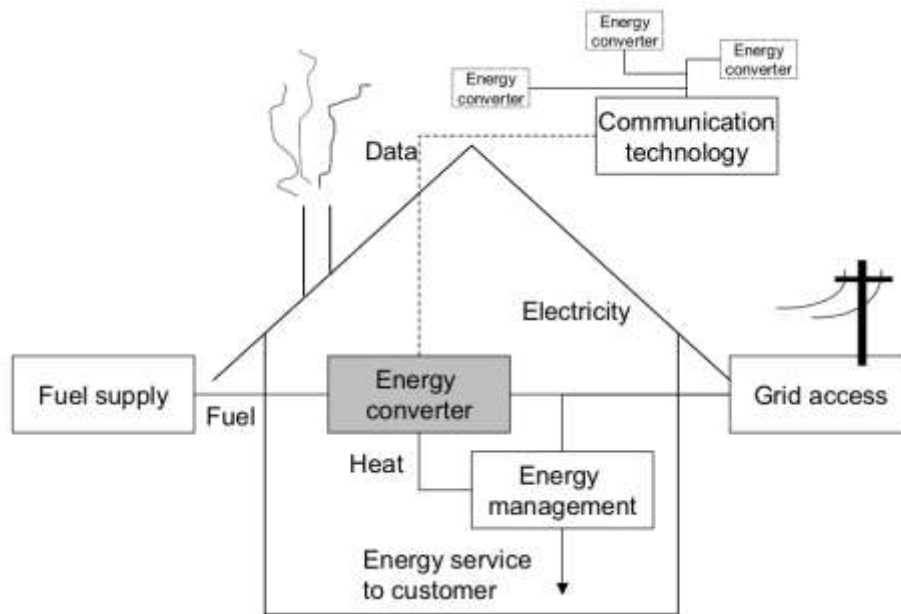


Figure 29. Example of microgeneration system [29].

Due to the possibility of working with thermal energy of relatively low temperature, the ORC (Organic Rankine Cycle) is a promising mean to exploit heat sources like heat from stationary solar collectors like FPC (Flat-Plate Collector) or CPC (Compound Parabolic Collector) from 100 °C to around 150 °C, or ETC-CPC (Evacuated Tube Collector-Compound Parabolic Collector) around 150 °C to 180 °C, or by tracking collectors like PTC (Parabolic Trough Collector) or Fresnel ones, at temperatures over 200 °C, etc.

Concentrating Solar Power (CSP) systems can be implemented with a variety of collectors such as the PTC, the LFC, the solar dish or the solar tower. Nowadays, most part of these systems are designed to provide thermal energy to a steam turbine connected to a cycle power block. This technology requires a minimum power of a few MWe in order to be competitive and involves high collector temperatures. Particularly in the case of small-scale systems, an organic Rankine cycle (ORC) system could be considered. For these kind of applications, at distributed level there are a number of advantages over the steam cycle. These include a lower working temperature, the absence of droplets during the expansion, the low maintenance requirements and the simplicity (fewer components) (S. Quoilin, 2011). Those strengths make the ORC technology interesting and therefore it deserves to be included within this overview. Despite medium-scale solar ORCs are already available on the market, work remains to be done for small-scale units (a few kWe), especially to reduce the specific investment costs and to control the system in order to avoid the need of an on-site operator. Few experimental studies are available from literature. (Kane, 2003) studied the coupling of linear Fresnel collectors with a cascaded 9 kWe ORC, using R123 and R134a as working fluids. An overall efficiency (solar to electricity) of 7.74% was obtained, with a collector efficiency of 57%. (Manolakos, 2007) studied a 2-kWe low-temperature solar ORC with R134a as working fluid and evacuated tube collectors: an overall efficiency below 4% was obtained. (Wang, 2010) studied a 1.6 kWe solar ORC using a rolling piston expander. An overall efficiency of 4.2% was obtained with evacuated tube collectors and 3.2% with flat-plate collectors. The difference in terms of efficiency was explained by lower collector efficiency (71% for the evacuated tube vs. 55% for

the plate technology) and lower collection temperature. As it's easy to understand a wide room for research and development is available on this field with many challenges still open.

The simplest regenerative Rankine machine is shown in Figure 30, together with a Ts diagram of a typical cycle:

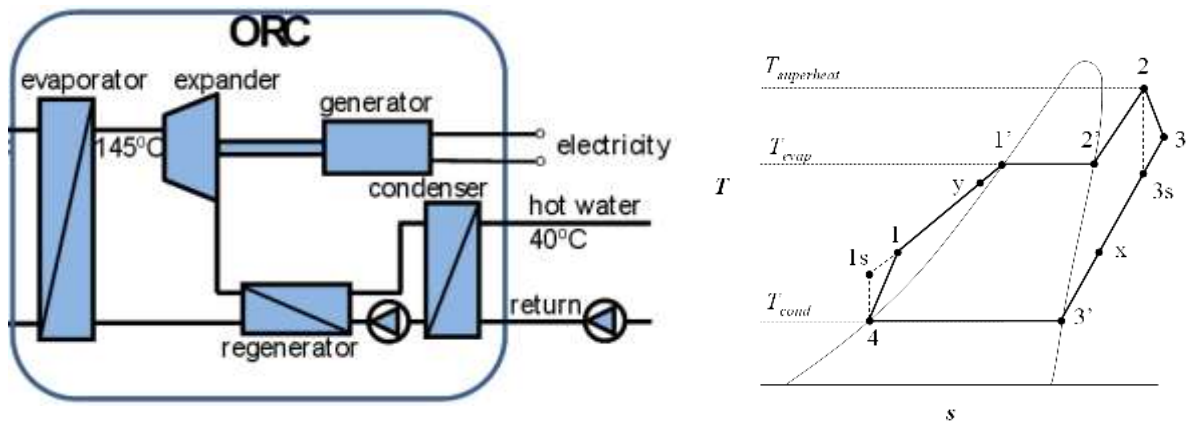


Figure 30. RORC system (a) and its typical Ts diagram (b) [32].

It comprises a pump and an expander (both of them can be either centrifugal or positive displacer machines), and three heat exchangers (an evaporator, a condenser and a regenerator).

The description of the thermodynamic cycle can be done starting on point 4 of the Figure 32b. It is desirable for this point to be in the liquid saturated line (it could be situated in the subcooled region as well). Utilizing a pump (generally driven by an electric motor) the pressure of the fluid is raised from a low value in the condenser to a higher value in the evaporator (point 1). Then the liquid passes through a regenerator to receive the heat given from the superheated vapour of the other part of the cycle going from 'point 1' to 'point y'. After that, the preheated fluid passes through the evaporator to receive more heat from an exterior source (as from a solar field, for example). At this stage the fluid passes from the subcooled region (point 1) to the overheated (or saturated) vapour region (point 2). Then the fluid expands from 'point 2' to 'point 3' into the expander, which runs an electric generator. The still superheated fluid then passes through the regenerator to transfer heat to the subcooled liquid. From 'point x' it enters the condenser to transfer more heat to the environment or to another application (cogeneration).

The condenser temperature (T_{cond}) determines if the utilization of a cogeneration device is possible or not. Due to the fact that the Rankine is a thermodynamic cycle, it is limited by the Carnot efficiency.

$$\eta_{\text{Carnot}} = \frac{T_{\text{max}} - T_{\text{min}}}{T_{\text{max}}}$$

This shows how it is affected adversely if the minimum temperature (T_{cond} in this case) is raised. It is necessary to study carefully possible combinations of ORC and cogeneration devices that allow to increase the global efficiency. To consider a cogeneration device linked to the heat transferred from the condenser of an ORC means always to introduce a penalization in the efficiency of the thermodynamic cycle.

4.2. INTRODUCTION TO SMALL SOLAR PLANTS

4.2.1. Case study: REELCOOP project

It was defined within REELCOOP project [32] a system which comprises a solar field, a storage medium, a biomass boiler and the RORC itself. The scheme of such a system is shown below (Figure 31):

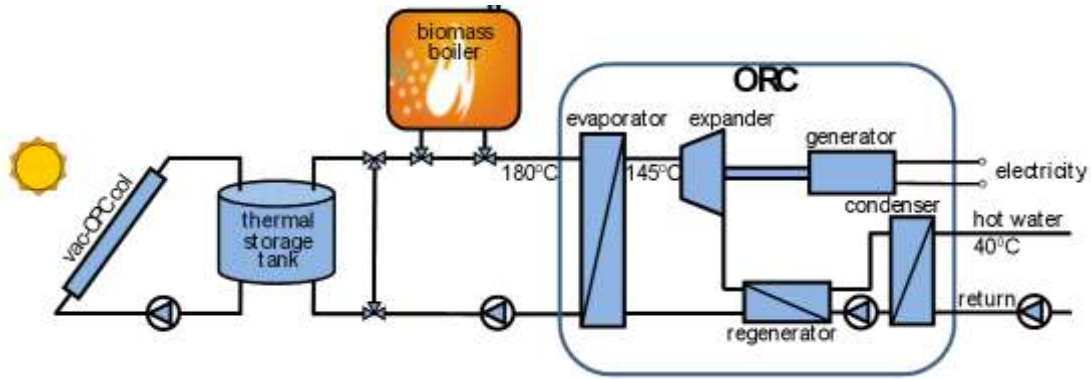


Figure 31. RORC system

The model was implemented entirely in Python. The characteristics of the different components are collected in the following table 11:

Table 11. Definition of the inputs for each component

Components		Inputs
CPC collector with evacuated tubes	Efficiency curve parameters: $\eta_0 = 0.623$; $a_1 = 0.59 \frac{W}{m^2K}$; $a_2 = 0.004 \frac{W}{m^2K^2}$	
	Flow rate = $0.557 \frac{kg}{s}$	
	Solar field area = $145.92 m^2$	
	Collector tilt: adjusted seasonally (fourth per year). Tilt = $51^\circ C$, $28^\circ C$, $8^\circ C$ and $30^\circ C$, depending on period	
	Collector azimuth = 0°	
	Fluid specific heat = $2620 \frac{J}{kgC}$ (oil THERMOL 5HT)	
Thermal storage	IAM data: file created through the values from Table X-IAM for the global irradiation (stationary model)	
	Tank volume = $8 m^3$	
	Not stratified	
	Tank losses: negligible	
	Cold side temperature (from Evaporator) = $140^\circ C$	
Boiler	Cold side flow rate (from Evaporator) = $0.379 kg/s$	
	Rated capacity = $80 kW$ Set point temperature = $180^\circ C$	
RORC	Evaporator	Useful heat $39.76 kW$
		Outlet temperature = $145^\circ C$ Superheating = $5^\circ C$
	Regenerator	Efficiency $\epsilon_{reg} = 0.82$
	Condenser	Condenser temperature = $45^\circ C$ or $90^\circ C$
		Subcooling = $2^\circ C$
	Expander	Efficiency $\eta_{exp} = 0.75$
Generator	Efficiency $\eta_{generator} = 0.95$	
	Net electrical power = $6 kW$	

Some of the inputs originally used for the REELCOOP project [32] have been modified here to show the different behaviour of an ORC system with and without a cogeneration application attached to it. For that reason the condenser temperature has been raised from the original $45^\circ C$

initially considered, to a value of $T_{\text{cond}} = 90 \text{ }^\circ\text{C}$. The last one is more compatible with a cogeneration device like an absorption system, for example.

Benguerir (Morocco) local climatic data was used in the model.

As shown in the Table 11, the RORC is conceived in order to give 6 kW of net electric power. Because the heat flow rate at the evaporator is about 40 kW at the design point for $T_{\text{cond}} = 45 \text{ }^\circ\text{C}$ and about 77 kW for $T_{\text{cond}} = 90 \text{ }^\circ\text{C}$ (lower than the value of 80 kW of the rated capacity of the boiler, in any event) the RORC can be run at the design point steadily (independently of the climatic conditions). The results and Ts diagrams representation of the cycles are shown below in Figure 32:

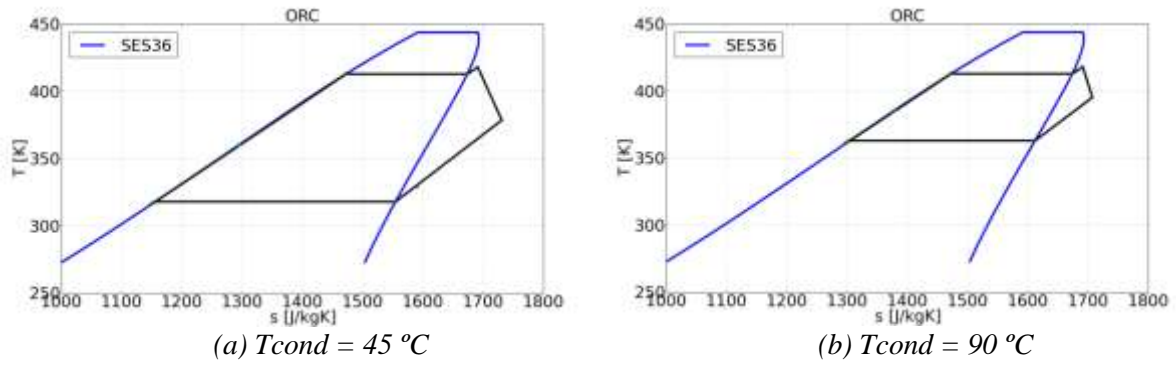


Figure 32. Ts diagram of the RORC (a) $T_{\text{cond}} = 45 \text{ }^\circ\text{C}$.(b) $T_{\text{cond}} = 90 \text{ }^\circ\text{C}$.

Table 12. RORC results for $T_{\text{cond}} = 45 \text{ }^\circ\text{C}$ and $T_{\text{cond}} = 90 \text{ }^\circ\text{C}$

		$T_{\text{cond}} = 45 \text{ }^\circ\text{C}$	$T_{\text{cond}} = 90 \text{ }^\circ\text{C}$
working fluid flowrate \dot{m}_{work} (kg/s)		0.241	0.590
Evaporator	\dot{Q}_{evap} (kW)	39.76	77.36
	\dot{Q}_{liquid} (kW)	18.04	24.03
	$\dot{Q}_{\text{phase change}}$ (kW)	19.98	49.05
	\dot{Q}_{vapour} (kW)	1.74	4.28
Regenerator	\dot{Q}_{reg} (kW)	10.84	16.35
	ϵ_{reg} (%)	0.82	0.82
	$\Delta T_{\text{min reg}}$ ($^\circ\text{C}$)	11.31	6.67
Condenser	\dot{Q}_{cond} (kW)	33.41	70.98
	\dot{Q}_{liquid} (kW)	0.52	1.44
	$\dot{Q}_{\text{phase change}}$ (kW)	30.51	65.95
	\dot{Q}_{vapour} (kW)	2.38	3.59
Expander \dot{W}_{exp} (kW)		6.65	6.98
Pump \dot{W}_{pump} (kW)		0.30	0.60
η_{cycle} (%)		15.97	8.25
Generator \dot{W}_{G} (kW)		6.32	6.63
Pump Motor $\dot{W}_{\text{Pump motor}}$ (kW)		0.32	0.63
$\eta_{\text{elec,NET,ORC}}$ (%)		15.09	7.76

Table 12 shows how doubling the value of the condenser temperature from $T_{\text{cond}} = 45 \text{ }^\circ\text{C}$ to $T_{\text{cond}} = 90 \text{ }^\circ\text{C}$, the value of $\eta_{\text{elec,NET,ORC}}$, defined in the following equation, falls from 15.09 % to 7.76 %, almost half of the initial value.

$$\eta_{\text{elec,NET,ORC}} = \frac{\dot{W}_{\text{G}} - \dot{W}_{\text{Pump motor}}}{\dot{Q}_{\text{evap}}}$$

For the whole system, monthly and annual values of solar radiation incident on the collector surface G_{coll} , useful heat gain on the solar collector fluid $Q_{\text{usef coll}}$, energy supplied by the boiler

Q_{aux} , efficiency of the solar field $\eta_{solar\ field}$, and efficiency of the overall system $\eta_{overall}$, defined below:

$$\eta_{solar\ field} = \frac{Q_{usef\ coll}}{G_{coll}}$$

$$\eta_{overall} = \eta_{solar\ field} \cdot \eta_{elec,NET,ORC}$$

have been represented in the following tables 13 and 14. The operating period considered for the system was 24 hours/day.

Table 13. Monthly and annual performance results for $T_{cond} = 45\ ^\circ C$

Month	G_{coll} (MWh)	$Q_{usef\ coll}$ (MWh)	Q_{aux} (MWh)	f
Jan	27.68	7.59	22.00	0.26
Feb	20.95	5.79	20.92	0.22
Mar	29.21	6.72	22.86	0.23
Apr	30.80	6.96	21.69	0.24
May	33.50	8.14	21.45	0.28
Jun	34.48	8.62	20.01	0.30
Jul	36.10	9.88	19.72	0.33
Aug	33.57	7.64	21.93	0.26
Sep	29.14	7.81	20.81	0.27
Oct	27.77	6.72	22.87	0.23
Nov	26.55	7.66	20.95	0.27
Dec	26.63	6.77	22.83	0.23
Annual	356.37	90.30	258.02	0.26

Table 14. Monthly and annual performance results for $T_{cond} = 90\ ^\circ C$.

Month	G_{coll} (MWh)	$Q_{usef\ coll}$ (MWh)	Q_{aux} (MWh)	f
Jan	27.68	7.84	49.72	0.14
Feb	20.95	5.96	46.02	0.11
Mar	29.21	6.93	50.62	0.12
Apr	30.80	7.19	48.51	0.13
May	33.50	8.42	49.13	0.15
Jun	34.48	8.91	46.79	0.16
Jul	36.10	10.24	47.31	0.18
Aug	33.57	7.89	49.67	0.14
Sep	29.14	8.09	47.61	0.15
Oct	27.77	6.94	50.61	0.12
Nov	26.55	7.95	47.75	0.14
Dec	26.63	6.98	50.58	0.12
Annual	356.37	93.35	584.31	0.14

The solar fraction f is defined as:

$$f = \frac{Q_{usef\ coll}}{Q_{usef\ coll} + Q_{aux}}$$

Defining an average "solar electrical efficiency" $\eta_{sol,electr}$ as the net electricity divided by auxiliary energy:

$$\eta_{sol,electr} = \frac{W_{\text{electricity NET}}}{Q_{\text{aux}}}$$

The annual 'global electrical efficiency' η_{electr} is defined as the total electrical energy generated during one year, divided by the sum of all annual energy inputs (boiler input energy plus solar incident radiation).

$$\eta_{\text{electr}} = \frac{W_{\text{electricity NET}}}{Q_{\text{aux}} + G_{\text{coll}}}$$

The results of those two defined efficiencies are given in the following tables 15 and 16:

Table 15. Annual boiler input energy ($Q_{\text{boiler annual}}$), annual average solar electrical efficiency ($\eta_{sol,electr}$) and the annual global electrical efficiency (η_{electr}) for $T_{\text{cond}} = 45^{\circ}\text{C}$

$Q_{\text{boiler annual}}$ (MWh)	$\eta_{sol,electr}$	η_{electr}
286.69	0.20	0.08

Table 16. Annual boiler input energy ($Q_{\text{boiler annual}}$), annual average solar electrical efficiency ($\eta_{sol,electr}$) and the annual global electrical efficiency (η_{electr}) for $T_{\text{cond}} = 90^{\circ}\text{C}$

$Q_{\text{boiler annual}}$ (MWh)	$\eta_{sol,electr}$	η_{electr}
649.23	0.09	0.05

As can be seen, η_{overall} is very low in both cases, but this situation changes if $\eta_{\text{cogeneration}}$, defined in equation 5, is considered instead of the previous $\eta_{\text{elec,NET,ORC}}$ in the calculation of η_{overall}

$$\eta_{\text{cogeneration}} = \frac{(\dot{W}_G - \dot{W}_{\text{Pump motor}}) + \dot{Q}_{\text{usefull}}}{\dot{Q}_{\text{evap}}}$$

$$\eta_{\text{overall,COG}} = \eta_{\text{solar field}} \cdot \eta_{\text{cogeneration}}$$

For example, if only half of the \dot{Q}_{cond} could be conceived as useful heat \dot{Q}_{usefull} in a cogeneration application, the global efficiency of the process with $T_{\text{cond}} = 90^{\circ}\text{C}$ would raise from the annual $\eta_{\text{overall}} = 2.04\%$ showed on table 4 to $\eta_{\text{overall,COG}} = 14.1\%$.

This calculus agreed well with the following estimation for an absorption refrigeration system, represented in the following Figure 33. The description of the cycle is given in many publications, for example in Moran et al. [30].

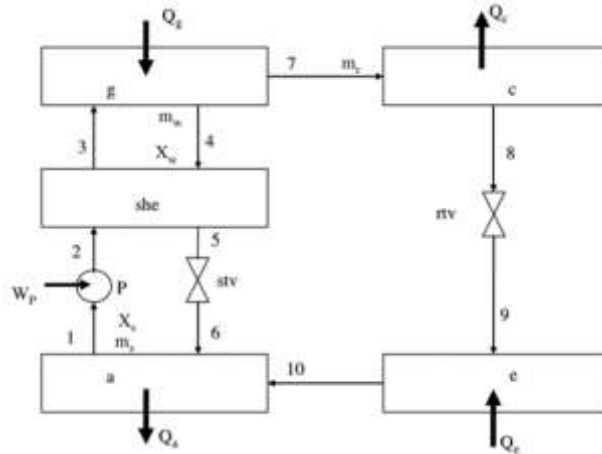


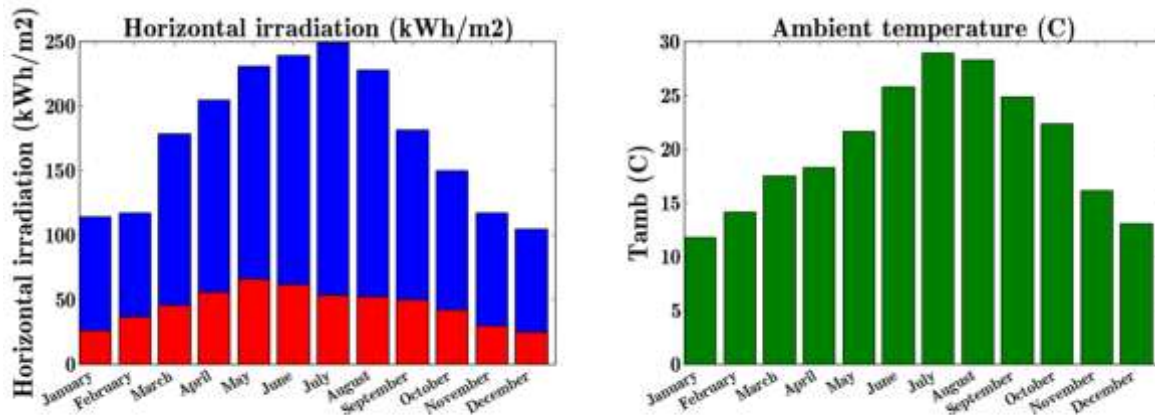
Figure 333. Schematic diagram of a single effect absorption refrigeration system [33].

In Figure 33 *g* is the generator, *she* is the solution heat exchanger, *a* is the absorber, *c* is the condenser and *e* is the evaporator. The definition of COP (coefficient of performance) is given below:

$$COP = \frac{\dot{Q}_e}{\dot{Q}_g + \dot{W}_p} \approx \frac{\dot{Q}_e}{\dot{Q}_g}$$

Where, according to IDAE [8], \dot{Q}_e can be recognized as useful heat for cogeneration. If the power of the pump \dot{W}_p is taken as negligible and \dot{Q}_g has exactly the same value of the heat power given by the ORC condenser \dot{Q}_{cond} , the global efficiency of the process with $T_{cond} = 90^\circ\text{C}$ and a representative $COP = 0.75$ would raise from the annual $\eta_{overall} = 2.04\%$ showed on table 4 to $\eta_{overall,COG} = 20.1\%$.

Below are represented some figures of meteorological data from Benguerir (Figure 34, 35).



(a) Horizontal Irradiation (kWh/m2)

(b) T_{amb} (°C)

Figure 344. Climatic conditions (monthly mean values at Benguerir, Morocco) (a) Horizontal Irradiation (kWh/m2) (b) Ambient Temperature (°C)

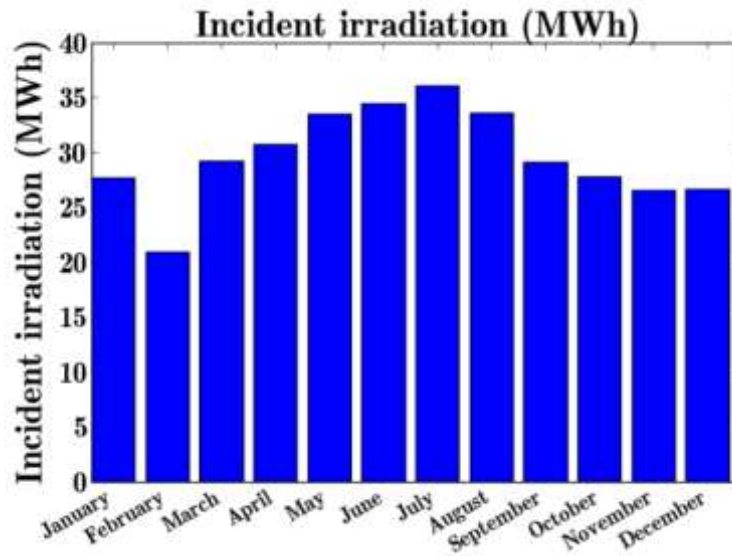
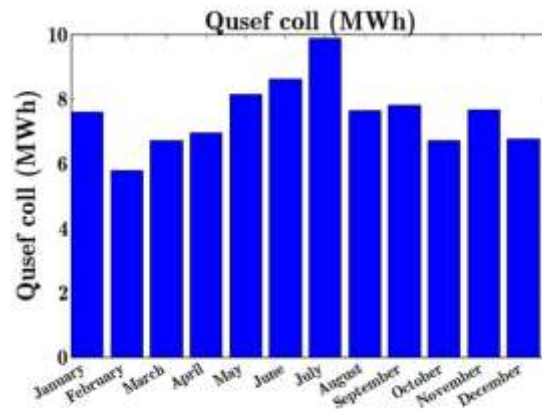
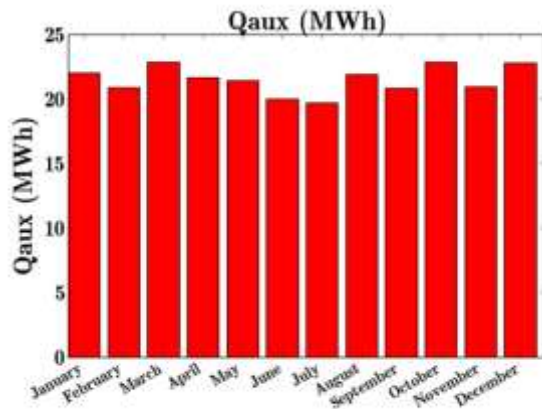


Figure 355. Incident irradiation (monthly mean values) (MWh)

The monthly values of auxiliary heat taken from the boiler Q_{aux} and the useful heat provided by the collectors $Q_{usef\ coll}$ are represented in the following bar diagrams: (Figures)



(a) Q_{aux} (MWh)

(b) Q_{usef} (MWh)

Figure 366. Heat provided to the RORC (monthly mean values) for the case of $T_{cond} = 45$ °C. (a) Auxiliar heat from the boiler Q_{aux} (MWh) (b) Usefull heat provided by the solar field Q_{usef} (MWh)

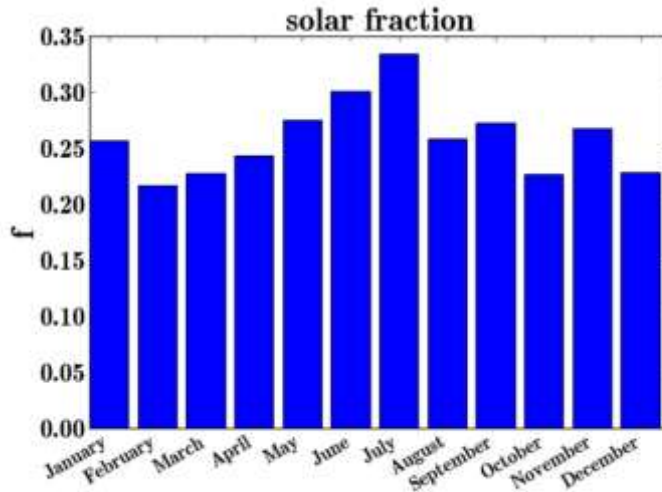
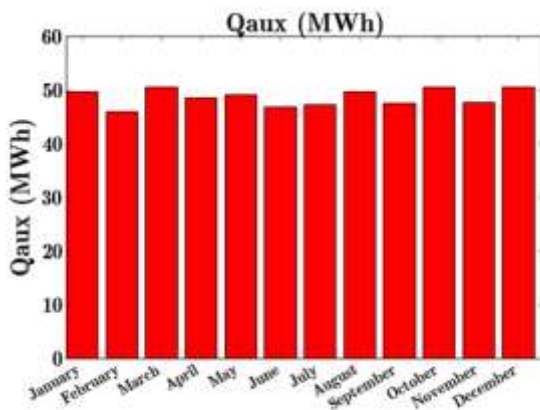
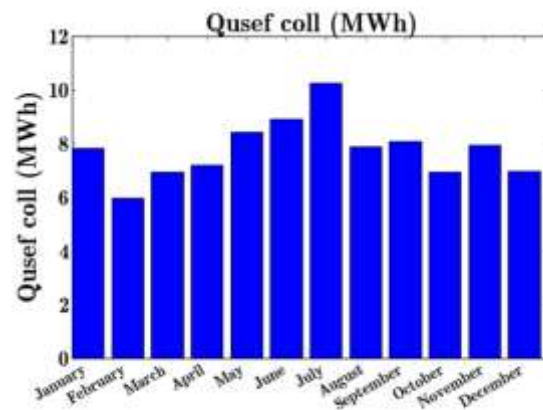


Figure 37. Solar fraction f (monthly mean values) for the case of $T_{cond} = 45\text{ }^{\circ}\text{C}$.



(a) Q_{aux} (MWh)



(b) Q_{usef} (MWh)

Figure 38. Heat provided to the RORC (monthly mean values) for the case of $T_{cond} = 90\text{ }^{\circ}\text{C}$. (a) Auxiliar heat from the boiler Q_{aux} (MWh) (b) Usefull heat provided by the solar field Q_{usef} (MWh)

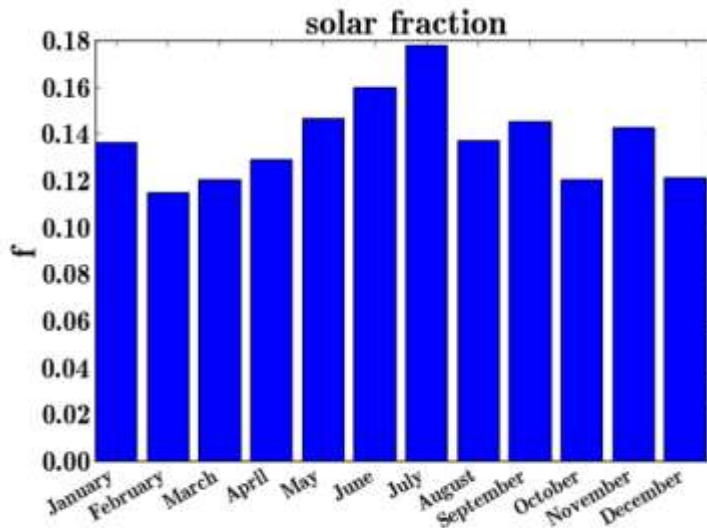


Figure 39. Solar fraction f (monthly mean values) for the case of $T_{cond} = 90\text{ }^{\circ}\text{C}$.

4.2.2. Case study: ORC coupling with storage and absorption systems

This study aims at analysing the coupling of a medium size CSP plant with absorption systems and storage. The input parameters are the size of the various items (solar field, storage, cold power etc.). The location of the plant is assumed to be fixed in the study, and is thus not included in the varying parameters. A special focus will be done on the equipment's performance level and on the cost of energy produced.

The temperature-power diagram shown in Figure 40 is certainly the most useful graph to present the various available technologies. It reflects the reality of existing plants or prototypes. Such map is also such a kind of photography of the market.

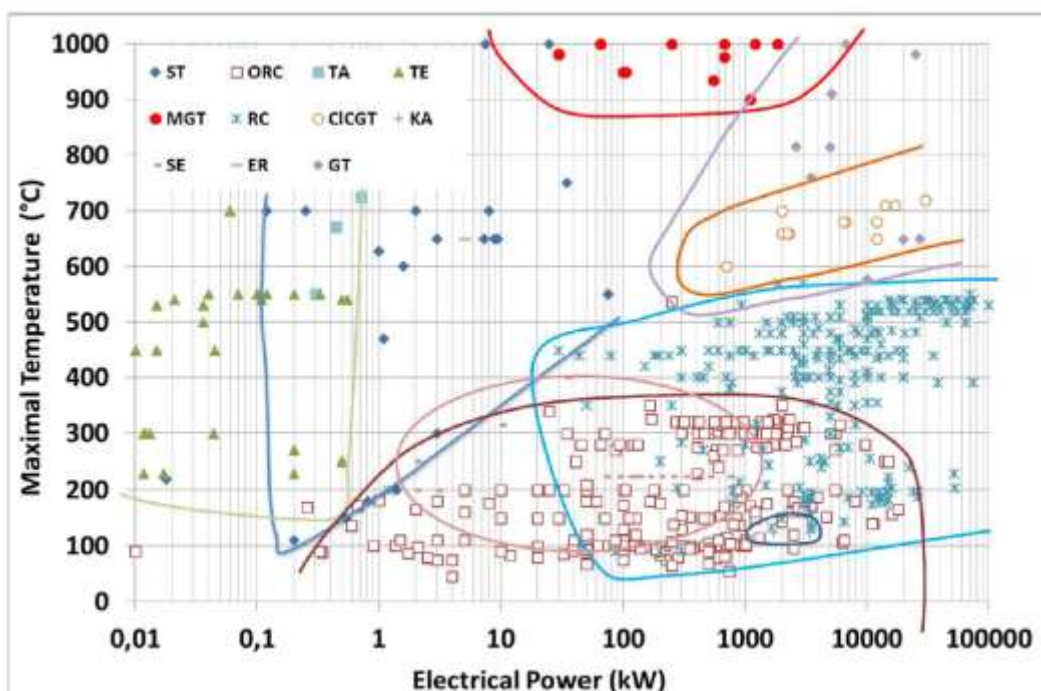


Figure 40. Temperature power diagram for different thermodynamic technologies.

In this second case study, the thermodynamic cycle used is an ORC using R245fa as working fluid.

Presentation of the tool – main hypothesis of the study

CEA is developing a calculation tool in order to simulate medium size CSP plants running an ORC cycle. The technology studied corresponds to the following items:

- Synthetic oil as thermal fluid in the solar field
- Fresnel mirrors
- Organic fluid turbine
- Cooling system upstream the turbine (air cooled heat exchanger)
- Dual thermocline storage system
- Absorption system
- The scheme of the plant given in the following drawing (see Figure 41):

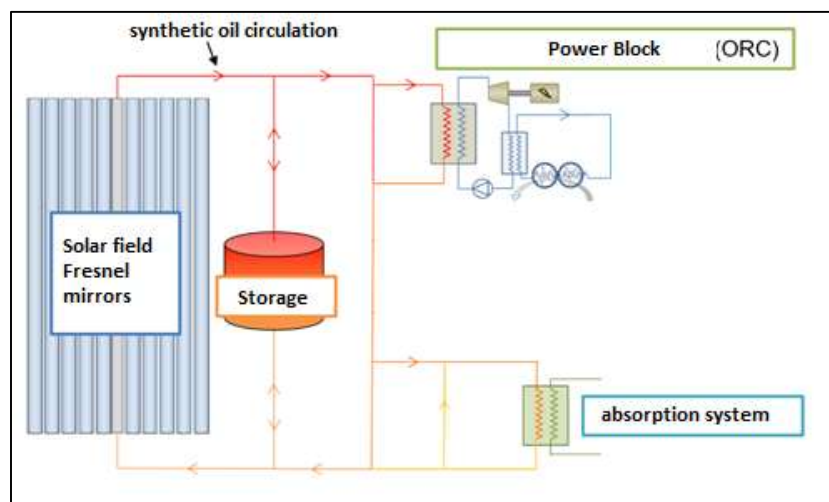


Figure 41. Schematic principle of the technology used in the case study

The basic configuration includes only the solar field and the power block (turbine and cooling system). The user can add any other item among storage, desalination, heat uptake and absorption systems. Desalination and heat uptake are not shown in the drawing above.

The geographical site chosen for the study is in the neighbours of the city of Larache in northern of Morocco. This city is on the sea coast and is 35.2°N latitude and -6.1°W longitude.

On the data used for the calculation, the overall year cumulated DNI leads to 2347 kWh/m²/yr. Figure 42 shows the evolution of the monthly cumulated DNI over the year.

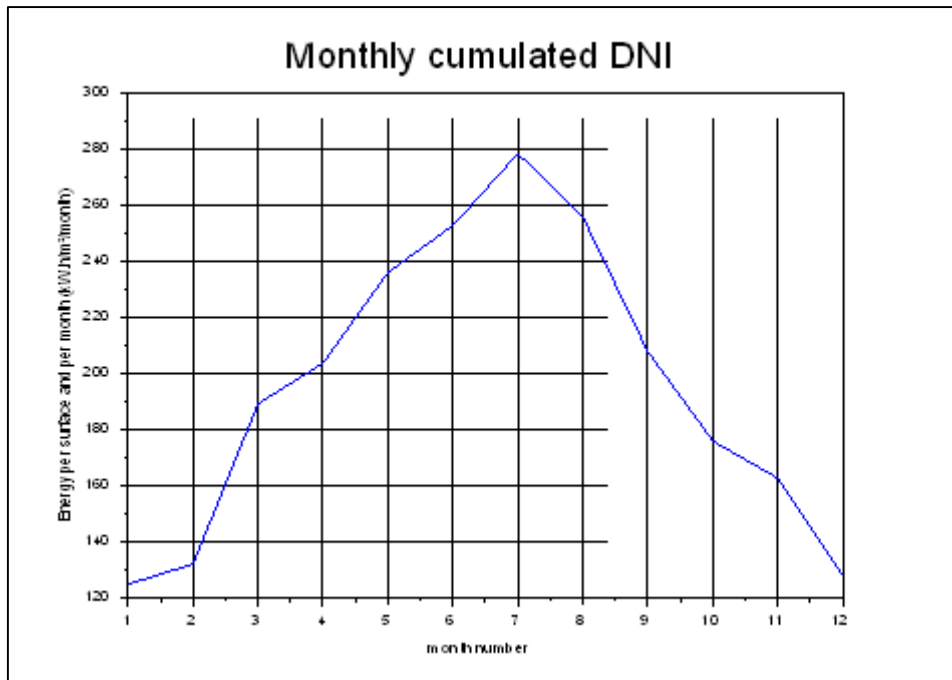


Figure 42. Monthly cumulated DNI in Larache (Morocco).

The reference plant corresponds to the following parameters:

- Solar multiple: 2
- Storage volume: 2500 m³
- ORC turbine nominal power: 5 MW_e

The flow rate in the solar field is adjusted in order to reach 300°C at the receiver outlet. The product of the mirrors total surface by the annual average DNI leads to an amount of energy of 293 GWh/yr.

With these characteristics, the global outputs of the plant are:

- Annual net electrical production: around 17.9 GWh_e
- Annual thermal energy stored: 34.1 GWh_{th}
- Annual thermal energy non valued: 10 GWh_{th}

Figure 43 shows the monthly net electrical production and the stored and solar thermal energy dumped along the year:

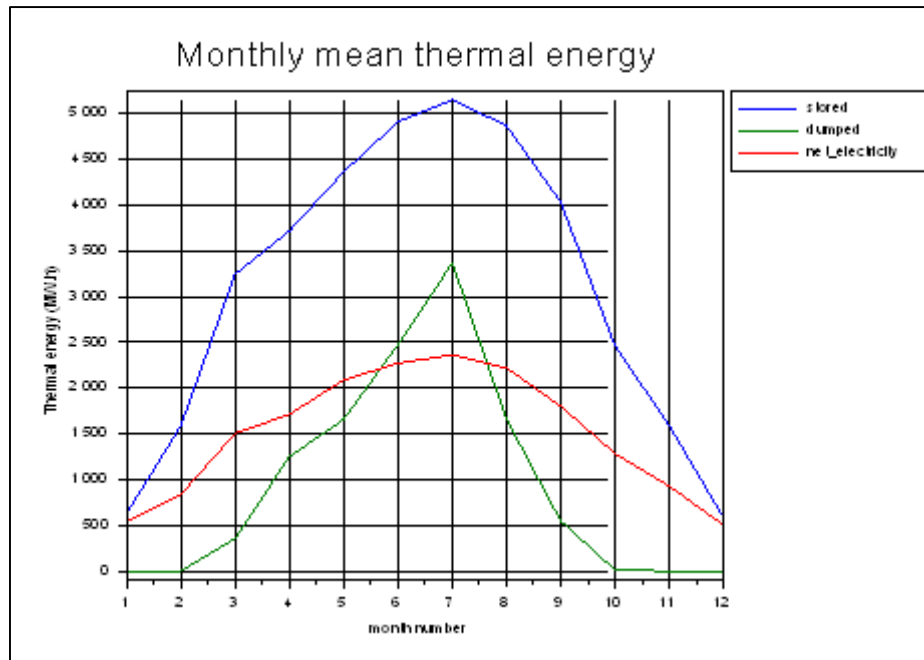


Figure 43. Monthly net electrical production in Larache (Morocco)

Study of coupling with absorption system

The absorption system modelled in the tool uses ammonia as the working fluid. Theoretically, it allows to reach negative temperatures (around -10°C) but in our example the choice of the cooling temperature is 6°C , which is suitable for district cooling, for instance.

The integration scheme chosen is a basic one, since the concentrator of the machine is fed with hot oil coming from ORC machine, after a mixing with a recirculation loop in order to decrease the temperature down to acceptable values. The condenser and absorber are cooled through an external loop whose fluid is itself cooled down by ambient air. The choice of this scheme is due to the flexibility on the cold temperatures reached by the system.

Some other schemes could have been designed, one example being the use of ORC heat waste to feed the absorption refrigerator concentrator. This could be feasible especially in the case where the plant is located close to the sea (for desalination purposes, for instance) and could use medium/low temperature [] sea water for the condenser and absorber uses.

In the following sections, the gain from running the absorption system using only the dumped power is studied, considered as an optimized running. This strategy seems to be consistent with the fact that cold production is mostly desired on the hottest months of the year, in the case of district cooling, for instance. The numerical tools allow also a “non-optimized” calculation, consisting in running the absorption system in parallel with electricity all day long. This strategy was tested for cost comparison (not presented among the performances below) with a 500 kW absorption machine.

We consider 4 maximum powers for the absorption machine: $500\text{ kW}_{\text{th-cold}}$, $1\text{ MW}_{\text{th-cold}}$, $5\text{ MW}_{\text{th-cold}}$ and $10\text{ MW}_{\text{th-cold}}$.

These powers correspond to the following approximated needs (according to the hypotheses given in the previous section):

	500 kW	1000 kW	5000 kW	10000 kW
Number of 4 people families	41	82	410	820
Number of office workers	250	500	2500	5000

With these values, the monthly heat produced is shown on the curves below for all the cases (see Figure 44):

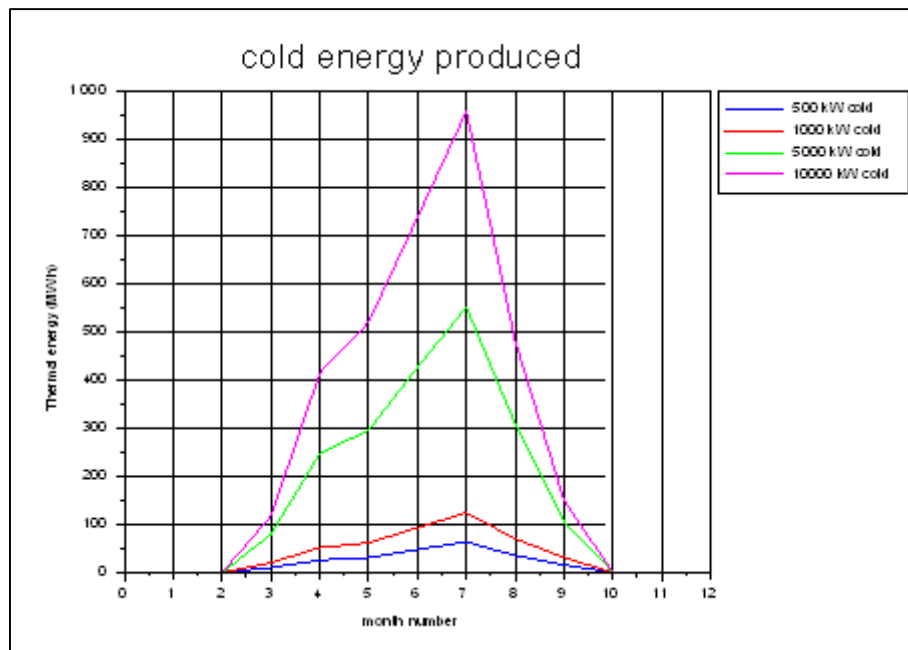


Figure 44. Monthly net electrical production coupling the studied system with absorption system.

The amount of cold produced is thus:

- 0.232 GWh if the limitation is 500 kW
- 0.454 GWh if the limitation is 1000 kW
- 2.02 GWh if the limitation is 5000 kW
- 3.40 GWh if the limitation is 10000 kW

The other output values are:

- Annual net electrical production: around 17.9 GWh_e
- Annual thermal energy stored: 34.1 GWh_{th}
- Annual thermal energy non valued for a 500 kW machine: 9.439 GWh_{th}
- Annual thermal energy non valued for a 1000 kW machine: 8.903 GWh_{th}
- Annual thermal energy non valued for a 5000 kW machine: 5.139 GWh_{th}
- Annual thermal energy non valued for a 10000 kW machine: 1.880 GWh_{th}

We can see that in the last case (10 MW_{th-cold}), almost all the dumped heat is used for cold production.

The calculations performed do not account for the output losses due to the starting-up and shutting-down transients of the absorption system.

Cost analysis

The aim of this section is to provide some first order estimates of the cost efficiency of each plant configuration studied in previous paragraphs. This will allow comparing the designs and strategies.

The cost analyses are always much more difficult to perform than energy study. They highly depend on various hypotheses as direct investment, loan rate and duration, taxes, etc. The country hosting the plant is also of primary importance. The goal of this report is not to perform a study of financial engineering. Therefore, all cases are calculated using the same costs hypotheses and it are chosen to give values normalized to a reference case. The main parameter studied will be the levelized cost of electricity (LCOE).

The histogram below (see Figure 45) shows the normalized LCOE for all the cases studied:

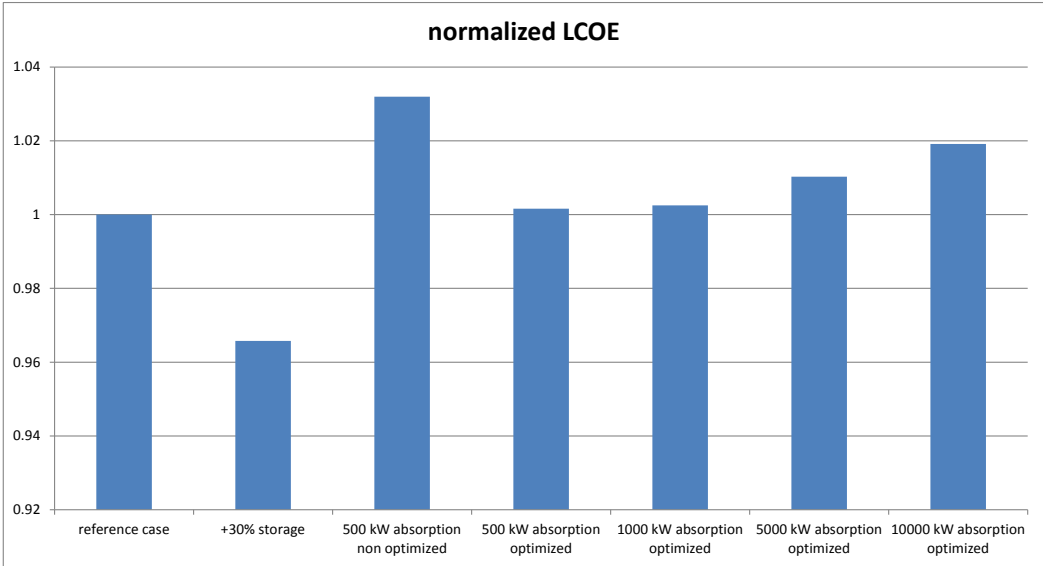


Figure 45. Normalized LCOE for different cases studied.

In order to account for cold production, it is proposed to convert the kW of the cooling system in electrical kW by using the usual compression cooling machine as a reference.

The absorption system is then compared to the compression refrigeration unit producing the same amount of cold but consuming more electricity. This electricity is thus estimated and added in the LCOE calculation.

For this need, we choose the Energy Efficiency Ratio (EER) cited in paragraph 4.4, which is a rather high value for a conventional equipment.

This leads to the following results, as reported in Table 17.

Table 17. Electrical consumption for different cases studied.

	cold heat produced (kWh th)	equivalent electrical consumption (kWh)
500 kW absorption non optimized	1,950,000	433,333
500 kW absorption - optimized	232,000	51,556
1000 kW absorption - optimized	454,000	100,889
5000 kW absorption - optimized	2,017,000	448,222
10000 kW absorption - optimized	3,380,500	751,222

These electrical consumptions are then included in the LCOE values which is shown in Figure 46 below as an adjusted value:

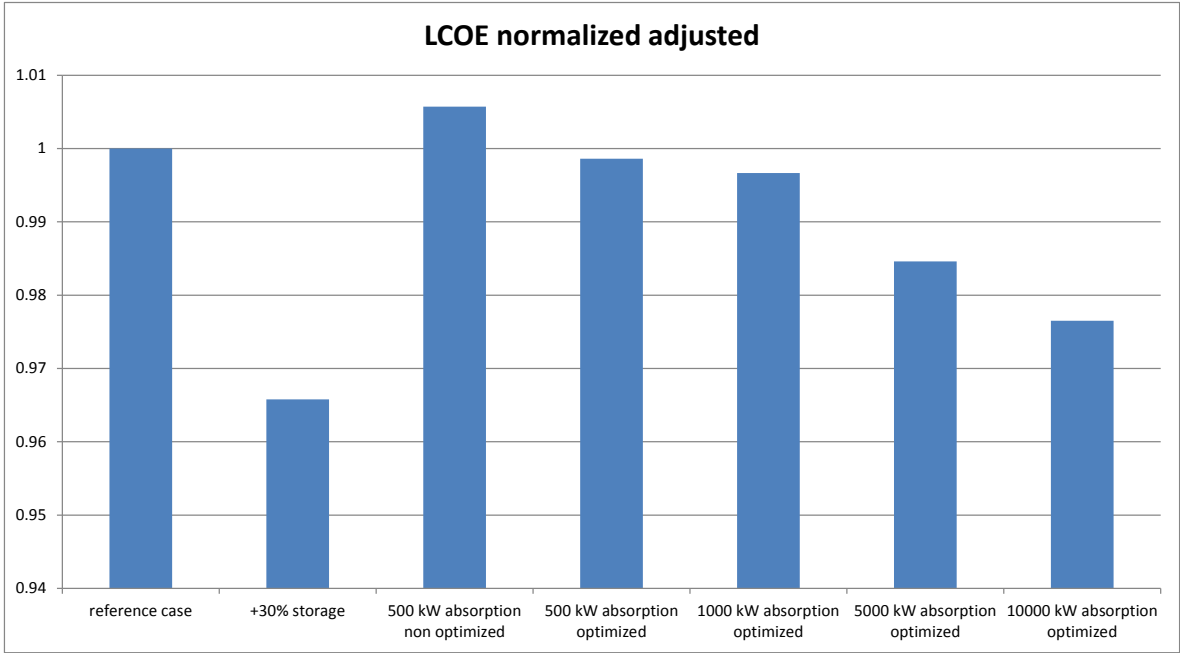


Figure 46. Adjusted LCOE for different cases studied.

We can see that using a 500 kW absorption system in a non-optimized strategy increases slightly the LCOE (+0.5%). However, this value is high when considering the small size of the unit, allowing the provision of cold power for few hundreds of people only. If the absorption system is run according to an optimized strategy, the LCOE decreases up to 2.5% (approximately) in the case of 10 MW of cold production. This case seems interesting given the size of the power plant in the Moroccan context.

4.3. TEMPERATURE LEVEL vs POWER CYCLE TECHNOLOGIES

In Table 18 are reported thermodynamic cycles that can be used in combination with a solar field. Other cycles like the Otto and Diesel ones are also used in cogeneration, but due to the fact that these are internal combustion engines, they cannot be used in combination with solar energy.

Table 18. Thermal cycles and maximum temperatures that can be reached with them

Thermal cycle		T_{\max} (°C)
Stirling		1500
Brayton		800 ÷ 1000
Rankine	Water	550
	Organic fluid	Depends on the fluid

As can be seen, the maximum temperature achievable by an ORC (Organic Rankine Cycle) depends on the characteristics of the employed fluid.

4.3.1. Analysed fluids for ORC: Selecting criteria

There are many possible working fluids available for an Organic Rankine Cycle. Choosing a suitable fluid for a given application must combine several properties hard to comply:

- suitable slope of the vapour saturated curve on the Ts diagram. The most appropriate selection for Rankine cycles with relatively low top temperature are dry and isentropic working fluids;
- costs;
- safety, health and environmental aspects.

Optimization of an objective function

In order to get the best fluid for a given application, an objective function has to be assumed. Different authors suggest the following objective functions:

- Heat transfer area net power produced (from Hettiarachchi et al. as cited in [21]): The use of this function is justified for applications with reduced value of thermal efficiency. It won't be used here;
- Overall recovery efficiency: Is the whole efficiency of the cycle taking into account the influence of heat exchangers like evaporator and condenser;
- Thermal efficiency: Is the thermal efficiency of the cycle only, without taking into account the influence of heat sources and sinks.

As said in [39], "overall recovery efficiency is the more meaningful parameter, but more difficult to determine". For that reason, thermal efficiency has been chosen as the objective function to optimize.

As any thermal cycle, a ceiling of thermal efficiency of a cycle is given by Carnot's well known formula.

$$\eta_{\text{Carnot}} = \frac{T_{\text{max}} - T_{\text{min}}}{T_{\text{max}}}$$

This expression shows us that efficiency grows up by increasing the maximum temperature and by lowering the minimum temperature of the cycle. Anyway, according to consulted literature, use of $T_{\text{superheat}} > T_{\text{evap}}$ has no positive consequences in ORC when dry or isentropic fluids are used. Increasing maximum temperature above the evaporation temperature ($T_{\text{superheat}} > T_{\text{evap}}$) is a necessary resource when a wet fluid is used (like water). But this measure is unnecessary when dry or isentropic fluids are employed. Besides, the use of $T_{\text{superheat}}$ diminishes the ratio $h1'2' / h12$ which, in turn, relieves the thermal efficiency of the Rankine cycle from that of the Carnot.

The thermal efficiency of an ORC is given by:

$$\eta_{\text{cycle}} = \frac{\dot{W}_{\text{expander}} - \dot{W}_{\text{pump}}}{\dot{Q}_{\text{evaporator}}}$$

Where the efficiency of the real cycle is always lower than the efficiency of the theoretical cycle ($\eta_{\text{cycle}} < \eta_{\text{Carnot}}$). $\dot{W}_{\text{expander}}$ and \dot{W}_{pump} are the work per unit of time (power) of the expander and the pump respectively. \dot{Q}_{hot} is the thermal power absorbed by the cycle. As seen in Figure 5b, this \dot{Q}_{hot} can be expressed as \dot{Q}_{1-2} or \dot{Q}_{y-2} depending on whether there is a regenerator or not. The thermal efficiency η_{cycle} is increased by growing the efficiency of the regenerator, η_{reg} and the efficiency of the expander, η_{expander}

Costs

There are two main costs to take into account when designing an ORC. Acquisition cost and operational cost.

Operational costs are related to the overall recovery efficiency (or the thermal efficiency, in first approximation), maintenance and replacement operations, etc.

On the other hand, acquisition costs are related to the dimensions of the different subsystems. Those dimensions are conditioned by parameters like the mass flux of working fluid [18,19,21] and, for the expander, the outlet volume flow rate $\dot{V}_3 = \dot{m}_{\text{work}} v_3 = \dot{m}_{\text{work}} / \rho_3$ [21]. The main goal is to keep them as low as possible.

Due to the technical nature of this text, attention is paid to parameters like the efficiency of the cycle η_{cycle} , the mass flux of working fluid \dot{m}_{work} and the expander's outlet volume flow rate \dot{V}_3 , that gives a good criterion to judge the merits of a choice without making an exhaustive economic analysis.

Safety, health and environmental aspects

Besides the costs and the slope of the vapour saturation curve on the Ts diagram, there are other important considerations to take into account.

As far as possible, fluids with the following characteristics should be chosen: (see Table 19)

- High stability.
- Low toxicity.
- High autoignition temperature. Autoignition temperature is the minimum temperature required to ignite a gas or vapour in air without the presence of a spark or flame [25]
- Non-corrosive/high compatibility with materials in contact.
- Low ozone depletion potential (ODP). ODP expresses the contribution to ozone depletion, based upon R11 = 1.0 [29].
- Low global warming potential (GWP). GWP expresses the contribution to the greenhouse effect, based upon CO₂ = 1. The timescale must be given (e.g. GWP₁₀₀: 100 years). [29]
- Moderate pressures in heat exchangers.

Table 19. Considered fluids (ordered according to their critical temperature)

	T _c (°C)	p _c (bar)	T _{NBP} (°C)	M (g/mol)	ODP	T _{Autoign} (°C)	GWP 100years
Water	374.15	220.9	100	18.02	n/a	n/a	n/a
Toluene	318.65	41.09	14.55	92.14	0	535	3.3
Benzene	289.01	48.99	80.15	78.11	0	560	3.4
Heptane	266.85	27.4	98.35	100.20	0	204	3
MM	245.6	19.39	100	162.37	n/a	340	n/a
Cycle pentane	238.55	45.1	49.25	70.13	0	320	< 2.5
SES36	177.55	28.49	35.6	184.85	0	n/a	n/a
Butane	152.0	37.96	-0.49	58.122	0	365	4
Isobutane	134.7	36.4	-11.75	58.122	0	460	3

In the Table 20 above T_c is the critical temperature, p_c is the critical pressure, T_{NBP} is the normal boiling point temperature, M is the molar mass, ODP is the ozone depletion potential, T_{autoign} is the autoignition temperature and GWP is the global warming potential.

Only benzene and toluene are toxic [40], but they are considered here for academic purposes. From the point of view of ODP and GWP, all fluids are suitable for this application. They have in addition a good compatibility with most metals commonly used in refrigeration engineering.

All fluids present an auto ignition temperature much higher than their own critical temperature, except heptane. This feature makes heptane not very appropriate for ORC.

Fluids on the bottom of the table have low critical temperature (Isobutane, Butane, SES36) and their use in applications with relatively high temperature heat sources would lead to supercritical cycles.

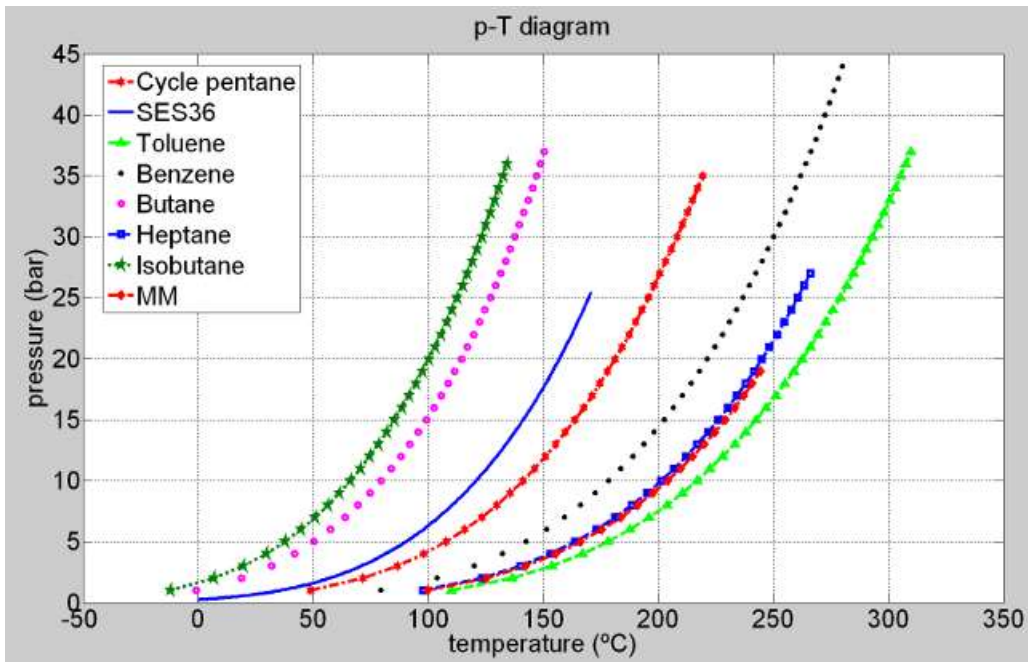


Figure 47. Saturation pressure as a function of saturation temperature for the fluids considered (except water)

In Figure 47 saturation pressures for the fluids considered are reported, showing for example that only Toluene, Benzene and Heptane could cope with evaporation temperatures T_{evap} above 250 °C in a non-supercritical cycle. For every T_{evap} considered, a fluid with the lowest p_{evap} is preferred. In the case of $T_{\text{evap}} = 250$ °C, Benzene has a lower p_{evap} and is better than Toluene and Heptane from that point of view.

In Figure 48 T_s diagrams for all the fluids considered are shown:

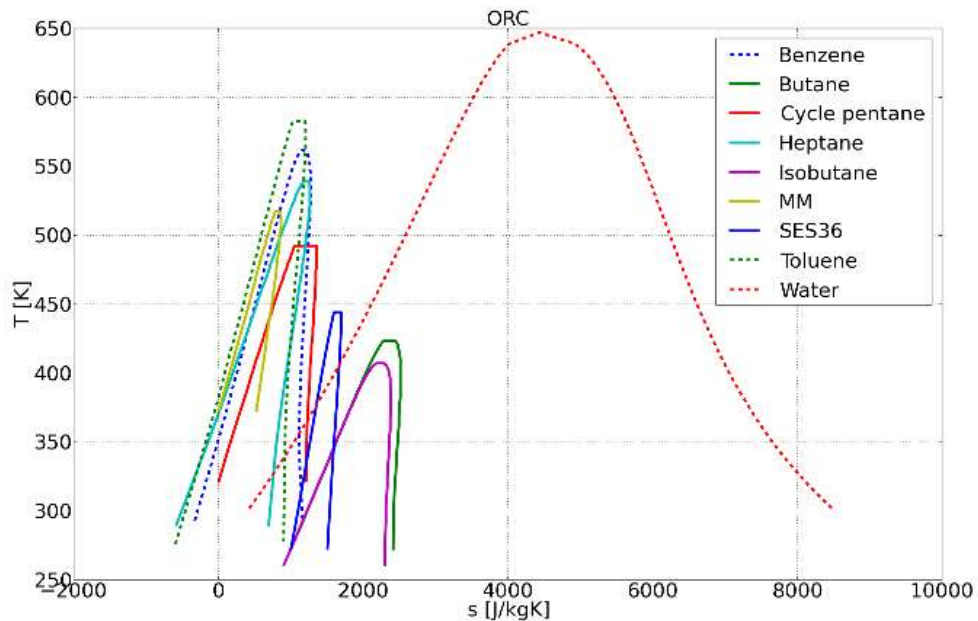


Figure 48. T_s diagram for saturated fluids considered.

Where butane, cycle pentane, isobutane and MM are represented for pressures higher than 1 bar.

4.3.2. Operating conditions

A selection criterion for an ORC fluid includes the evaporating and condensing temperatures. In effect, apart from cycle efficiency results, the operational conditions of a given working fluid, in terms of its pressure/temperature conditions under the ORC operating regime, are of paramount importance in the fluid selection process. Such conditions are related to both evaporation and condensation temperature regimes.

The maximum temperature of the cycle (T_{\max}) is conditioned, among other factors, by the working fluid stability and safety-related aspects. It must be taken into account that the higher the maximum temperature in the cycle, the more efficient the ORC, but the lower efficiency of the solar collector's field. T_{\max} is indirectly linked to the different collector technologies and this fact is taken into account for their estimation in the following study.

Possible collectors to be considered are:

Stationary Solar Collectors

- Flat Plate Collectors (FPC): They can produce heat for low and medium temperatures around 100 °C;
- Evacuated Tube Collectors (ETC): They can produce heat for low and medium temperatures from 100 °C to around 150 °C;
- Evacuated Tube Collectors - Compound Parabolic Concentrators (ETC-CPC.). They can produce heat for low and medium temperatures around 150 °C to 180 °C.

Sun Tracking Concentrating Collectors

- Parabolic Trough Collectors (PTC): They produce heat at temperatures over 200 °C;
- Linear Fresnel Collectors (LFC): They also can produce heat at temperatures over 200 °C.

The condensing temperature (T_{cond}) is the temperature related with practical aspects as the pressure associated to it (it is desirable to maintain the value of the condensing pressure superior to the atmospheric one, in order to avoid air from outside entering the system). On the other hand, it can be useful to increase the condensing temperature when it is foreseen to use the heat rejected by the ORC in any other process (e.g., desalination or cooling). In the present text, T_{cond} will be estimated according to the usual values achieved in practical cooling systems and in cogeneration applications.

Values commonly encountered in literature are:

- Water cooling. An approximate value for the minimum achievable end temperature of the process medium could be about 20 °C [26].
- Water-Air cooling. An approximate value for the minimum achievable end

temperature of the process medium could be about 30 °C [26].

- Air cooling. An approximate value for the minimum achievable end temperature of the process medium could be about 40 °C [26].

Other three T_{cond} (80 °C, 90 °C and 100 °C) are considered to cover possible cogeneration applications like desalination or absorption refrigeration. Additionally a $T_{\text{cond}} = 150$ °C has been thought to cover process heat applications:

For that reason, the analysis will be focused on a system with the following characteristics:

- T_{max} will be one of these seven values: 100 °C, 150 °C, 200 °C, 250 °C, 300 °C, 350 °C or 400 °C.;
- T_{cond} will be one of these seven values: 20 °C, 30 °C, 40 °C, 80 °C, 90 °C, 100 °C or 150°C;
- ε_{reg} (efficiency of the regenerator) will be 0 (without regenerator) or 0.8 (with it);
- η_{t} (efficiency of the expander) will be set at a value of 0.8;
- η_{p} (efficiency of the pump) will be fixed at a value of 0.8.

The mass flow of working fluid (\dot{m}) will vary for every fluid in accordance to the imposed thermal power in evaporator ($\dot{Q}_{\text{evaporator}} = 60$ kW).

These give rise to some different theoretical case studies for each fluid (according to different possible combinations of T_{evap} and T_{cond} for each regenerator condition) but, in fact, much of them can't withstand some or several combinations. In Table 20 below are represented all the studied possibilities.

Table 20. Fluids represented in the "Results" section

			T_{evap}		
			FPC	ETC	ETC-CPC
			100 °C = 373 K	150 °C = 423.15 K	200 °C = 473.15 K
T_{cond}	cooling systems	20 °C = 293.15 K	Benzene, Butane, Heptane, Isobutane, SES36, Toluene	Benzene, Heptane, SES36, Toluene	Benzene, Heptane, Toluene
		30 °C = 303.15 K	Benzene, Butane, Heptane, Isobutane, SES36, Toluene	Benzene, Heptane, SES36, Toluene	Benzene, Heptane, Toluene
		40 °C = 313.15 K	Benzene, Butane, Heptane, Isobutane, SES36, Toluene, Water	Benzene, Heptane, SES36, Toluene, Water	Benzene, Heptane, Toluene, Water
	other applications	80 °C = 353.15 K	-	Benzene, Cycle pentane, Heptane, SES36, Toluene, Water	Benzene, Cycle pentane, Heptane, Toluene, Water
		90 °C = 363.15 K	-	Benzene, Cycle pentane, Heptane, SES36, Toluene, Water	Benzene, Cycle pentane, Heptane, Toluene, Water
		100 °C = 373.15 K	-	Benzene, Cycle pentane, Heptane, MM, SES36, Toluene, Water	Benzene, Cycle pentane, Heptane, MM, Toluene, Water

Table 21. Fluids represented in the Appendix

		T_{max}						
		100 °C = 373.15 K	150 °C = 423.15 K	200 °C = 473.15 K	250 °C = 523.15 K	300 °C = 573.15 K	350 °C = 623.15 K	400 °C = 673.15 K
T_{cond}	20 °C = 293.15 K	(a), (b), (d), (e), (g), (h)	(a), (b), (d), (e), (g), (h)	(a), (b), (d), (e), (h)	(a), (d), (h)	(a), (d), (h)	(a), (h)	-
	30 °C = 303.15 K	(a), (b), (d), (e), (g), (h)	(a), (b), (d), (e), (g), (h)	(a), (b), (d), (e), (h)	(a), (d), (h)	(a), (d), (h)	(a), (h)	-
	40 °C = 313.15 K	(a), (b), (d), (e), (g), (h), (i)	(a), (b), (d), (e), (g), (h), (i)	(a), (b), (d), (e), (h), (i)	(a), (d), (h), (i)	(a), (d), (h), (i)	(a), (h), (i)	(i)
	80 °C = 353.15 K	-	(a), (b), (c), (d), (e), (g), (h), (i)	(a), (b), (c), (d), (e), (h), (i)	(a), (c), (d), (h), (i)	(a), (d), (h), (i)	(a), (h), (i)	(i)
	90 °C = 363.15 K	-	(a), (b), (c), (d), (e), (g), (h), (i)	(a), (b), (c), (d), (e), (h), (i)	(a), (c), (d), (h), (i)	(a), (d), (h), (i)	(a), (h), (i)	(i)
	100 °C = 373.15 K	-	(a), (b), (c), (d), (e), (f), (g), (h), (i)	(a), (b), (c), (d), (e), (f), (h), (i)	(a), (c), (d), (f), (h), (i)	(a), (d), (f), (h), (i)	(a), (h), (i)	(i)
	150 °C = 423.15 K	-	-	(a), (c), (d), (f), (h), (i)	(a), (c), (d), (f), (h), (i)	(a), (d), (f), (h), (i)	(a), (h), (i)	(i)

In Table 21 are reported fluids represented in the APPENDIX measurements, like benzene (a), butane (b), cycle pentane (c), heptane (d), isobutane (e), MM (f), SES36 (g), toluene (h) and water (i). The cycles working with overheated fluids have been highlighted in red in the previous table. The criterion for doing this has been:

- For water, given an imposed maximum temperature ($T_{\text{superheat}}$), T_{evap} is calculated in order to have point 3 (exit of the expander) as saturated vapour (without any possibility for regeneration). This is done because water is a wet fluid;
- For other fluids, given an imposed maximum temperature ($T_{\text{superheat}}$), T_{evap} is calculated as being near the critical point, without exceeding it (subcritical cycle).

4.3.3. Preliminary Conclusions

The election of the best fluid depends on a variety of factors like toxicity, risk of inflammation, stability, ozone depletion potential, etc., but also on its performance for a particular application. For that reason, an analysis with different maximum and minimum cycle temperatures has been done and, from the results, some conclusions can be inferred:

Regeneration increases η_{cycle} whatever the fluid chosen, but some of them, like heptane and SES36, seems to be particularly sensitive to the presence of a regenerator (more than the other analysed fluids).

Best fluid to be used with $T_{\text{max}} = 100 \text{ }^\circ\text{C}$

The best fluids for $T_{\text{max}} = 100 \text{ }^\circ\text{C}$ and T_{cond} compatible with ordinary cooling systems ($T_{\text{cond}} = 20 \text{ }^\circ\text{C}$, $T_{\text{cond}} = 30 \text{ }^\circ\text{C}$ and $T_{\text{cond}} = 40 \text{ }^\circ\text{C}$) are SES36 and butane using regeneration. They exhibit the highest value of η_{cycle} in all cases. SES36 has a slightly better efficiency and lower values of pressure than butane, but also a stronger sensitivity to the presence of a regenerator.

Best fluids to be used with $T_{\text{max}} = 200 \text{ }^\circ\text{C}$

If $T_{\text{evap}} = 200 \text{ }^\circ\text{C}$ is reached, the best fluid election depends on T_{cond} (regeneration considered in all cases):

- Heptane for $T_{\text{cond}} = 20 \text{ }^\circ\text{C}$, $30 \text{ }^\circ\text{C}$ and $40 \text{ }^\circ\text{C}$ has the highest values of η_{cycle} but it has a large dependence on the presence of a regenerator as compared with the possible use of benzene or toluene (both of them are toxic);
- Cycle pentane for $T_{\text{cond}} = 80 \text{ }^\circ\text{C}$ and $90 \text{ }^\circ\text{C}$;
- Benzene for $T_{\text{cond}} = 100 \text{ }^\circ\text{C}$ has the largest efficiency value of the cycle for the fluids considered, but due to its toxicity it should be replaced by another one. If cycle pentane is chosen instead of benzene, a fall of the cycle efficiency has to be accepted, from $\eta_{\text{cycle}} = 16.3\%$ (benzene) to $\eta_{\text{cycle}} = 15.0\%$ (cycle pentane);
- Toluene for $T_{\text{cond}} = 150 \text{ }^\circ\text{C}$ has the largest cycle efficiency value among the fluids considered, but due to its toxicity it should be replaced by another one. If heptane is chosen instead of toluene, a fall of the cycle efficiency has to be accepted from $\eta_{\text{cycle}} = 9.8\%$ (toluene) to $\eta_{\text{cycle}} = 9.0\%$ (heptane).

Best fluids to be used with $T_{\max} = 250\text{ }^{\circ}\text{C}$

From the point of view of the cycle efficiency, the best fluid to be used when $T_{\max} = 250\text{ }^{\circ}\text{C}$ is toluene with regeneration, independently of the temperature in the condenser, T_{cond} . The exception is for $T_{\text{cond}} = 100\text{ }^{\circ}\text{C}$, where the best option is benzene. Because both of them (benzene and toluene) are toxic, another fluid should be used instead. For a temperature T_{cond} between $20\text{ }^{\circ}\text{C}$ and $40\text{ }^{\circ}\text{C}$ the solution could be to use heptane instead, but taking into account that its $T_{\text{autoignition}} = 204\text{ }^{\circ}\text{C}$ (lower than the value of $250\text{ }^{\circ}\text{C}$ considered as the maximum cycle temperature).

For temperatures T_{cond} between $80\text{ }^{\circ}\text{C}$ and $100\text{ }^{\circ}\text{C}$, cycle-pentane with regeneration could be utilized advantageously to avoid the use of toluene or benzene without excessive loss of cycle efficiency.

For $T_{\text{cond}} = 150\text{ }^{\circ}\text{C}$ MM could be used if a fall in its efficiency from 15.0% (toluene) to 12.3% (MM) is acceptable.

Best fluids to be used with $T_{\max} = 300\text{ }^{\circ}\text{C}$

For $T_{\max} = 300\text{ }^{\circ}\text{C}$ the only fluids considered are benzene, toluene, heptane and water. All of them have drawbacks. Benzene and toluene are toxic, heptane has an autoignition temperature much lower than the maximum temperature of the cycle and water could be better employed in a profitable way by raising the evaporation pressure in a cycle with reheating and regeneration.

Anyway, from the point of view of the efficiency of the cycle, benzene is better than toluene for T_{cond} between $20\text{ }^{\circ}\text{C}$ and $40\text{ }^{\circ}\text{C}$ and between $90\text{ }^{\circ}\text{C}$ and $100\text{ }^{\circ}\text{C}$. For T_{cond} of $80\text{ }^{\circ}\text{C}$ and $150\text{ }^{\circ}\text{C}$ the best fluid is toluene.

Best fluids to be used with $T_{\max} = 350\text{ }^{\circ}\text{C}$

For $T_{\max} = 350\text{ }^{\circ}\text{C}$ the only fluids considered are benzene, toluene and water. All of them have drawbacks. Benzene and toluene are toxic and water could be better profited raising the evaporation pressure in a cycle with reheating and regeneration.

Anyway, from the point of view of the efficiency of the cycle, benzene is better than toluene for T_{cond} between $20\text{ }^{\circ}\text{C}$ and $40\text{ }^{\circ}\text{C}$ and for $T_{\text{cond}} = 100\text{ }^{\circ}\text{C}$. Toluene is better for a T_{cond} value of $80\text{ }^{\circ}\text{C}$, $90\text{ }^{\circ}\text{C}$ and $150\text{ }^{\circ}\text{C}$.

Best fluids to be used with $T_{\max} = 400\text{ }^{\circ}\text{C}$

For $T_{\max} = 400\text{ }^{\circ}\text{C}$ (and $T_{\text{cond}} \geq 40\text{ }^{\circ}\text{C}$) the only fluid considered is water. This is due to the fact that fluids other than water need a very high degree of overheating and their evaporation

pressures raises to prohibitive values. It must be noted that, accordingly with the increase in the condenser temperature T_{cond} , the evaporation temperature raises as well. This is a result of the imposed rule for having point 3 (condition of the working fluid at the exit of the expander) as saturated vapour. Cycle efficiency goes from 22.4 % with $T_{\text{cond}} = 40 \text{ }^\circ\text{C}$ to 16.8 % with $T_{\text{cond}} = 150 \text{ }^\circ\text{C}$.

Water is not a good choice for this application because it needs superheating in order to avoid having point 3 (see points nomenclature in Figure 5b) on the phase change zone. This measure prevents water droplets from entering the expander and causing abnormal erosion and/or corrosion but it also turns drastically away the real efficiency of the cycle η_{cycle} from the maximum efficiency obtainable η_{Carnot} . Moreover, the overheating temperature applied to water in this document is calculated as a high enough value in order to have point 3 as saturated vapour, which doesn't allow the use of a regenerator.

4.4. CASE STUDIES: a short introduction

Within the subtask “schemes of integration in thermal application and power cycle for small scale system” will be analysed three industrial applications as case studies: a cork industry, a municipal solid waste treatment plant and a pharmaceutical industry (Digespo project).

Case study I – Insulation cork board (ICB) production

Among the several industrial processes utilized by the cork industry there is one that presents a high potential of integration of CST technologies: the insulation cork board (ICB) production. ICB is traditionally used as a thermal, acoustic and vibrational insulator and has recently acquired a broader range of applications with functional and decorative applications.

The ICB is an agglomerated material exclusively made of cork granules. The granules are bonded by moulds due to their own resins defined by the autoclave walls where they undergo light compression followed by steaming at more than 300°C , usually between 17 to 30 minutes. The superheated steam passes through the granule mass resulting in the secretion of the cork resins to the granules' surfaces and in an increase in their volume, which determines their agglutination. ICB is a completely natural product since its agglomeration process is due to the cork natural resins and to the granules expansion, without using any glues or additives or other materials than cork⁷. Process is described in Figures 49 and 50.

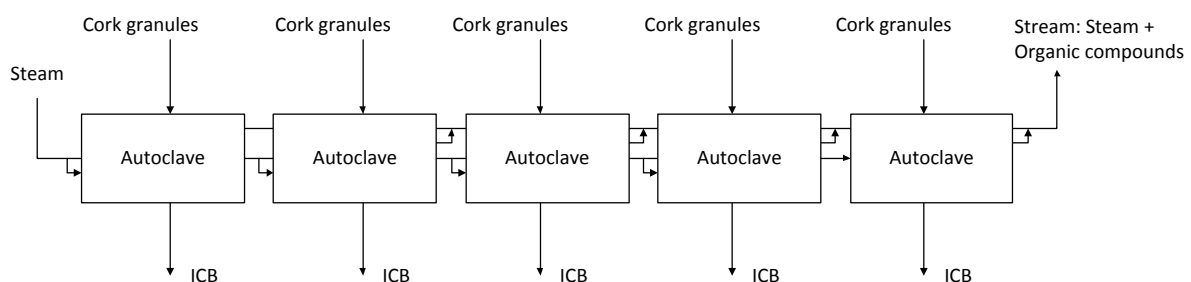


Figure 49. Process diagram for ICB manufacturing.

⁷ Gil, L. (2007). *Technical manual: Cork as a building material*. St.^a M.^a de Lamas: APCOR.

Current ICB production lines produce the required steam in boilers using cork dust as fuel or, in some cases, fossil fuels. Feeding the production line with steam produced by solar heat would reduce the usage of such fuels. In the case of units still burning fossil fuels this would represent obvious environmental as well as expected economic benefits. The replacement of cork dust would also be beneficial, since cork dust retains economic value that could be exploited by further processing such as the production of pellets or bricks which could be used as renewable fuel (biomass) in other industries or for domestic hot water and heating production.

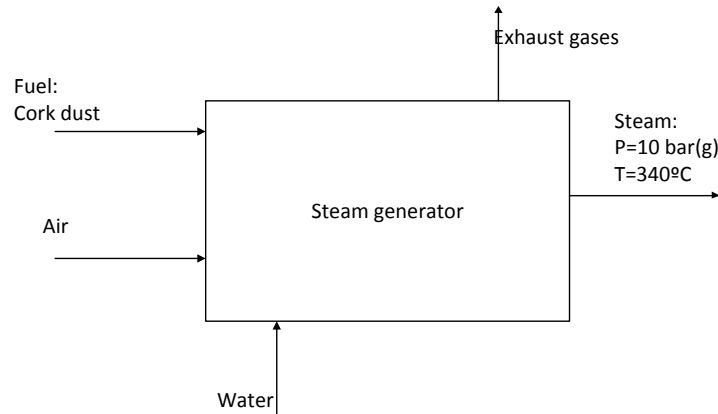


Figure 50. Actual process diagram for superheated steam production in cork industry.

The integration of CST systems in a particular ICB plant is being analysed as a case study under the project STAGE-STE and the results of this analysis will be available under milestone 43.

Case study II – Refused derived fuel (RDF) drying

Refused derived fuel (RDF) is a solid fuel obtained from non-hazardous waste (mainly municipal solid waste) after a mechanical biological treatment (MBT). It can be used as substitute fuel in cement kilns. However, the use of RDF as alternative fuel is limited by its humidity level (typically around 40 to 50%). It is then needed to dry the RDF produced at the end of the MBT, reducing its humidity level to values around 10% creating economic value for the RDF which can then be sold as fuel to co-incineration applications and reduces the amount of waste placed in landfills.

Concentrated solar energy can be used to supply heat to the drying process where hot air is used in rotating drums or belt dryers at temperature within the range of 80 °C to 100°C. Both co-generation or dedicated heat production schemes can be devised. In the first case the drying air could be heated by steam provided from a back-pressure turbine powered by the solar field, enabling the production of electricity to power the mechanical systems used in the MBT and thermal energy for the drying process. In the second case the solar field would be dedicated to the production of hot heat transfer fluid that would be used in a liquid-air heat exchanger to heat the air used in the drying process.

The integration of CST systems in a particular municipal waste treatment plant is being analysed as a case study under the project STAGE-STE and the results of this analysis will be available under MS43.

Case study III– micro-cogeneration for industrial and domestic application

The integration of solar fields in the industry had been developed inside the DIGESPO project. The aim was to integrate solar process heat into the company as micro cogeneration system for the chain production. The technology is able to provide steam, hot water and electricity.

The system is a modular 1-3 kWe, 3-9 kWth micro Combined Heat and Power (m-CHP) system based on innovative Concentrated Solar Power (CSP) and Stirling engine technology. This CSP m-CHP will provide electrical power, heating and cooling for single and multiple domestic dwellings and other small buildings.

The developed system integrates small-scale concentrator optics with moving and tracking components, solar absorbers in the form of evacuated tube collectors, a heat transfer fluid, a Stirling engine with generator, and heating and/or cooling systems. It incorporates them into buildings in an architecturally acceptable manner, with low visual impact. (See Figure 51)



Figure 51. The complete small scale m-CHP system developed in DIGESPO project.

Two Cer.Met. coatings have been modelled, realized and tested. The up scaled receiver, in form of Cer.Met. coating based on $\text{TiO}_2\text{-Nb}$, has confirmed an absorbance of 0.94 and emittance of 0.1 (at a temperature of 350°C). A second Cer.Met. coating based on $\text{SiO}_2\text{-W}$ has demonstrated an absorbance of 0.93 and emittance of 0.09 (at a temperature of 350°C). A full-evacuated solar tube has been designed and realized, with an absorber of 12 mm in diameter and a length of 2 meters. The system presents a concentration ratio of 12:1, and a single module is 200 cm long, 40 cm wide and 20-25 cm high. Two or more modules can be combined. The evacuated solar tube, located on the focus, has the selective absorber in a tube with a diameter of 12 mm. A very thin glass mirror has been developed (thickness < 1 mm). The overall mirror reflectivity has been measured with a detected value of 0,954.

Research has proposed a high energy density, double acting Stirling engine, provided of innovative heat exchangers realized through Selective Laser Melting process. The engine is a low speed (250 RPM), high pressure (130 bar) and compact solution able to be run at 300°C and to generate 3.5 kW of nominal power.

A solar plant based on the DIGESPO concept has been installed in Malta, supplying the industrial process of generating steam at 180°C and 6 bar absolute pressure in a first phase, and supporting the tests for improved technologies in a second stage. The solar collector's efficiency is around 50% in presence of 900 W/m^2 of direct solar radiation and at 300°C .

5. MARKET ANALYSIS AND BUSINESS MODELS

5.1. INDUSTRIAL FUEL PRICING IN EUROPEAN COUNTRIES.

The aim of this paragraph is to gather the industrial fuel pricing which is used by countries in European Union, especially in those countries with the highest solar irradiation, which consequently have a higher potential for the use of medium temperature collectors in industrial processes, in order to reduce energy production from fossil fuels.

In the following paragraphs it is reached the reasonable conclusion that when the viability of a solar thermal installation on an industrial process is analysed, the cost of heat generated by the existing fossil fuel based boiler needs to be taken into account. It thus derives that boilers employing Natural Gas are the worst scenario, as the cost in €/kWh is in general lower than the cost of natural gas.

In addition, in order to properly calculate the full energy costs, other costs must be considered related to different factors: inefficiencies of existing boilers working out of full loads, operating and maintenance costs, etc. This will have an important impact on the heat cost in the industrial process, making solar thermal technology even more interesting as energy source for different applications and processes.

5.1.1. Fuels employed at industrial processes.

Natural Gas and Electricity are the most commonly used energy sources in industries inside European Countries, although renewables, especially biomasses, already are having an important role too. (See Figure 52)

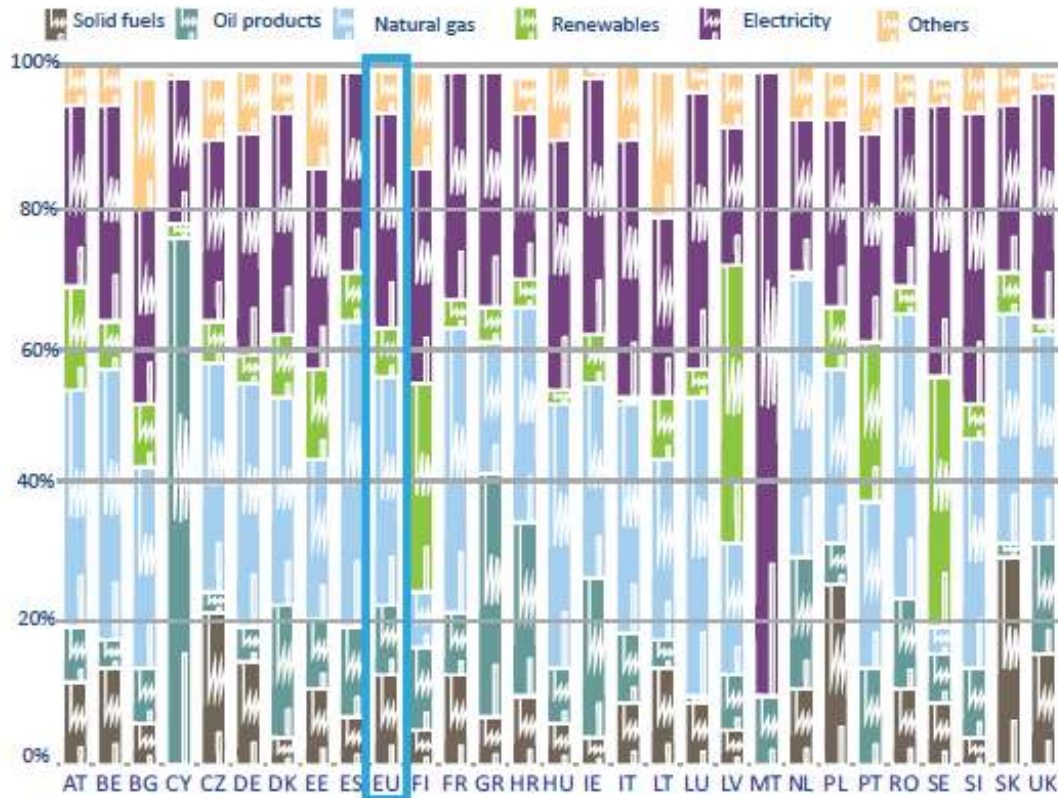


Figure 52. Industrial use of energy by source in 2013 [87].

For process heat generation, in some parts of the world coal still is the primary energy source but in Europe and North America, industrial boilers and heat transfer fluid heaters mainly employ fossil fuels (natural gas, LPG, diesel fuel, fuel oil). There are also electrical systems especially for the lowest thermal output models in which electricity utilization is common. Biomass is widely used in countries such as India and it is becoming interesting also in Europe as a Renewable Energy Source.

Typically, for low and medium temperatures (below 400°C), process heat is supplied via steam (commonly generated by fossil fuels in steam boilers at high conversion efficiencies of about 90%).

When defining the target cost of thermal energy provided by a solar thermal installation in a given process, a comparison with the most widely used energy sources needs to be done. Here, natural gas has a principal importance as it is by far the most used fuel in industrial processes.

5.1.2. Natural Gas and Electricity price survey methodology.

In year 2007 the methodology for the price survey of electricity and natural gas for industrial end-users (non-domestic users) was significantly modified to improve the transparency in a liberalized energy market. In year 2008 this Directive was recasted (Directive 2008/92/EC) [88]. Some prices are reported in Tables 22 and 23.

The principal changes introduced were:

- Introduction of consumption bands instead of the standard consumers (characterized by predefined annual consumption).
- Prices based on half yearly averages instead of fixed prices on 1st of January.
- National price data are employed and regional data are considered obsolete.

Table 22. Gas price categories for industrial end-users [88].

Industrial end-user	Annual gas consumption (Gj)	
	Lowest	Highest
Band-I1		< 1 000
Band-I2	1 000	< 10 000
Band-I3	10 000	< 100 000
Band-I4	100 000	< 1 000 000
Band-I5	1 000 000	<= 4 000 000

Table 23. Electricity price categories for industrial end-users [88].

Industrial end-user	Annual electricity consumption (MWh)	
	Lowest	Highest
Band IA		< 20
Band IB	20	< 500
Band IC	500	< 2 000
Band ID	2 000	< 20 000
Band IE	20 000	< 70 000
Band IF	70 000	<= 150 000

5.1.3. Natural gas and electricity prices for industrial end-users.

In the next tables, prices for natural gas and electricity in different countries are shown according to the methodology explained above.

Natural gas.

Table 24 shows the natural gas prices (c€/kWh) for industrial consumers with an annual consumption in the band I4 (100.000GJ-1.000.000GJ). They include excise duties and exclude value-added taxes. Important differences are seen between different countries.

Table 24. Natural Gas prices for industrial end-users - annual consumptions [89].

reference period	Germany	Belgium	Bosnia and Herzegovina	Bulgaria	Denmark	Estonia	Finland	France	Greece
1st half 2008	3,74	3,14	-	1,95	2,81	2,29	2,70	2,96	-
2nd half 2008	4,09	3,56	-	2,48	2,89	2,87	3,20	3,51	-
1st half 2009	3,59	3,17	-	2,93	2,51	2,56	2,95	3,06	-
2nd half 2009	3,29	3,15	-	1,88	2,08	2,21	2,81	2,68	-
1st half 2010	3,32	2,37	-	2,16	2,75	2,76	2,84	2,73	-
2nd half 2010	3,48	2,51	-	2,74	3,29	2,74	3,26	2,77	-
1st half 2011	3,61	2,66	-	2,65	3,62	2,70	4,06	2,72	-
2nd half 2011	3,62	2,78	5,45	2,93	3,57	3,01	4,73	2,86	-
1st half 2012	3,45	2,87	5,66	3,33	3,54	3,59	4,59	3,03	-
2nd half 2012	3,49	2,90	5,66	3,69	3,69	3,42	4,67	3,08	5,32
1st half 2013	3,71	2,99	5,66	3,28	3,93	3,57	4,74	3,19	4,93
2nd half 2013	3,80	3,02	5,31	3,17	3,78	3,42	4,75	3,31	4,52
1st half 2014	3,54	2,75	5,31	3,17	3,18	3,44	4,45	3,14	4,36
2nd half 2014	3,19	2,63	5,31	3,06	3,09	3,62	4,38	3,06	4,28 _p
1st half 2015	3,16	2,61	5,32	2,84	3,12	3,35	4,34	3,04	3,79 _p

reference period	Ireland	Italy	Croatia	Latvia	Liechtenstein	Lithuania	Luxembourg	Macedonia	Netherlands
1st half 2008	2,90	3,00	-	2,81	-	2,91	2,12	-	3,02
2nd half 2008	3,26	3,68	2,31	3,81	-	3,84	2,53	-	3,27
1st half 2009	3,14	3,28	2,64	3,73	-	2,59	2,67	-	3,21
2nd half 2009	2,31	2,45	2,68	2,48	-	2,30	2,54	-	2,89
1st half 2010	2,31	2,63	3,40	2,45	-	2,87	2,45	-	2,57
2nd half 2010	2,50	2,65	3,94	3,00	-	3,14	2,78	-	2,63
1st half 2011	2,86	2,79	4,05	2,80	-	3,38	3,32	3,79	2,76
2nd half 2011	2,70	3,07	4,32	3,27	-	4,13	3,77	4,08	2,78
1st half 2012	3,11	3,57	3,71	3,52	-	4,38	3,59	4,59	2,94
2nd half 2012	3,26	3,52	4,74	3,83	-	4,61	4,06	4,72	3,07
1st half 2013	3,48	3,41	4,17	3,58	-	4,23	4,15	4,06	3,21
2nd half 2013	3,59	3,32	3,61	3,54	-	4,18	3,51	3,80	3,08
1st half 2014	3,35	3,16	3,11	3,29	-	3,80	3,28	3,76	3,40
2nd half 2014	3,05	2,96	3,80	3,38	-	3,15	3,14	-	2,78
1st half 2015	3,01	2,92	3,58	3,31	-	2,02	3,15	-	3,07

reference period	Austria	Poland	Portugal	Romania	Serbia	Sweden	Slovakia	Slovenia	Spain
1st half 2008	-	2,67	2,37	2,43	-	4,65	3,10	3,31	2,57
2nd half 2008	-	2,98	2,61	2,62	-	4,40	4,35	4,19	3,04
1st half 2009	2,62	2,49	2,56	2,13	-	3,17	3,64	-	2,69
2nd half 2009	2,57	2,56	2,30	1,86	-	3,90	2,92	2,72	2,34
1st half 2010	2,47	2,66	2,60	2,05	-	4,08	2,97	4,07	2,44
2nd half 2010	2,76	2,85	2,90	1,92	-	4,38	3,02	3,59	2,52
1st half 2011	2,93	2,87	2,88	2,12	-	4,78	3,04	-	2,62
2nd half 2011	3,07	2,74	3,35	2,31	-	4,95	3,25	-	3,05
1st half 2012	3,67	3,04	3,56	2,68	-	4,88	3,33	4,82	3,32
2nd half 2012	3,80	3,36	3,69	2,42	-	4,97	3,21	4,64	3,44
1st half 2013	3,95	3,25	3,66	2,48	3,83	4,89	3,57	4,11	3,48
2nd half 2013	3,64	3,22	3,61	2,42	3,75	4,72	3,47	4,02	3,38
1st half 2014	3,68	3,27	3,64	2,66	3,71	4,24	3,40	3,65	3,36
2nd half 2014	3,39	3,17	3,81	2,76	3,80	4,04	3,45	3,57	3,47
1st half 2015	3,43	3,21	3,55	2,60	4,35	4,19	3,24	3,25	3,24

reference period	Czech Republic	Turkey	Hungary	United Kingdom
1st half 2008	2,96	2,48	2,73	2,62
2nd half 2008	3,68	3,26	3,75	2,99
1st half 2009	3,04	2,74	3,20	2,56
2nd half 2009	2,41	2,17	3,12	1,95
1st half 2010	2,73	2,26	2,80	2,02
2nd half 2010	3,16	2,31	3,40	2,14
1st half 2011	2,94	2,12	3,57	2,37
2nd half 2011	3,28	2,09	3,95	2,57
1st half 2012	3,19	2,55	4,46	2,95
2nd half 2012	3,17	2,99	4,21	3,05
1st half 2013	3,10	2,99	4,17	3,14
2nd half 2013	3,05	2,63	3,96	3,11
1st half 2014	2,99	2,38	3,31	3,09
2nd half 2014	2,81	2,61	2,87	2,86
1st half 2015	2,71	2,77	2,78	2,93

When analysing natural gas prices, there is the need to take into account its expected future evolution. A solar thermal installation in an industrial process will guarantee an energy generation also in the years after the installation, thus its comparison against fossil fuel based solutions needs to be done considering the expected prices in those years.

Considering the uncertainty in this evolution, in this report expected prices in the next years are not given and current price values are considered. Anyway, in the report by Solarconcentra technological platform [90] it is shown the expected evolution for the price of natural gas for the next years at different scenarios (low, medium and high). See Table 25.

Table 25. Price estimation for natural gas in industries in Spain – 2015/2035. Source: Solarconcentra.

CONSUMIDOR INDUSTRIAL	ESCENARIO	PRECIO (€/kWh _{th})		
		2015	2025	2035
Grupo I1	Alto	0.0576	0.1151	0.1725
	Medio	0.0548	0.0835	0.1122
	Bajo	0.0533	0.0677	0.0821
Grupo I2	Alto	0.0504	0.1040	0.1576
	Medio	0.0477	0.0745	0.1013
	Bajo	0.0464	0.0598	0.0732
Grupo I3	Alto	0.0401	0.0725	0.1050
	Medio	0.0385	0.0547	0.0709
	Bajo	0.0377	0.0458	0.0539
Grupo I4	Alto	0.0364	0.0637	0.0910
	Medio	0.0350	0.0487	0.0623
	Bajo	0.0343	0.0412	0.0480
Grupo I5	Alto	0.0352	0.0692	0.1032
	Medio	0.0335	0.0505	0.0675
	Bajo	0.0327	0.0412	0.0497
Grupo I6	Alto	0.0343	0.0667	0.0992
	Medio	0.0327	0.0489	0.0651
	Bajo	0.0319	0.0400	0.0481

As explained, even if natural gas prices are expected to have an important evolution, for estimation, current gas prices can be used. Also, for the calculation of the cost of energy for an industrial process it needs to be taken into account the efficiency of the employed boiler-heater.

This efficiency highly depends on many factors such as the employed fuel, boiler type, control, flue gas temperatures, maintenance status, working load, etc. With all this, as a reference value for Spain, for an industrial process with a consumption in band I3 (natural gas price of 0.037€/kWh), and considering a boiler efficiency of 0.87, the current cost of energy based on natural gas is of **0.042 €/kWh_{th}**. Similar estimations can be done with the available data in this report for different countries.

Electricity

Table 26 shows electricity prices (c€/kWh) for industrial consumers with an annual consumption in the band ID (2.000MWh-20.000MWh). They include excise duties and exclude value-added tax. As in the case of the natural gas prices, important differences are seen between different countries.

Table 26. Electricity prices for industrial end-users - annual consumptions [89].

reference period	Germany	Belgium	Bosnia and Herzegovina	Bulgaria	Denmark	Estonia	Finland	France	Greece
1st half 2008	9,59	9,34	-	4,96	8,98	4,83	6,10	5,84	7,37
2nd half 2008	9,57	9,62	-	5,93	10,06	5,23	6,42	5,61	7,98
1st half 2009	10,02	10,09	-	5,98	8,46	5,63	6,57	6,86	8,29
2nd half 2009	10,07	9,88	-	5,83	9,03	5,72	6,64	6,12	8,11
1st half 2010	9,93	9,41	-	5,78	9,17	6,68	6,79	6,96	8,25
2nd half 2010	10,58	9,39	-	5,98	9,36	7,22	6,68	6,26	8,95
1st half 2011	11,21	9,71	-	5,84	9,66	7,18	7,33	7,42	8,85
2nd half 2011	11,39	10,20	-	5,93	9,02	7,27	7,23	7,00	9,20
1st half 2012	11,45	10,00	6,60	6,34	9,41	7,70	7,20	8,11	10,22
2nd half 2012	11,69	9,70	6,63	6,98	9,67	8,06	7,18	7,00	10,59
1st half 2013	12,78	9,32	6,47	7,01	10,01	9,05	7,12	8,34	10,68
2nd half 2013	12,73	10,00	6,57	6,30	9,72	8,98	7,17	7,42	10,70
1st half 2014	13,76	9,58	6,65	6,79	9,36	8,40	6,97	8,30	10,88
2nd half 2014	13,26	9,73	6,55	6,81	9,63	8,51	7,01	7,88	10,64
1st half 2015	13,16	9,56	6,52	6,20	8,97	8,19	6,63	8,78	10,02

reference period	Ireland	Italy	Croatia	Latvia	Liechtenstein	Lithuania	Luxembourg	Malta	Macedonia
1st half 2008	12,01	12,48	6,19	5,86	-	7,01	-	9,18	-
2nd half 2008	12,76	14,21	8,08	7,12	-	7,04	-	13,23	-
1st half 2009	10,70	13,33	7,31	8,49	-	7,81	9,35	12,30	-
2nd half 2009	9,71	12,24	7,81	8,35	-	6,66	9,36	8,60	-
1st half 2010	8,38	12,09	8,00	8,26	-	9,17	7,81	14,90	-
2nd half 2010	8,66	12,98	7,77	8,50	-	10,23	7,95	16,00	-
1st half 2011	8,73	12,95	7,75	9,05	-	10,21	7,31	15,80	-
2nd half 2011	9,77	13,93	7,62	9,89	-	10,26	7,32	15,70	-
1st half 2012	10,38	16,29	7,56	9,90	-	10,75	7,34	15,90	-
2nd half 2012	11,96	16,78	8,03	10,00	-	10,74	7,90	15,80	-
1st half 2013	11,59	15,37	8,11	10,44	-	11,88	7,46	15,90	7,64
2nd half 2013	11,64	15,91	7,99	10,65	-	11,34	7,23	15,50	6,98
1st half 2014	11,58	15,23	8,15	10,75	-	11,64	6,55	15,70	6,43
2nd half 2014	11,36	15,91	7,82	10,68	-	11,70	6,73	15,80	6,33
1st half 2015	11,64	14,89	7,91	10,81	-	9,06	6,39	13,50	6,74

reference period	Montenegro	Netherlands	Norway	Austria	Poland	Portugal	Romania	Serbia	Sweden
1st half 2008	-	9,03	6,57	9,26	8,34	8,07	7,83	-	6,20
2nd half 2008	-	9,15	6,78	9,65	7,94	8,17	7,99	-	6,86
1st half 2009	-	10,11	6,87	10,86	8,05	8,44	7,34	-	5,91
2nd half 2009	-	9,85	6,72	10,81	8,42	8,27	7,14	-	6,01
1st half 2010	-	8,85	8,87	10,32	8,53	8,01	7,16	-	7,18
2nd half 2010	-	8,68	7,90	10,32	8,59	8,05	6,94	-	7,36
1st half 2011	4,94	8,62	9,60	10,12	8,62	9,03	7,03	-	7,89
2nd half 2011	4,92	8,41	7,62	10,14	7,89	9,27	7,03	-	7,08
1st half 2012	5,39	8,44	7,43	9,83	8,14	10,55	7,30	-	7,13
2nd half 2012	5,90	8,60	6,96	9,85	8,45	10,40	6,70	-	6,73
1st half 2013	6,25	8,66	7,89	9,84	7,96	10,41	7,61	4,91	6,90
2nd half 2013	6,18	8,32	7,13	9,80	7,53	10,25	7,06	5,08	6,72
1st half 2014	6,35	9,37	6,45	9,60	7,04	10,10	7,87	4,61	6,35
2nd half 2014	6,17	8,43	6,54	9,37	7,13	10,09	7,30	6,02	5,98
1st half 2015	6,15	8,17	6,19	8,97	7,68	10,32	7,48	5,62	5,45

reference period	Slovakia	Slovenia	Spain	Czech Republic	Turkey	Hungary	United Kingdom	Cyprus	Kosovo
1st half 2008	10,83	7,67	8,38	9,25	6,43	9,99	8,80	13,17	-
2nd half 2008	11,70	8,03	8,91	9,39	7,96	10,88	10,10	17,16	-
1st half 2009	12,70	8,10	9,53	9,40	7,24	11,03	10,18	10,83	-
2nd half 2009	12,63	7,98	9,34	9,78	7,21	11,46	9,00	13,62	-
1st half 2010	10,58	8,46	9,27	9,40	8,24	9,42	8,74	14,00	-
2nd half 2010	10,86	8,65	8,97	9,69	8,44	9,41	8,87	16,20	-
1st half 2011	11,56	8,49	9,16	9,96	6,99	9,38	8,93	15,15	-
2nd half 2011	11,76	8,44	9,37	9,67	6,80	9,35	9,30	19,73	-
1st half 2012	12,18	8,41	10,15	9,69	7,68	9,16	10,33	20,94	-
2nd half 2012	11,59	8,45	10,03	9,72	8,71	9,65	10,88	22,10	-
1st half 2013	11,83	8,64	10,46	9,72	8,86	9,37	10,61	19,52	6,89
2nd half 2013	11,49	8,42	10,80	9,55	7,59	9,61	11,03	18,97	6,81
1st half 2014	10,37	7,64	10,39	7,85	6,89	8,89	11,73	16,37	6,83
2nd half 2014	10,53	7,55	10,29	7,71	7,26	8,75	12,14	17,42	7,06
1st half 2015	10,10	7,23	9,68	7,18	7,88	8,52	13,71	12,56	7,18

Similar to the case of the natural gas pricing per kWh, in the case of electricity the expected cost evolution should also need to be taken into account. In the same report by Solarconcentra technological platform [90], expected evolution for electricity prices for industrial end-users are explained under low, medium and high scenarios. See Table 27.

Table 27. Price estimation for electricity in industries in Spain – 2015/2035 [90].

Consumidor Industrial	ESCENARIO	Precio del kWh (€)		
		2015	2025	2035
Grupo IA	Alto	0.3034	0.6413	0.9792
	Medio	0.2865	0.4555	0.6244
	Bajo	0.2781	0.3626	0.4470
Grupo IB	Alto	0.1614	0.2746	0.3877
	Medio	0.1558	0.2123	0.2689
	Bajo	0.1529	0.1812	0.2095
Grupo IC	Alto	0.1215	0.1888	0.2561
	Medio	0.1181	0.1518	0.1854
	Bajo	0.1164	0.1333	0.1501
Grupo ID	Alto	0.1038	0.1579	0.2121
	Medio	0.1011	0.1281	0.1552
	Bajo	0.0997	0.1132	0.1268
Grupo IE	Alto	0.0801	0.1109	0.1418
	Medio	0.0785	0.0940	0.1094
	Bajo	0.0778	0.0855	0.0932
Grupo IF	Alto	0.0760	0.1276	0.1792
	Medio	0.0734	0.0992	0.1250
	Bajo	0.0721	0.085	0.0979
Grupo IG	Alto	0.0633	0.1168	0.1702
	Medio	0.0607	0.0874	0.1141
	Bajo	0.0593	0.0727	0.0861

As in the case of gas, when using electricity for industrial heat generation, the efficiency of the boiler-heater needs to be taken into account. In this case, efficiency values are much higher and near a value of 100%, with minor losses. So, for an initial calculation, the cost of energy employing electricity for an industrial consumer, even for the highest consumption, is **greater than 0.06 €/kWh**. Similar calculations can be done for other countries also.

5.1.4. Petroleum derivative prices.

The price of the petroleum highly depends on many factors such as political decision, market strategies, demand changes, currency exchange rates, etc. Having this into account, it is understood why different derivatives employed as industrial fuels such as Heating Gas Oil and fuel oil have such a high price variability with time. (See Table 28)

Table 28. Prices in force on 14/12/2015 inclusive of duties and taxes. Source: <https://ec.europa.eu/energy/en/statistics/weekly-oil-bulletin>.

	Heating gas oil	Fuel oil - (III) Soufre <= 1% Sulphur <= 1% Schwefel <= 1%
	1000L	t
Austria	583,17	292,70
Belgium	442,00	178,51
Bulgaria	557,73	
Croatia	555,88	359,62
Cyprus	735,96	501,88
Czech Republic	561,09	242,08
Denmark	1.145,82	679,40
Estonia	691,00	
Finland	720,00	
France	597,75	271,89
Germany	510,00	
Greece	810,00	297,13
Hungary	1.038,02	354,32
Ireland	564,43	524,91
Italy	1.080,35	267,61
Latvia	644,64	
Lithuania	449,23	
Luxembourg	431,72	
Malta	1.000,00	
Netherlands	1.029,00	501,00
Poland	556,78	322,47
Portugal	970,00	453,92
Romania	982,50	406,05
Slovakia		351,73
Slovenia	810,00	447,24
Spain	558,10	273,89
Sweden	974,47	733,10
United Kingdom	517,09	
CE/EC/EG EUR 28 (IV) Moyenne pondérée Weighted average Gewichteter Durchschnitt	580,74	352,51

In the same report by Solarconcentra technological platform [90], Fuel Oil and Heating Diesel Oil prices are gathered from the same source (Oil bulletin, European Commission).

Current (year 2015) and future expected prices in €/kWh for different evolution scenarios (low, medium and high) are published in this report, as shown in the next tables. Information is shown for Spanish market and also for Europe (average). In particular in Tables 29 and 30 Spanish prices are shown.

Table 29. Price and its expected evolution for Fuel Oil. Source: Solarconcentra.

	ESCENARIO	PRECIO (€/kWh)		
		2015	2025	2035
Fuel Oil	Alto	0,0372 ²	0.084	0.132
	Medio		0.060	0.084
	Bajo		0.049	0.060

Table 30. Price and its expected evolution for heating Gas Oil. Source: Solarconcentra.

	ESCENARIO	PRECIO (€/kWh)		
		2015	2025	2035
Gasoleo C	Alto	0.0773 ³	0.146	0.215
	Medio		0.111	0.146
	Bajo		0.094	0.111

In these cases also, similar to the cases employing Natural Gas and Electricity, boiler-heater efficiencies need to be taken into account to calculate the final cost of energy produced employing these fuels.

6. CONCLUSIONS

The Solar Heat Industrial Process (SHIP) sector is one of the direct and more exploitable directions for CSP systems. A lot of components optimization, system engineering and schemes for integration between solar technologies and industrial plants, either in hybrid mode or with energy storage media, is available. Further studies are required to define a combination of technical requirements with economic aspects required at the market level. Constraints on the CAPEX, OPEX and LCOE are major elements to be considered and evaluated by each single project or initiative to be successful in proposing a solution. Modularization and standardization of components for main system categories will introduce a simplification in the system proposed to the end-users, where their interest to be leveraged, their acceptance on the decarbonization target (eventually supported by proper incentives) is still a major priority for a successful implementation of CSP technologies in industries. Reliable business models with in-depth analyses on learning curves, target costs, market potential divided by specific sector are indeed required to create an European roadmap towards an important decarbonization of the thermal and power consumption in the industrial sector.

7. REFERENCES

- [1] EDEN Annex I - “Description of Work”, final version, 16.07.2012;
- [2] EDEN Consortium Agreement, final version signed by partners, 28.03.2012;
- [3] D5.4 - “Establish exploitation and dissemination plan”, WP5, V.1, October 2014;
- [4] EDEN Grant Agreement Number 303472, final version, 22.08.2012;
- [5] “Energy storage Technology Roadmap”, IEA Technology Annex, March 2014;
- [6] “2013 Technology Map of the European Strategic Energy Technology Plan (SET-Plan)”, Joint Research Centre – Institute for Energy and Transport, 2014;
- [7] Kane, M. L. (2003). Small hybrid solar power system. *Energy* 28, 1427–1443.
- [8] Manolakos, D. P. (2007). Experimental evaluation of an autonomous low-temperature solar Rankine cycle system for reverse osmosis desalination. *Desalination* 203, 366–374.
- [9] S. Quoilin, M. O. (2011). Performance and design optimization of a low-cost solar organic Rankine cycle for remote power generation. *Solar Energy* 85, 955-966.
- [10] Wang, X. Z. (2010). Performance evaluation of a low-temperature solar Rankine cycle system utilizing R245fa. *Solar Energy* 84, 353–364.
- [11] FEASIBILITY ASSESSMENT OF SOLAR PROCESS HEAT APPLICATIONS
Christoph Lauterbach, Shahrdad Javid Rad, Bastian Schmitt, Klaus Vajen Kassel University, Institute of Thermal Engineering, Kassel (Germany) www.solar.uni-kassel.de
- [12] SOLAIR : Requirements on the design and configuration of small and medium sized solar air-conditioning applications.
- [13] N. Tauveron, S. Colasson, J-A. Gruss (2015). Conversion of waste heat to electricity: cartography of possible cycles due to hot source characteristics. *Proceeding of ECOS 2015*.
- [14] Häberle, A. (2012): 19 - Concentrating solar technologies for industrial process heat and cooling. In: Keith Lovegrove und Wes Stein (Hg.): *Concentrating Solar Power Technology : Woodhead Publishing Series in Energy*: Woodhead Publishing, S. 602–619. <http://www.sciencedirect.com/science/article/pii/B9781845697693500194>.
- [15] Kempener, Ruud; Burch, Jay; Brunner, Christoph; Navntoft, Christian; Mugnier, Daniel (2015): *Solar Heat for Industrial Processes*. Technology Brief. Hg. v. IEA-ETSAP and IRENA. www.irena.org/Publications, zuletzt geprüft am 10.03.2015.
- [16] Muster, Bettina; Hassine, Ilyes Ben; Helmke, Annabell; Stefan Heß; Krummenacher, Pierre; Schmitt, Bastian; Schnitzer, Hans (2015): *Integration Guideline*. Guideline for solar planners, energy consultants and process engineers giving a general procedure to integrate solar heat into industrial processes by identifying and ranking suitable integration points and solar thermal system concepts. http://task49.iea-shc.org/Data/Sites/7/150218_iea-task-49_d_b2_integration_guideline-final.pdf, zuletzt geprüft am 20.07.2015.

- [17] Schweiger, Hans (2001): POSHIP The Potential of Solar Heat for Industrial Processes. Final Project Report. Hg. v. AguaSol Ingeniería. Barcelona, Spain, zuletzt geprüft am 07.03.2015.
- [18] A. Schuster, S. Karellas, E. Kakaras, H. Spliethoff, Energetic and economic investigation of Organic Rankine Cycle applications *Applied Thermal Engineering* 29 (2009) 1809-1817
- [19] A. Schuster, S. Karellas, R. Aumann, Efficiency optimization potential in supercritical Organic Rankine Cycles *Energy* 35 (2010) 1033 – 1039
- [20] Agustín M. Delgado-Torres, Lourdes García-Rodríguez, Preliminary assessment of solar organic Rankine cycles for driving a desalination system *Desalination* 216 (2007) 252-275
- [21] Agustín M. Delgado-Torres, Lourdes García-Rodríguez, Analysis and optimization of the lowtemperature solar organic Rankine cycle (ORC), *Energy Conversion and Management* 51 (2010) 2846-2856
- [22] Anna Stoppato, Energetic and economic investigation of the operation management of an Organic Rankine Cycle cogeneration plant *Energy* 41 (2012) 3e9
- [23] Bertrand Fankam Tchance, George Papadakis, Gregory Lambrinos, Antonios Frangoudakis, Fluid selection for a low-temperature solar organic Rankine cycle *Applied Thermal Engineering* 29 (2009) 2468-2476
- [24] Bo-Tau Liu, Kuo-Hsiang Chien, Chi-Chuan Wang, Effect of working fluids on organic Rankine cycle for waste heat recovery, *Energy* 29 (2004) 1207-1217
- [25] Guía técnica para la medida y determinación del calor útil, de la electricidad y del ahorro de energía primaria de cogeneración de alta eficiencia. Instituto para la Diversificación y Ahorro de la Energía. Ministerio de Industria, Turismo y Comercio. Gobierno de España, 2008
- [26] Integrated Pollution Prevention and Control (IPPC), Reference Document on the application of Best Available Techniques to Industrial Cooling Systems, December 2001.
- [27] J. Sirchis, Combined Production of Heat and Power (Cogeneration) Elsevier Applied Science 2005
- [28] Jorge Facão, Ana Palmero-Marrero and Armando C. Oliveira, Analysis of a solar assisted micro-cogeneration ORC system *International Journal of Low Carbon Technologies*
- [29] Martin Pehnt, Martin Cames, Corinna Fischer, Barbara Praetorius, Lambert Schneider, Katja Schumacher, Jan-Peter Vo_, *Micro Cogeneration Towards Decentralized Energy Systems* Springer-Verlag Berlin Heidelberg 2006
- [30] Michael J. Moran, Howard N. Shapiro, Bruce R. Munson, David P. DeWitt, *Introduction to Thermal Systems Engineering*, 5th Edition, John Wiley and Sons, Inc. (2006)
- [31] NIST REFPROP data base

- [32] Research Cooperation in Renewable Energy Technologies for Electricity Generation, REELCOOP <<http://www.reelcoop.com>> [accessed 20.12.15]
- [33] S.C. Kaushik, Akhilesh Arora Energy and exergy analysis of single effect and series flow double effect water-lithium bromide absorption refrigeration systems International Journal of Refrigeration 32 (2009) 1247-1258
- [34] S. Quoilin, M. Orosz, H. Hemond, V. Lemort, Performance and design optimization of a lowcost solar organic Rankine cycle for remote power generation Solar Energy 85 (2011) 955-966
- [35] Soteris A. Kalogirou, Solar Energy Engineering Processes and Systems Academic Press Elsevier Inc, Second edition 2014
- [36] Supplementary Material (ESI) for Green Chemistry, The Royal Society of Chemistry 2010
- [37] T. Guo, H.X. Wang, S.J. Zhang, Selection of working fluids for a novel low-temperature geothermally-powered ORC based cogeneration system Energy Conversion and Management 52 (2011) 2384-2391
- [38] T. Guo, H.X. Wang, S.J. Zhang, Fluids and parameters optimization for a novel cogeneration system driven by low-temperature geothermal sources Energy 36 (2011) 2639e2649
- [39] Ulli Drescher, Dieter Bruggemann, Fluid selection for the Organic Rankine Cycle (ORC) in biomass power and heat plants Applied Thermal Engineering 27 (2007) 223-228
- [40] Agency for Toxic Substances and Disease Registry (ATSDR), <http://www.atsdr.cdc.gov/substances/toxsubstance.asp?toxid=14> [accessed 21.12.15]
- [41] <http://www.dowcorning.com/> [accessed 15.06.15]
- [42] http://www.engineeringtoolbox.com/fuels-ignition-temperatures-d_171.html (accessed 15.06.15)
- [43] <http://www.epa.gov> [accessed 11.06.15]
- [44] <http://www3.epa.gov/chp/basic/> [accessed 14.12.2015]
- [45] <http://www.inchem.org/documents/icsc/icsc/eics0353.htm> [accessed 15.06.15]
- [46] Solkane software http://softadvice.informer.com/Solkane_8.html
- [47] <http://webbook.nist.gov/> [accessed 11.06.15]
- [48] Kane, M. L. (2003). Small hybrid solar power system. Energy 28, 1427–1443.
- [49] Manolakos, D. P. (2007). Experimental evaluation of an autonomous low-temperature solar Rankine cycle system for reverse osmosis desalination. Desalination 203, 366–374.
- [50] S. Quoilin, M. O. (2011). Performance and design optimization of a low-cost solar organic Rankine cycle for remote power generation. Solar Energy 85, 955-966.

- [51] Wang, X. Z. (2010). Performance evaluation of a low-temperature solar Rankine cycle system utilizing R245fa. *Solar Energy* 84, 353–364.
- [52] FEASIBILITY ASSESSMENT OF SOLAR PROCESS HEAT APPLICATIONS
Christoph Lauterbach, Shahraddad Javid Rad, Bastian Schmitt, Klaus Vajen Kassel University, Institute of Thermal Engineering, Kassel (Germany) www.solar.uni-kassel.de
- [53] Strategic Research Priorities for Solar Thermal Technology, RHC-Platform, 2012. (http://www.rhc-platform.org/fileadmin/Publications/Solar_thermal_SRP.pdf)
- [54] Solar Heating and Cooling application factsheet, GLOBAL SOLAR WATER HEATING PROJECT, Project partners: Domestic hot water for single family houses, ESTIF (http://www.estif.org/fileadmin/estif/content/publications/downloads/UNEP_2015/factsheet_single_family_houses_v05.pdf)
- [55] Solar Heating and Cooling application factsheet, GLOBAL SOLAR WATER HEATING PROJECT, Project partners: Domestic hot water for single family houses, (http://www.estif.org/fileadmin/estif/content/publications/downloads/UNEP_2015/factsheet_multi_family_houses_v06.pdf)
- [56] Solar Heating and Cooling application factsheet, GLOBAL SOLAR WATER HEATING PROJECT, Project partners: Solar thermal cooling, (http://www.estif.org/fileadmin/estif/content/publications/downloads/UNEP_2015/factsheet_solar_thermal_cooling_v06.pdf)
- [57] Solar Thermal Markets in Europe, 2014 (published June 2015), ESTIF (http://www.estif.org/fileadmin/estif/content/market_data/downloads/2014_solar_thermal_markets_LR.pdf)
- [58] IEA-SHC (2013), “Executive Summary: Solar Cooling Position Paper”, Task 38: Solar Air-Conditioning and Refrigeration, December 2013, (<http://www.iea-shc.org/data/sites/1/publications/IEA-SHC-Solar-Cooling-Position-Paper--Executive-Summary.pdf>)
- [59] Solar Heat for Industrial Processes Technology Brief, IEA-ETSAP and IRENA© Technology Brief E21 – January 2015 (http://www.irena.org/DocumentDownloads/Publications/IRENA_ETSAP_Tech_Brief_E21_Solar_Heat_Industrial_2015.pdf)
- [60] State of the art – Survey on new solar cooling developments, A technical report of subtask C, 31st October 2010, Task 38 Solar Air-Conditioning and Refrigeration
- [61] Augsten, E. (2012), “Europe/Asia: Solar Cooling Gains Traction”, *Solar Thermal World*, 3 September 2012, <http://solarthermalworld.org/content/europeasia-solar-cooling-gains-traction>.
- [62] IEA (2012), “Solar Heating and Cooling Roadmap”, http://www.iea.org/publications/freepublications/publication/Solar_Heating_Cooling_Roadmap_2012_WEB.pdf
- [63] Jakob, U. (2014), “Technologies and Perspectives of Solar Cooling systems”, AHK Conference Sydney, Australia, 24th March 2014, http://www.docstoc.com/docs/169908741/DrJakob_Green_Chiller_Assoc.pdf.

- [64] SOLAR THERMAL MARKETS IN EUROPE Trends and Market Statistics 2014, June 2015, ESTIF
- [65] Mujumdar, A. S. (2007): Handbook of industrial drying. 3rd ed. Boca Raton, FL: CRC.
- [66] Kemp, Ian C. (2011): Fundamentals of Energy Analysis of Dryers. In: Evangelos Tsotsas und Arun S. Mujumdar (Hg.): Modern Drying Technology. Weinheim, Germany: Wiley-VCH Verlag GmbH & Co. KGaA, S. 1–45.
- [67] Ekechukwu, O.V; Norton, B. (1999): Review of solar-energy drying systems II: an overview of solar drying technology. In: Energy Conversion and Management 40 (6), S. 615–655. DOI: 10.1016/S0196-8904(98)00093-4.
- [68] Girovich, M. J. (1996): Biosolids Treatment and Management: Processes for Beneficial Use: Taylor & Francis. Online verfügbar unter <https://books.google.es/books?id=TW5b-kb9gnEC>.
- [69] Kudra, T.; Mujumdar, A. S. (2009): Advanced Drying Technologies, Second Edition: CRC Press. Online verfügbar unter https://books.google.es/books?id=Ksn4Z1_YQdAC.
- [70] Flash Dryer. Online verfügbar unter <http://www.gea.com/global/de/products/flash-dryer.jsp>, zuletzt geprüft am 22.11.2015.
- [71] Ducept, F. (2002): Superheated steam dryer: simulations and experiments on product drying. In: Chemical Engineering Journal 86 (1-2), S. 75–83. DOI: 10.1016/S1385-8947(01)00275-3.
- [72] Air Impingement Dryers - Industrial Air Dryers, Hot Air Impingement Dryers. Online verfügbar unter <http://www.arrowhead-dryers.com/air-impingement-dryers.html>, zuletzt geprüft am 22.11.2015.
- [73] Through drying, Technical Information Paper TIP 0404-25 (2014). Online verfügbar unter <http://www.tappi.org/Bookstore/Standards-TIPs/TIPs/Engineering/0108040425.aspx>, zuletzt geprüft am 22.11.2015.
- [74] Komatsu, Yosuke; Sciazko, Anna; Zakrzewski, Marcin; Kimijima, Shinji; Hashimoto, Akira; Kaneko, Shozo; Szmyd, Janusz S. (2015): An experimental investigation on the drying kinetics of a single coarse particle of Belchatow lignite in an atmospheric superheated steam condition. In: Fuel Processing Technology 131, S. 356–369. DOI: 10.1016/j.fuproc.2014.12.005.
- [75] Concentrated solar power - Airlight Energy. CSP collector data sheet. Online verfügbar unter <http://www.airlightenergy.com/csp/>, zuletzt geprüft am 22.11.2015.
- [76] DLR, G.A. (2007). *Aqua-CSP Study Report, Concentrating Solar Power for Seawater Desalination, Final Report*. Stuttgart: DLR.
- [77] Casimiro, S., Cardoso, J., Alarcón-Padilla, D., Turchi, C., Ioakimidis, C., & Mendes, J. (2014). Modeling multi effect distillation powered by CSP in TRNSYS. *Energy Procedia*, 49, 2241-2250.
- [78] Association, I. D. (2014). *IDA Desalination Yearbook 2014-2015*. Oxford: Media Analytics, Ltd.

- [79] Sommariva, C. (2010). *Desalination and Advanced Water Treatment - Economics and Financing*. Hopkinton: Balaban Desalination Publications.
- [80] Temstet, C., Canton, G., Laborie, J., & Durante, A. (1996). A large high-performance MED plant in Sicily. *Desalination*, 105(1-2), 109-114.
- [81] Palenzuela, P., Alarcón-Padilla, D., & Zaragoza, G. (2015). Large-scale solar desalination by combination with CSP: Techno-economic analysis of different options for the Mediterranean Sea and the Arabian Gulf. *Desalination*, 366, 130-138.
- [82] Programme, U. N. (2008). *Resource and Guidance Manual for Environmental Impact Assessments*. Nairobi: United Nations Environment Programme.
- [83] Ahmed, M., Cardoso, J., Mendes, J., & Casimiro, S. (2015). Reverse osmosis powered by concentrating solar power (CSP): a case study for Trapani, Sicily. *EUROMED 2015: Desalination for Clean Water and Energy*. Palermo. (to be published in *Desalination and Water Treatment*)
- [84] Fytili, D., & Zabaniotou, A. (2008). Utilization of sewage sludge in EU application of old and new methods - A review. *Renewable and Sustainable Energy Reviews*, 12(1), 116-140.
- [85] Neyens, E., & Baeyens, J. (2003). A review of thermal sludge pre-treatment processes to improve dewaterability. *Journal of Hazardous Materials*, 98(1-3), 51-67.
- [86] INTECUS GmbH and C&E Consulting and Engineering GmbH. (2014). *Technical Guide on the Treatment and Recycling Techniques for Sludge from municipal Wastewater Treatment with references to Best Available Techniques (BAT)*. Dessau-Rosslau: Federal Environment Agency (Umweltbundesamt).
- [87] (Briefing Statistical Spotlight April 2015. European Parliament)
- [88] DIRECTIVE 2008/92/EC OF THE EUROPEAN PARLIAMENT AND OF THE COUNCIL of 22 October 2008
- [89] Source: Eurostat, Energy Statistics – prices
- [90] MERCADO POTENCIAL EN ESPAÑA Y APLICACIONES EN TECNOLOGÍAS SOLARES DE CONCENTRACIÓN DE MEDIA TEMPERATURA, December, 2015)
- [91] Glorius, T., Tubergen, J. v., Pretz, T., Khoury, A., & Uepping, R. (s.d.). *BREF "Waste Treatment" Solid Recovered Fuels*. European Recovered Fuel Organisation.
- [92] *What is SRF*. (s.d.), From European Recovered Fuel Organisation: <http://erfo.info>; Accessed 6 January 2016
- [93] Organization, W. H. (2007). *Desalination for Safe Water Supply, Guidance for the Health and Environmental Aspects Applicable to Desalination*. Geneva: World Health Organization.
- [94] Casimiro, S. (2015). *Concentrating Solar Power + Desalination Plants (CSP+D): Models and Performance Analysis*, PhD Thesis. Lisboa: Universidade de Lisboa - Instituto Superior Técnico.

8. APPENDIX

The results of the simulations of an ORC with a heat power exchange in the evaporator of 60 kW and different fluids are presented here. The values on the tables are:

- η_{reg} the regenerator efficiency
- Q_{hot} the evaporator heat power
- Q_{reg} the regenerator heat power
- Q_{cold} the condenser heat power
- W_p the pump mechanical power
- W_{exp} the expander mechanical power
- m_{work} the mass flow of working fluid
- v_3 the specific volume of working fluid at the exit of the expander
- V_3 the volume flow of working fluid at the exit of the expander
- $h_{1'2'}/h_{y2}$ the percentage of heat used to change the phase of the fluid in the evaporator
- $h_{3'4'}/h_{x4}$ the percentage of heat used to change the phase of the fluid in the condenser
- p_{max} the pressure in the evaporator
- p_{cond} the pressure in the condenser
- η_{cycle} the efficiency of the cycle

Results for $T_{\text{cond}} = 20 \text{ }^\circ\text{C}$ and $T_{\text{max}} = 100 \text{ }^\circ\text{C}$

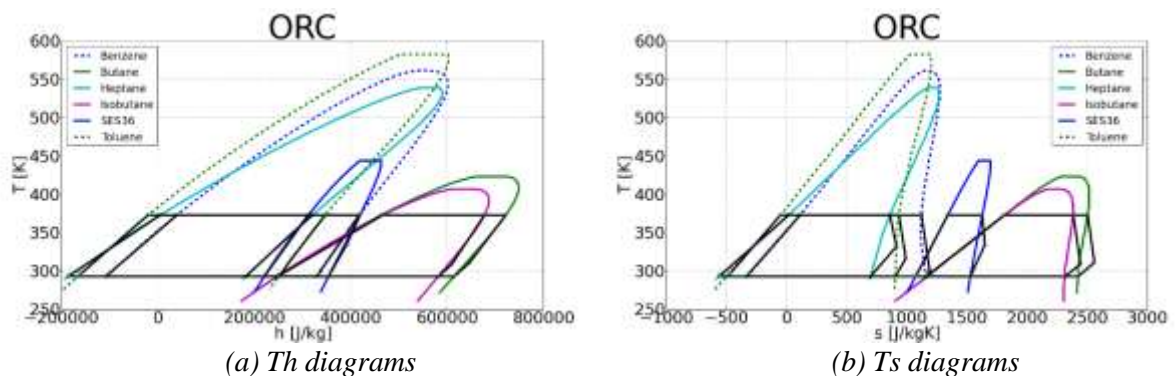


Figure 1: ORC with $T_{\text{cond}} = 20 \text{ }^\circ\text{C}$ and $T_{\text{max}} = 100 \text{ }^\circ\text{C}$

Table 1: Results of the cycle for $T_{cond} = 20.0\text{ }^{\circ}\text{C}$ and $T_{max} = 100.0\text{ }^{\circ}\text{C}$

	ϵ_{reg} (%)	\dot{Q}_{hot} (kW)	\dot{Q}_{reg} (kW)	\dot{Q}_{cold} (kW)	W_p (kW)	W_{exp} (kW)	\dot{m}_{work} (kg/s)	v_3 (m ³ /kg)	\dot{V}_3 (m ³ /s)	$\frac{h_{12}}{h_{y2}}$ (%)	$\frac{h_{34}}{h_{x4}}$ (%)	P_{evap} (bar)	P_{cond} (bar)	η_{cycle} (%)
Benzene	0.0	60.0	0.0	-50.9	0.1	9.1	0.114	3.172	0.363	72.2	98.1	1.8	0.1	15.1
	80.0	60.0	0.7	-50.8	0.1	9.2	0.116	3.172	0.367	73.0	99.4	1.8	0.1	15.3
Butane	0.0	60.0	0.0	-50.9	0.4	9.6	0.128	0.197	0.025	54.9	92.0	15.3	2.1	15.4
	80.0	60.0	3.2	-50.4	0.4	10.1	0.135	0.197	0.027	57.9	97.9	15.3	2.1	16.2
Heptane	0.0	60.0	0.0	-51.6	0.1	8.5	0.119	4.290	0.509	62.4	84.6	1.1	0.1	14.1
	80.0	60.0	7.0	-50.6	0.1	9.5	0.132	4.290	0.568	69.7	96.4	1.1	0.1	15.7
Isobutane	0.0	60.0	0.0	-50.9	0.5	9.5	0.140	0.132	0.018	49.4	92.3	19.9	3.0	14.9
	80.0	60.0	3.2	-50.4	0.6	10.0	0.148	0.132	0.019	52.0	98.1	19.9	3.0	15.7
SES36	0.0	60.0	0.0	-51.7	0.2	8.5	0.303	0.253	0.077	54.2	78.0	6.3	0.6	13.9
	80.0	60.0	10.5	-50.2	0.2	10.0	0.356	0.253	0.090	63.8	94.4	6.3	0.6	16.3
Toluene	0.0	60.0	0.0	-52.3	0.1	8.2	0.118	2.650	0.312	72.2	94.1	0.8	0.1	13.6
	80.0	60.0	2.3	-52.0	0.1	8.5	0.122	2.650	0.324	75.0	98.2	0.8	0.1	14.2

Results for $T_{cond} = 20\text{ }^{\circ}\text{C}$ and $T_{max} = 150\text{ }^{\circ}\text{C}$

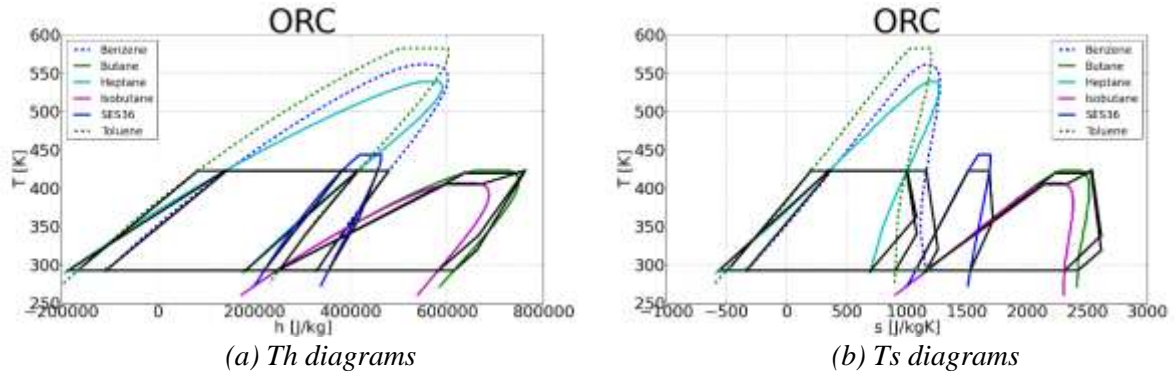


Figure 2: ORC with $T_{cond} = 20\text{ }^{\circ}\text{C}$ and $T_{max} = 150\text{ }^{\circ}\text{C}$

Table 2: Results of the cycle for $T_{cond} = 20.0\text{ }^{\circ}\text{C}$ and $T_{max} = 150.0\text{ }^{\circ}\text{C}$

	ϵ_{reg} (%)	\dot{Q}_{hot} (kW)	\dot{Q}_{reg} (kW)	\dot{Q}_{cold} (kW)	W_p (kW)	W_{exp} (kW)	\dot{m}_{work} (kg/s)	v_3 (m ³ /kg)	\dot{V}_3 (m ³ /s)	$\frac{h_{12}}{h_{y2}}$ (%)	$\frac{h_{34}}{h_{x4}}$ (%)	P_{evap} (bar)	P_{cond} (bar)	η_{cycle} (%)
Benzene	0.0	60.0	0.0	-47.8	0.1	12.2	0.103	3.380	0.347	57.5	93.5	5.8	0.1	20.2
	80.0	60.0	2.5	-47.3	0.1	12.7	0.107	3.380	0.361	59.9	98.4	5.8	0.1	21.1
Butane	0.0	60.0	0.0	-49.0	0.8	11.9	0.119	0.200	0.024	20.4	88.7	35.0	2.1	18.5
	80.0	60.0	4.4	-48.2	0.9	12.8	0.127	0.200	0.025	21.9	96.7	35.0	2.1	19.9
Heptane	0.0	60.0	0.0	-49.2	0.1	10.8	0.100	4.620	0.462	45.8	74.7	3.8	0.1	17.9
	80.0	60.0	11.9	-47.1	0.1	12.9	0.120	4.620	0.554	54.9	93.6	3.8	0.1	21.4
Isobutane	0.0	60.0	0.0	-49.4	0.8	11.3	0.118	0.149	0.018	14.5	80.0	35.0	3.0	17.4
	80.0	60.0	8.8	-47.9	1.0	13.0	0.135	0.149	0.020	16.7	94.7	35.0	3.0	20.0
SES36	0.0	60.0	0.0	-49.7	0.4	10.7	0.257	0.273	0.070	31.6	68.7	17.6	0.6	17.1
	80.0	60.0	15.3	-47.1	0.5	13.4	0.322	0.273	0.088	39.7	91.0	17.6	0.6	21.5
Toluene	0.0	60.0	0.0	-49.1	0.1	11.3	0.104	2.687	0.279	57.7	88.3	2.8	0.1	18.8
	80.0	60.0	4.7	-48.2	0.1	12.2	0.112	2.687	0.301	62.2	96.9	2.8	0.1	20.3

Results for $T_{cond} = 20\text{ }^{\circ}\text{C}$ and $T_{max} = 200\text{ }^{\circ}\text{C}$

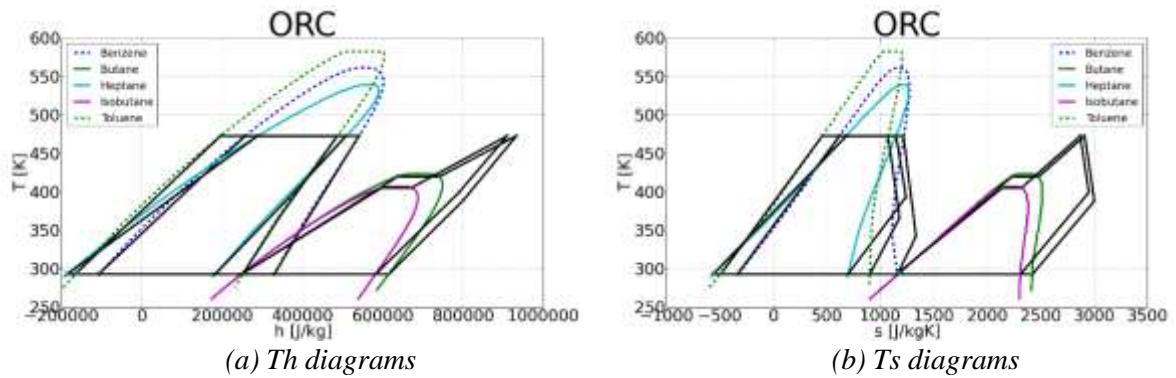


Figure 3: ORC with $T_{cond} = 20\text{ }^{\circ}\text{C}$ and $T_{max} = 200\text{ }^{\circ}\text{C}$

Table 3: Results of the cycle for $T_{cond} = 20.0\text{ }^{\circ}\text{C}$ and $T_{max} = 200.0\text{ }^{\circ}\text{C}$

	ϵ_{reg} (%)	\dot{Q}_{hot} (kW)	\dot{Q}_{reg} (kW)	\dot{Q}_{cold} (kW)	\dot{W}_p (kW)	\dot{W}_{exp} (kW)	\dot{m}_{work} (kg/s)	v_3 (m ³ /kg)	\dot{V}_3 (m ³ /s)	$\frac{h_{12}}{h_{y2}}$ (%)	$\frac{h_{34}}{h_{y4}}$ (%)	P _{evap} (bar)	P _{cond} (bar)	η_{cycle} (%)
Benzene	0.0	60.0	0.0	-45.8	0.2	14.4	0.093	3.610	0.336	43.9	88.7	14.4	0.1	23.7
	80.0	60.0	4.3	-44.7	0.2	15.4	0.100	3.610	0.360	47.1	97.2	14.4	0.1	25.4
Butane	0.0	60.0	0.0	-48.8	0.6	11.9	0.089	0.256	0.023	15.3	66.6	35.0	2.1	18.7
	80.0	60.0	16.2	-45.8	0.8	15.1	0.113	0.256	0.029	19.4	90.2	35.0	2.1	23.8
Heptane	0.0	60.0	0.0	-47.9	0.2	12.2	0.086	5.022	0.434	31.7	66.5	9.8	0.1	20.1
	80.0	60.0	16.3	-44.6	0.2	15.5	0.110	5.022	0.552	40.4	90.8	9.8	0.1	25.5
Isobutane	0.0	60.0	0.0	-49.6	0.7	11.0	0.091	0.181	0.017	11.2	61.7	35.0	3.0	17.2
	80.0	60.0	20.0	-46.1	0.9	14.6	0.122	0.181	0.022	15.0	88.5	35.0	3.0	23.0
Toluene	0.0	60.0	0.0	-46.8	0.1	13.4	0.092	2.775	0.256	44.8	82.3	7.5	0.1	22.2
	80.0	60.0	7.3	-45.2	0.1	15.1	0.104	2.775	0.288	50.2	95.5	7.5	0.1	24.9

Results for $T_{cond} = 20\text{ }^{\circ}\text{C}$ and $T_{max} = 250\text{ }^{\circ}\text{C}$

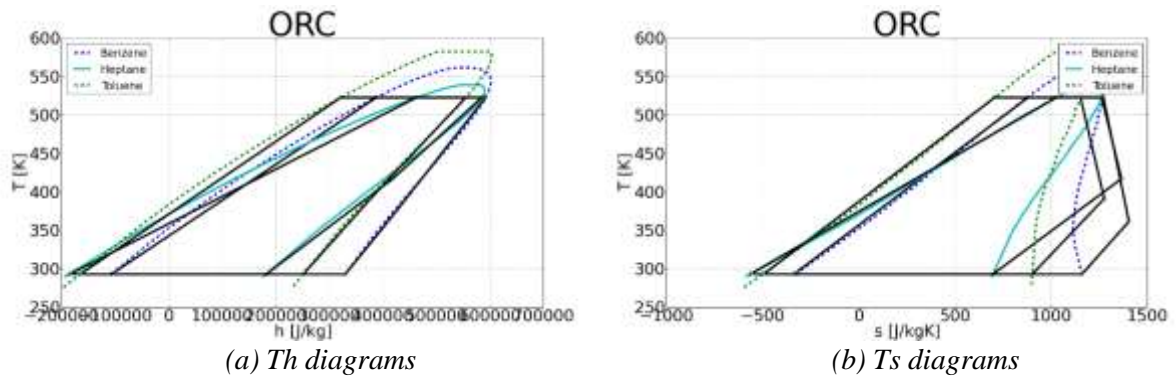


Figure 4: ORC with $T_{cond} = 20\text{ }^{\circ}\text{C}$ and $T_{max} = 250\text{ }^{\circ}\text{C}$

Table 4: Results of the cycle for $T_{cond} = 20.0\text{ }^{\circ}\text{C}$ and $T_{max} = 250.0\text{ }^{\circ}\text{C}$

	ϵ_{reg} (%)	\dot{Q}_{hot} (kW)	\dot{Q}_{reg} (kW)	\dot{Q}_{cold} (kW)	\dot{W}_p (kW)	\dot{W}_{exp} (kW)	\dot{m}_{work} (kg/s)	v_3 (m ³ /kg)	\dot{V}_3 (m ³ /s)	$\frac{h_{12}}{h_{y2}}$ (%)	$\frac{h_{34}}{h_{y4}}$ (%)	P _{evap} (bar)	P _{cond} (bar)	η_{cycle} (%)
Benzene	0.0	60.0	0.0	-44.6	0.4	15.7	0.086	3.816	0.330	29.4	84.5	29.9	0.1	25.6
	80.0	60.0	5.9	-43.1	0.4	17.3	0.095	3.816	0.362	32.3	96.1	29.9	0.1	28.2
Heptane	0.0	60.0	0.0	-47.2	0.3	13.0	0.078	5.334	0.417	15.9	60.9	21.5	0.1	21.2
	80.0	60.0	19.5	-43.1	0.4	17.3	0.103	5.334	0.552	21.1	88.4	21.5	0.1	28.1
Toluene	0.0	60.0	0.0	-45.3	0.2	14.8	0.083	2.973	0.248	32.4	76.8	16.7	0.1	24.4
	80.0	60.0	9.7	-42.9	0.2	17.2	0.097	2.973	0.288	37.7	94.2	16.7	0.1	28.3

Results for $T_{cond} = 20\text{ }^{\circ}\text{C}$ and $T_{max} = 300\text{ }^{\circ}\text{C}$

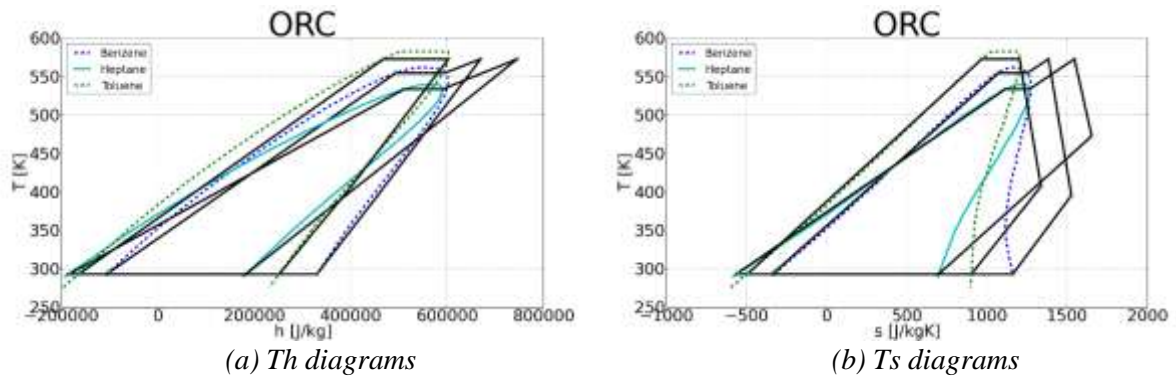


Figure 5: ORC with $T_{cond} = 20\text{ }^{\circ}\text{C}$ and $T_{max} = 300\text{ }^{\circ}\text{C}$

Table 5: Results of the cycle for $T_{cond} = 20.0\text{ }^{\circ}\text{C}$ and $T_{max} = 300.0\text{ }^{\circ}\text{C}$

	ϵ_{reg} (%)	\dot{Q}_{hot} (kW)	\dot{Q}_{reg} (kW)	\dot{Q}_{cold} (kW)	\dot{W}_p (kW)	\dot{W}_{exp} (kW)	\dot{m}_{work} (kg/s)	v_3 (m ³ /kg)	\dot{V}_3 (m ³ /s)	$\frac{\dot{W}_{reg}}{\dot{Q}_{hot}}$ (%)	$\frac{\dot{W}_{exp}}{\dot{Q}_{hot}}$ (%)	P_{evap} (bar)	P_{cond} (bar)	η_{cycle} (%)
Benzene	0.0	60.0	0.0	-43.8	0.5	16.7	0.078	4.176	0.325	13.2	77.6	45.0	0.1	26.9
	80.0	60.0	8.8	-41.5	0.6	19.1	0.089	4.176	0.373	15.1	94.1	45.0	0.1	30.9
Heptane	0.0	60.0	0.0	-47.4	0.3	12.9	0.065	6.060	0.392	8.6	50.3	25.0	0.1	21.0
	80.0	60.0	27.3	-41.6	0.4	18.7	0.094	6.060	0.571	12.5	83.3	25.0	0.1	30.5
Toluene	0.0	60.0	0.0	-44.5	0.4	15.8	0.079	3.099	0.243	17.6	73.6	32.7	0.1	25.7
	80.0	60.0	11.0	-41.7	0.4	18.7	0.093	3.099	0.288	20.8	93.1	32.7	0.1	30.5

Results for $T_{cond} = 20\text{ }^{\circ}\text{C}$ and $T_{max} = 350\text{ }^{\circ}\text{C}$

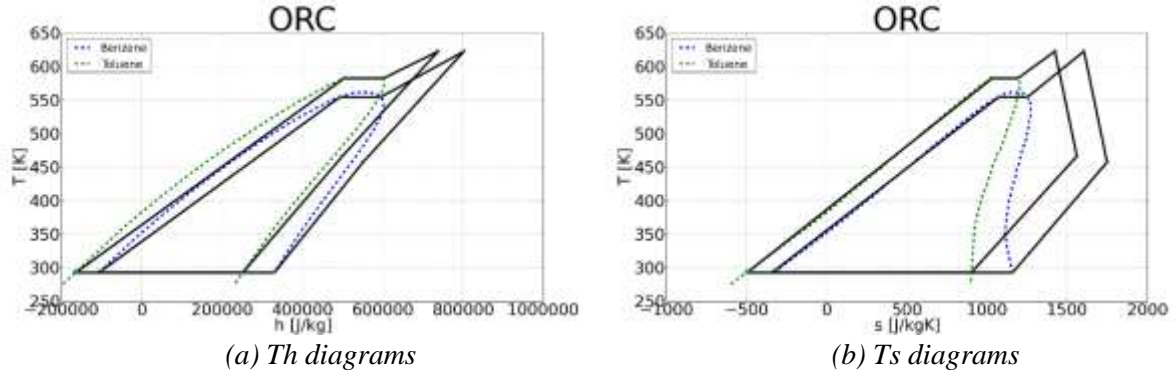


Figure 6: ORC with $T_{cond} = 20\text{ }^{\circ}\text{C}$ and $T_{max} = 350\text{ }^{\circ}\text{C}$

Table 6: Results of the cycle for $T_{cond} = 20.0\text{ }^{\circ}\text{C}$ and $T_{max} = 350.0\text{ }^{\circ}\text{C}$

	ϵ_{reg} (%)	\dot{Q}_{hot} (kW)	\dot{Q}_{reg} (kW)	\dot{Q}_{cold} (kW)	\dot{W}_p (kW)	\dot{W}_{exp} (kW)	\dot{m}_{work} (kg/s)	v_3 (m ³ /kg)	\dot{V}_3 (m ³ /s)	$\frac{\dot{W}_{reg}}{\dot{Q}_{hot}}$ (%)	$\frac{\dot{W}_{exp}}{\dot{Q}_{hot}}$ (%)	P_{evap} (bar)	P_{cond} (bar)	η_{cycle} (%)
Benzene	0.0	60.0	0.0	-43.7	0.4	16.7	0.067	4.838	0.322	11.3	66.4	45.0	0.1	27.1
	80.0	60.0	14.4	-39.8	0.5	20.7	0.082	4.838	0.399	13.9	90.4	45.0	0.1	33.6
Toluene	0.0	60.0	0.0	-44.4	0.4	15.9	0.067	3.565	0.238	10.9	62.7	37.0	0.1	26.0
	80.0	60.0	16.9	-40.0	0.5	20.4	0.086	3.565	0.305	14.0	89.2	37.0	0.1	33.2

Results for $T_{\text{cond}} = 30\text{ }^{\circ}\text{C}$ and $T_{\text{max}} = 100\text{ }^{\circ}\text{C}$

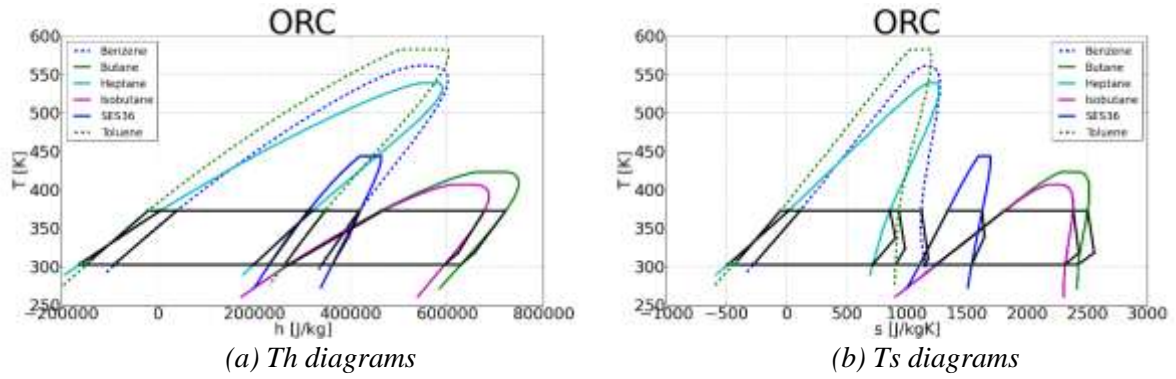


Figure 7: ORC with $T_{\text{cond}} = 30\text{ }^{\circ}\text{C}$ and $T_{\text{max}} = 100\text{ }^{\circ}\text{C}$

Table 7: Results of the cycle for $T_{\text{cond}} = 30.0\text{ }^{\circ}\text{C}$ and $T_{\text{max}} = 100.0\text{ }^{\circ}\text{C}$

	ϵ_{reg} (%)	\dot{Q}_{bot} (kW)	\dot{Q}_{reg} (kW)	\dot{Q}_{cold} (kW)	W_p (kW)	W_{exp} (kW)	\dot{m}_{work} (kg/s)	v_3 (m ³ /kg)	\dot{V}_3 (m ³ /s)	$\frac{h_{12}-h_{v2}}{h_{v2}}$ (%)	$\frac{h_{34}-h_{v4}}{h_{v4}}$ (%)	P _{evap} (bar)	P _{cond} (bar)	η_{cycle} (%)
Benzene	0.0	60.0	0.0	-51.9	0.1	8.2	0.119	1.655	0.196	74.8	98.1	1.8	0.2	13.6
	80.0	60.0	0.7	-51.9	0.1	8.3	0.120	1.655	0.198	75.6	99.3	1.8	0.2	13.7
Butane	0.0	60.0	0.0	-51.5	0.4	8.7	0.134	0.144	0.019	57.7	92.7	15.3	2.9	13.9
	80.0	60.0	3.1	-51.1	0.4	9.2	0.141	0.144	0.020	60.6	98.3	15.3	2.9	14.6
Heptane	0.0	60.0	0.0	-52.6	0.1	7.7	0.125	1.966	0.245	65.7	85.9	1.1	0.1	12.8
	80.0	60.0	6.3	-51.8	0.1	8.5	0.138	1.966	0.271	72.5	96.3	1.1	0.1	14.2
Isobutane	0.0	60.0	0.0	-52.3	0.5	8.1	0.149	0.101	0.015	52.4	92.1	19.9	4.0	12.6
	80.0	60.0	3.3	-51.9	0.6	8.5	0.157	0.101	0.016	55.3	98.0	19.9	4.0	13.3
SES36	0.0	60.0	0.0	-52.5	0.2	7.7	0.320	0.178	0.057	57.2	79.7	6.3	0.8	12.5
	80.0	60.0	9.8	-51.3	0.2	8.9	0.372	0.178	0.066	66.6	94.9	6.3	0.8	14.6
Toluene	0.0	60.0	0.0	-53.2	0.1	7.4	0.123	1.802	0.221	75.1	94.6	0.8	0.2	12.4
	80.0	60.0	1.9	-53.0	0.1	7.7	0.127	1.802	0.228	77.5	98.0	0.8	0.2	12.8

Results for $T_{\text{cond}} = 30\text{ }^{\circ}\text{C}$ and $T_{\text{max}} = 150\text{ }^{\circ}\text{C}$

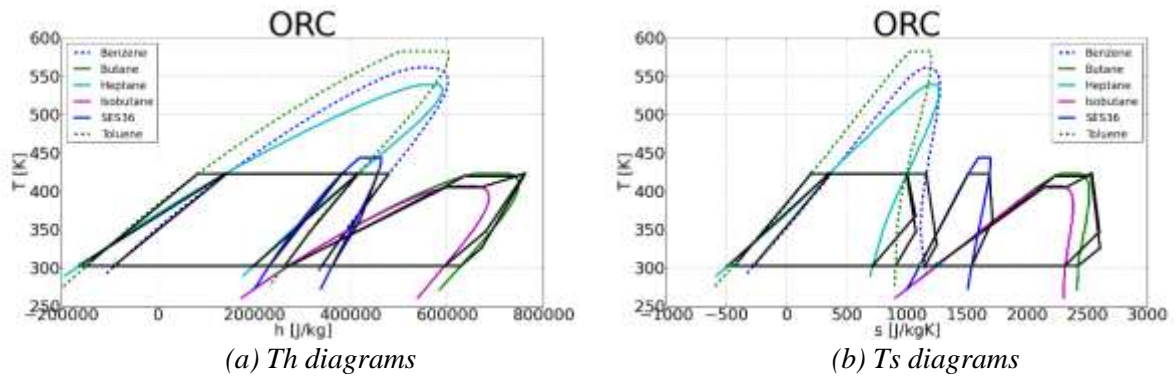
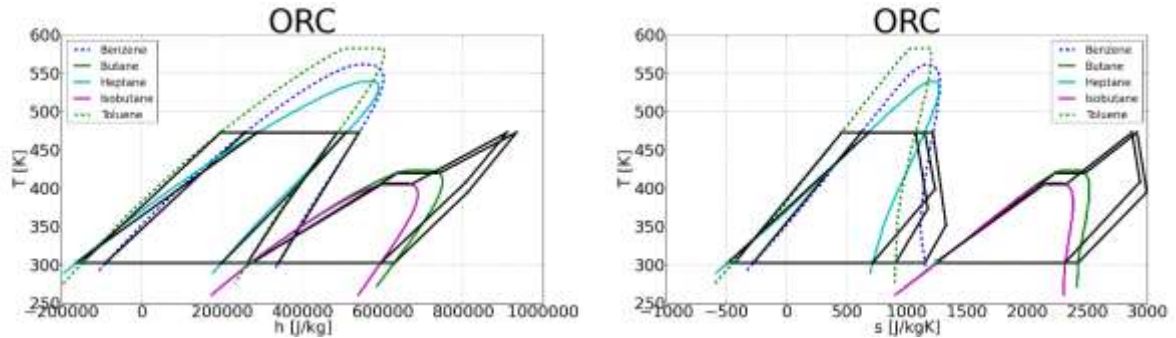


Figure 8: ORC with $T_{\text{cond}} = 30\text{ }^{\circ}\text{C}$ and $T_{\text{max}} = 150\text{ }^{\circ}\text{C}$

Table 8: Results of the cycle for $T_{\text{cond}} = 30.0\text{ }^{\circ}\text{C}$ and $T_{\text{max}} = 150.0\text{ }^{\circ}\text{C}$

	ϵ_{reg} (%)	\dot{Q}_{bot} (kW)	\dot{Q}_{reg} (kW)	\dot{Q}_{cold} (kW)	W_p (kW)	W_{exp} (kW)	\dot{m}_{work} (kg/s)	v_3 (m ³ /kg)	\dot{V}_3 (m ³ /s)	$\frac{h_{12}-h_{v2}}{h_{v2}}$ (%)	$\frac{h_{34}-h_{v4}}{h_{v4}}$ (%)	P _{evap} (bar)	P _{cond} (bar)	η_{cycle} (%)
Benzene	0.0	60.0	0.0	-48.6	0.1	11.4	0.106	1.742	0.184	59.2	93.3	5.8	0.2	18.9
	80.0	60.0	2.6	-48.1	0.1	11.9	0.110	1.742	0.192	61.8	98.4	5.8	0.2	19.7
Butane	0.0	60.0	0.0	-49.5	0.9	11.2	0.124	0.149	0.018	21.4	89.3	35.0	2.9	17.2
	80.0	60.0	4.3	-48.8	0.9	12.0	0.133	0.149	0.020	22.9	97.1	35.0	2.9	18.5
Heptane	0.0	60.0	0.0	-50.0	0.1	10.2	0.104	2.111	0.220	47.8	75.4	3.8	0.1	16.8
	80.0	60.0	11.5	-48.1	0.1	12.1	0.124	2.111	0.262	57.0	93.5	3.8	0.1	20.1
Isobutane	0.0	60.0	0.0	-50.7	0.9	10.1	0.124	0.114	0.014	15.3	79.2	35.0	4.0	15.3
	80.0	60.0	9.4	-49.2	1.0	11.6	0.144	0.114	0.016	17.7	94.3	35.0	4.0	17.7
SES36	0.0	60.0	0.0	-50.4	0.4	10.0	0.269	0.191	0.051	33.1	69.7	17.6	0.8	16.0
	80.0	60.0	14.9	-48.0	0.5	12.5	0.336	0.191	0.064	41.3	91.3	17.6	0.8	19.9
Toluene	0.0	60.0	0.0	-49.9	0.1	10.7	0.107	1.820	0.196	59.7	88.6	2.8	0.2	17.8
	80.0	60.0	4.5	-49.1	0.1	11.5	0.116	1.820	0.210	64.2	96.7	2.8	0.2	19.1

Results for $T_{\text{cond}} = 30\text{ }^{\circ}\text{C}$ and $T_{\text{max}} = 200\text{ }^{\circ}\text{C}$



(a) Th diagrams

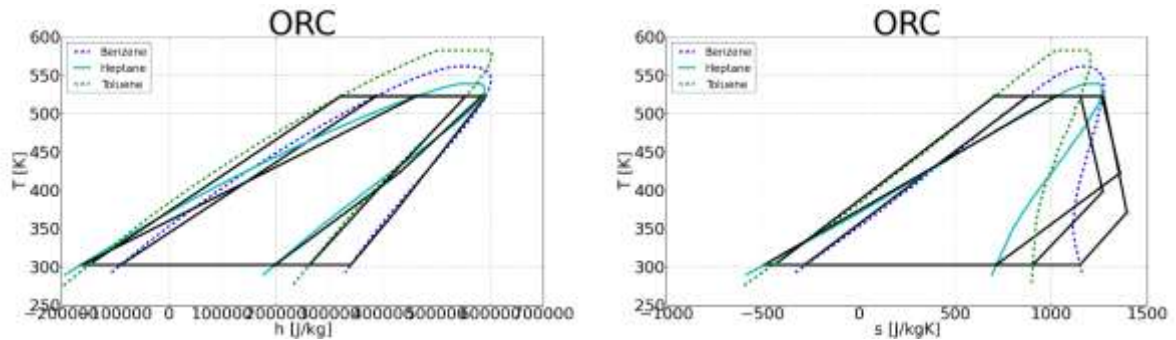
(b) Ts diagrams

Figure 9: ORC with $T_{\text{cond}} = 30\text{ }^{\circ}\text{C}$ and $T_{\text{max}} = 200\text{ }^{\circ}\text{C}$

Table 9: Results of the cycle for $T_{\text{cond}} = 30.0\text{ }^{\circ}\text{C}$ and $T_{\text{max}} = 200.0\text{ }^{\circ}\text{C}$

	ϵ_{reg} (%)	\dot{Q}_{hot} (kW)	\dot{Q}_{reg} (kW)	\dot{Q}_{cold} (kW)	W_p (kW)	W_{exp} (kW)	\dot{m}_{work} (kg/s)	v_3 (m ³ /kg)	\dot{V}_3 (m ³ /s)	$\frac{h_{1-2}}{h_{y2}}$ (%)	$\frac{h_{3-4}}{h_{x4}}$ (%)	P_{evap} (bar)	P_{cond} (bar)	η_{cycle} (%)
Benzene	0.0	60.0	0.0	-46.4	0.2	13.7	0.095	1.794	0.171	45.1	88.3	14.4	0.2	22.5
	80.0	60.0	4.6	-45.4	0.2	14.7	0.103	1.794	0.184	48.5	97.3	14.4	0.2	24.2
Butane	0.0	60.0	0.0	-49.5	0.6	11.1	0.092	0.189	0.017	15.8	66.1	35.0	2.9	17.4
	80.0	60.0	17.0	-46.5	0.8	14.2	0.118	0.189	0.022	20.3	90.2	35.0	2.9	22.3
Heptane	0.0	60.0	0.0	-48.5	0.2	11.6	0.089	2.296	0.205	32.8	66.8	9.8	0.1	19.1
	80.0	60.0	16.3	-45.3	0.2	14.8	0.114	2.296	0.261	41.7	90.8	9.8	0.1	24.3
Isobutane	0.0	60.0	0.0	-50.9	0.7	9.7	0.095	0.138	0.013	11.7	60.4	35.0	4.0	15.1
	80.0	60.0	0.0	-50.9	0.7	9.7	0.095	0.138	0.013	11.7	60.4	35.0	4.0	15.1
Toluene	0.0	60.0	0.0	-47.5	0.1	12.9	0.095	1.906	0.182	46.2	82.4	7.5	0.2	21.4
	80.0	60.0	7.2	-46.0	0.1	14.5	0.107	1.906	0.203	51.7	95.3	7.5	0.2	23.9

Results for $T_{\text{cond}} = 30\text{ }^{\circ}\text{C}$ and $T_{\text{max}} = 250\text{ }^{\circ}\text{C}$



(a) Th diagrams

(b) Ts diagrams

Figure 10: ORC with $T_{\text{cond}} = 30\text{ }^{\circ}\text{C}$ and $T_{\text{max}} = 250\text{ }^{\circ}\text{C}$

Table 10: Results of the cycle for $T_{\text{cond}} = 30.0\text{ }^{\circ}\text{C}$ and $T_{\text{max}} = 250.0\text{ }^{\circ}\text{C}$

	ϵ_{reg} (%)	\dot{Q}_{hot} (kW)	\dot{Q}_{reg} (kW)	\dot{Q}_{cold} (kW)	W_p (kW)	W_{exp} (kW)	\dot{m}_{work} (kg/s)	v_3 (m ³ /kg)	\dot{V}_3 (m ³ /s)	$\frac{h_{1-2}}{h_{y2}}$ (%)	$\frac{h_{3-4}}{h_{x4}}$ (%)	P_{evap} (bar)	P_{cond} (bar)	η_{cycle} (%)
Benzene	0.0	60.0	0.0	-45.2	0.4	15.0	0.089	1.906	0.169	30.1	84.0	29.9	0.2	24.4
	80.0	60.0	6.3	-43.7	0.4	16.6	0.098	1.906	0.186	33.3	96.1	29.9	0.2	27.0
Heptane	0.0	60.0	0.0	-47.6	0.3	12.5	0.080	2.439	0.196	16.4	61.0	21.5	0.1	20.2
	80.0	60.0	19.7	-43.6	0.4	16.5	0.107	2.439	0.260	21.7	88.6	21.5	0.1	26.9
Toluene	0.0	60.0	0.0	-45.9	0.2	14.4	0.086	2.039	0.175	33.3	76.8	16.7	0.2	23.6
	80.0	60.0	9.8	-43.6	0.2	16.7	0.100	2.039	0.203	38.8	93.9	16.7	0.2	27.4

Results for $T_{\text{cond}} = 30 \text{ }^\circ\text{C}$ and $T_{\text{max}} = 300 \text{ }^\circ\text{C}$

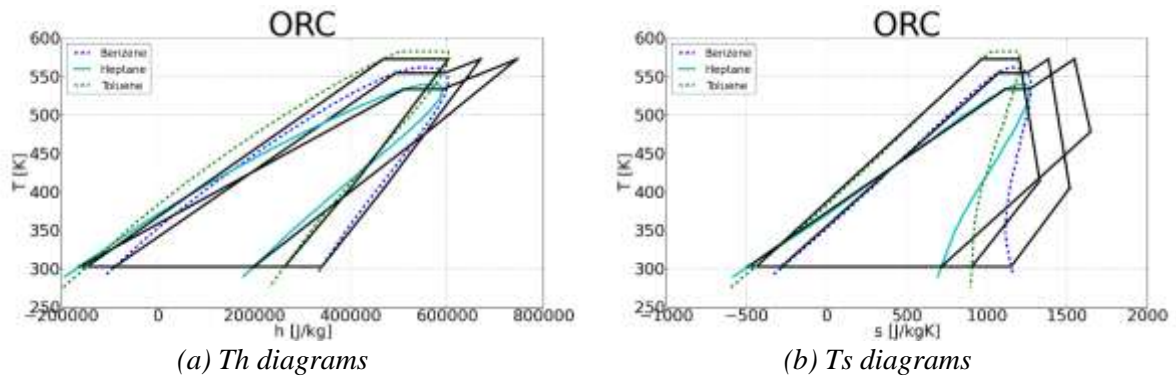


Figure 11: ORC with $T_{\text{cond}} = 30 \text{ }^\circ\text{C}$ and $T_{\text{max}} = 300 \text{ }^\circ\text{C}$

Table 11: Results of the cycle for $T_{\text{cond}} = 30.0 \text{ }^\circ\text{C}$ and $T_{\text{max}} = 300.0 \text{ }^\circ\text{C}$

	ϵ_{reg} (%)	\dot{Q}_{hot} (kW)	\dot{Q}_{reg} (kW)	\dot{Q}_{cold} (kW)	\dot{W}_p (kW)	\dot{W}_{exp} (kW)	\dot{m}_{work} (kg/s)	v_3 (m ³ /kg)	\dot{V}_3 (m ³ /s)	$\frac{\dot{h}_{12}}{\dot{h}_{y2}}$ (%)	$\frac{\dot{h}_{34}}{\dot{h}_{x4}}$ (%)	P_{evap} (bar)	P_{cond} (bar)	η_{cycle} (%)
Benzene	0.0	60.0	0.0	-44.5	0.5	16.0	0.080	2.070	0.165	13.5	76.9	45.0	0.2	25.7
	80.0	60.0	9.3	-42.1	0.6	18.4	0.092	2.070	0.190	15.6	93.9	45.0	0.2	29.7
Heptane	0.0	60.0	0.0	-47.8	0.3	12.3	0.066	2.772	0.184	8.8	50.1	25.0	0.1	20.0
	80.0	60.0	27.9	-42.1	0.4	18.0	0.097	2.772	0.269	12.8	83.3	25.0	0.1	29.3
Toluene	0.0	60.0	0.0	-44.9	0.4	15.3	0.080	2.124	0.170	18.0	73.4	32.7	0.2	24.8
	80.0	60.0	11.3	-42.0	0.5	18.2	0.095	2.124	0.202	21.3	93.2	32.7	0.2	29.5

Results for $T_{\text{cond}} = 30 \text{ }^\circ\text{C}$ and $T_{\text{max}} = 350 \text{ }^\circ\text{C}$

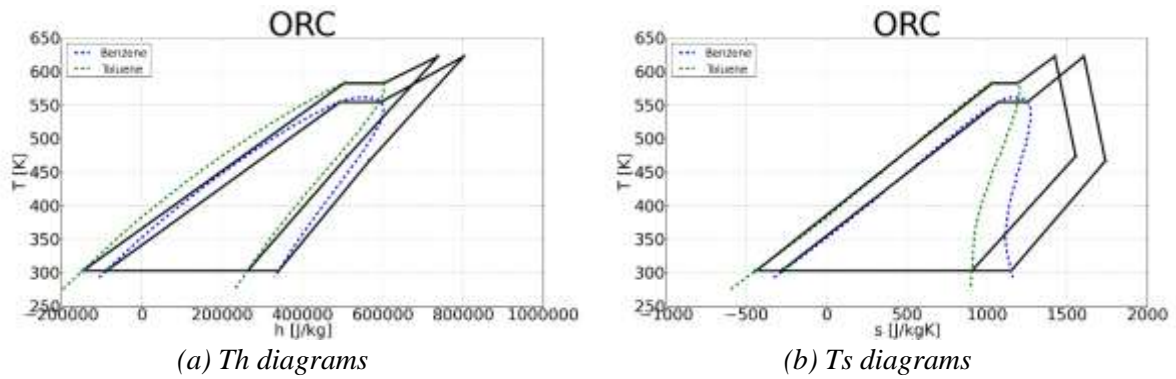


Figure 12: ORC with $T_{\text{cond}} = 30 \text{ }^\circ\text{C}$ and $T_{\text{max}} = 350 \text{ }^\circ\text{C}$

Table 12: Results of the cycle for $T_{\text{cond}} = 30.0 \text{ }^\circ\text{C}$ and $T_{\text{max}} = 350.0 \text{ }^\circ\text{C}$

	ϵ_{reg} (%)	\dot{Q}_{hot} (kW)	\dot{Q}_{reg} (kW)	\dot{Q}_{cold} (kW)	\dot{W}_p (kW)	\dot{W}_{exp} (kW)	\dot{m}_{work} (kg/s)	v_3 (m ³ /kg)	\dot{V}_3 (m ³ /s)	$\frac{\dot{h}_{12}}{\dot{h}_{y2}}$ (%)	$\frac{\dot{h}_{34}}{\dot{h}_{x4}}$ (%)	P_{evap} (bar)	P_{cond} (bar)	η_{cycle} (%)
Benzene	0.0	60.0	0.0	-44.4	0.4	16.0	0.068	2.450	0.166	11.5	65.5	45.0	0.2	25.9
	80.0	60.0	15.2	-40.5	0.5	20.0	0.085	2.450	0.208	14.4	90.1	45.0	0.2	32.4
Toluene	0.0	60.0	0.0	-44.8	0.4	15.4	0.068	2.439	0.166	11.1	62.3	37.0	0.2	25.0
	80.0	60.0	17.3	-40.5	0.5	19.8	0.088	2.439	0.214	14.4	89.0	37.0	0.2	32.3

Results for $T_{cond} = 40\text{ }^{\circ}\text{C}$ and $T_{max} = 100\text{ }^{\circ}\text{C}$

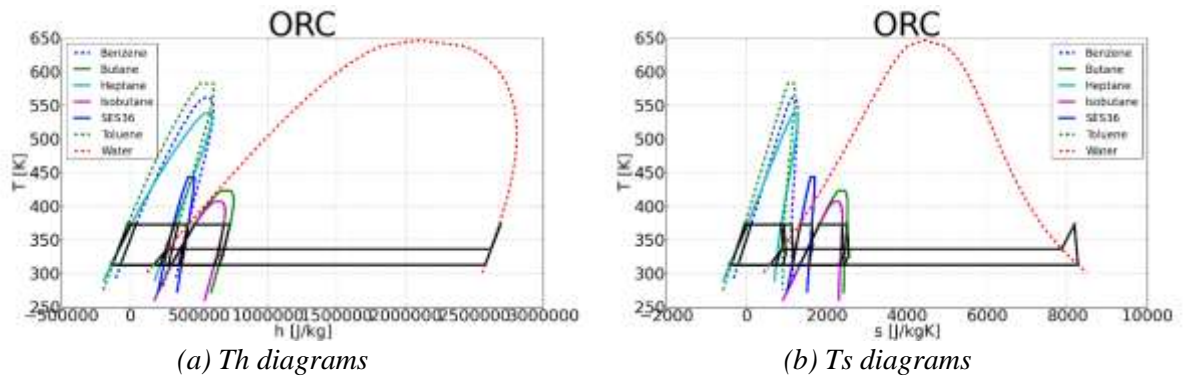


Figure 13: ORC with $T_{cond} = 40\text{ }^{\circ}\text{C}$ and $T_{max} = 100\text{ }^{\circ}\text{C}$

Table 13: Results of the cycle for $T_{cond} = 40.0\text{ }^{\circ}\text{C}$ and $T_{max} = 100.0\text{ }^{\circ}\text{C}$

	ϵ_{reg} (%)	\dot{Q}_{hot} (kW)	\dot{Q}_{reg} (kW)	\dot{Q}_{cool} (kW)	\dot{W}_p (kW)	\dot{W}_{exp} (kW)	\dot{m}_{cool} (kg/s)	v_3 (m ³ /kg)	\dot{V}_3 (m ³ /s)	$\frac{\dot{W}_{reg}}{\dot{W}_{y2}}$ (%)	$\frac{\dot{Q}_{reg}}{\dot{Q}_{y4}}$ (%)	P_{evap} (bar)	P_{cond} (bar)	η_{cycle} (%)
Benzene	0.0	60.0	0.0	-53.0	0.1	7.2	0.123	1.120	0.138	77.5	98.0	1.8	0.3	11.9
	80.0	60.0	0.7	-52.9	0.1	7.2	0.124	1.120	0.139	78.4	99.3	1.8	0.3	12.0
Butane	0.0	60.0	0.0	-52.7	0.4	7.4	0.142	0.110	0.016	60.9	92.9	15.3	3.8	11.8
	80.0	60.0	3.2	-52.3	0.4	7.8	0.149	0.110	0.016	64.2	98.5	15.3	3.8	12.4
Heptane	0.0	60.0	0.0	-53.6	0.1	6.9	0.131	1.275	0.168	69.2	87.2	1.1	0.2	11.4
	80.0	60.0	5.6	-53.0	0.1	7.5	0.144	1.275	0.183	75.6	96.3	1.1	0.2	12.5
Isobutane	0.0	60.0	0.0	-54.1	0.5	6.5	0.159	0.078	0.012	56.0	91.7	19.9	5.3	9.9
	80.0	60.0	3.5	-53.7	0.6	6.9	0.168	0.078	0.013	59.3	97.7	19.9	5.3	10.5
SES36	0.0	60.0	0.0	-53.4	0.2	6.8	0.339	0.126	0.043	60.7	81.4	6.3	1.2	11.0
	80.0	60.0	9.0	-52.4	0.2	7.8	0.390	0.126	0.049	69.8	95.4	6.3	1.2	12.6
Toluene	0.0	60.0	0.0	-54.2	0.1	6.6	0.127	1.366	0.174	78.0	95.2	0.8	0.2	11.0
	80.0	60.0	1.6	-54.0	0.1	6.8	0.131	1.366	0.179	80.1	98.0	0.8	0.2	11.3
Water	0.0	60.0	0.0	-57.3	0.1	2.7	0.024	19.404	0.462	93.3	100.0	0.2	0.1	4.4

Results for $T_{cond} = 40\text{ }^{\circ}\text{C}$ and $T_{max} = 150\text{ }^{\circ}\text{C}$

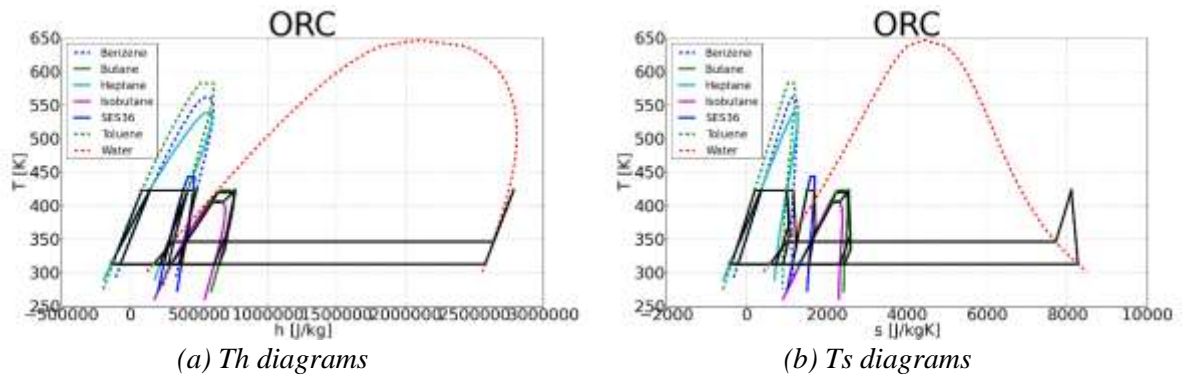
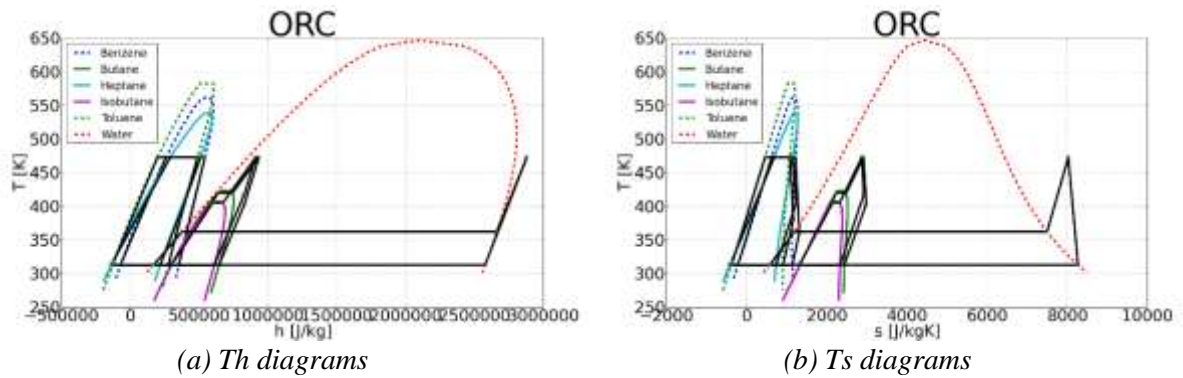


Figure 14: ORC with $T_{cond} = 40\text{ }^{\circ}\text{C}$ and $T_{max} = 150\text{ }^{\circ}\text{C}$

Table 14: Results of the cycle for $T_{cond} = 40.0\text{ }^{\circ}\text{C}$ and $T_{max} = 150.0\text{ }^{\circ}\text{C}$

	ϵ_{reg} (%)	\dot{Q}_{hot} (kW)	\dot{Q}_{reg} (kW)	\dot{Q}_{cool} (kW)	\dot{W}_p (kW)	\dot{W}_{exp} (kW)	\dot{m}_{cool} (kg/s)	v_3 (m ³ /kg)	\dot{V}_3 (m ³ /s)	$\frac{\dot{W}_{reg}}{\dot{W}_{y2}}$ (%)	$\frac{\dot{Q}_{reg}}{\dot{Q}_{y4}}$ (%)	P_{evap} (bar)	P_{cond} (bar)	η_{cycle} (%)
Benzene	0.0	60.0	0.0	-49.5	0.1	10.6	0.109	1.167	0.127	61.1	93.2	5.8	0.3	17.5
	80.0	60.0	2.7	-49.0	0.1	11.1	0.114	1.167	0.133	63.9	98.4	5.8	0.3	18.3
Butane	0.0	60.0	0.0	-50.5	0.9	10.1	0.131	0.114	0.015	22.5	89.3	35.0	3.8	15.4
	80.0	60.0	4.4	-49.8	1.0	10.9	0.140	0.114	0.016	24.1	97.1	35.0	3.8	16.5
Heptane	0.0	60.0	0.0	-50.8	0.1	9.5	0.109	1.383	0.151	49.9	76.2	3.8	0.2	15.7
	80.0	60.0	11.2	-49.1	0.1	11.3	0.129	1.383	0.179	59.2	93.5	3.8	0.2	18.6
Isobutane	0.0	60.0	0.0	-52.3	0.9	8.6	0.131	0.088	0.012	16.1	78.2	35.0	5.3	12.9
	80.0	60.0	10.1	-51.0	1.1	10.1	0.153	0.088	0.013	18.9	93.7	35.0	5.3	15.1
SES36	0.0	60.0	0.0	-51.2	0.4	9.3	0.282	0.136	0.039	34.8	70.7	17.6	1.2	14.7
	80.0	60.0	14.5	-49.0	0.5	11.5	0.351	0.136	0.048	43.2	91.7	17.6	1.2	18.3
Toluene	0.0	60.0	0.0	-50.6	0.1	10.0	0.111	1.376	0.153	61.7	88.9	2.8	0.2	16.6
	80.0	60.0	4.4	-49.9	0.1	10.8	0.119	1.376	0.164	66.2	96.6	2.8	0.2	17.9
Water	0.0	60.0	0.0	-55.3	0.1	4.8	0.023	8.919	0.205	89.0	100.0	0.4	0.1	7.9

Results for $T_{\text{cond}} = 40 \text{ }^\circ\text{C}$ and $T_{\text{max}} = 200 \text{ }^\circ\text{C}$

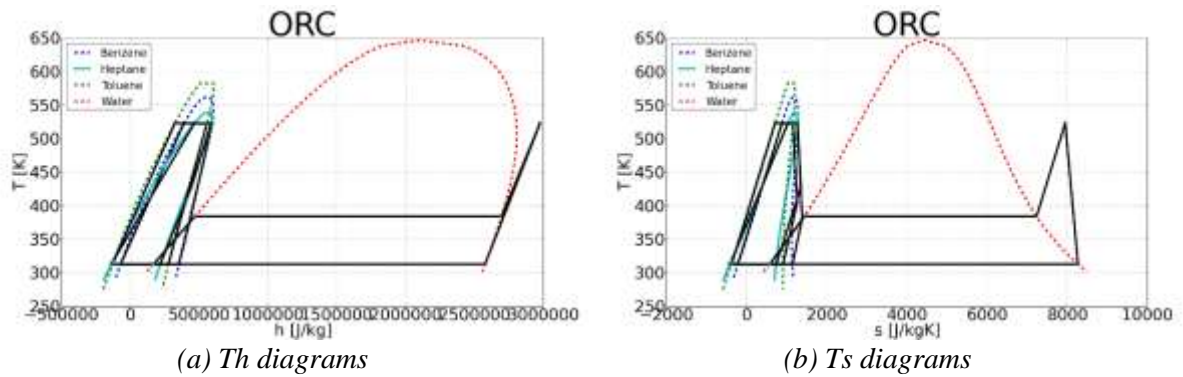


(a) Th diagrams (b) Ts diagrams
Figure 15: ORC with $T_{\text{cond}} = 40 \text{ C}$ and $T_{\text{max}} = 200 \text{ C}$

Table 15: Results of the cycle for $T_{\text{cond}} = 40.0 \text{ C}$ and $T_{\text{max}} = 200.0 \text{ C}$

	ϵ_{reg} (%)	\dot{Q}_{hot} (kW)	\dot{Q}_{reg} (kW)	\dot{Q}_{cold} (kW)	\dot{W}_{p} (kW)	\dot{W}_{exp} (kW)	\dot{m}_{work} (kg/s)	v_3 (m ³ /kg)	V_3 (m ³ /s)	$\frac{n_{1,2}}{n_{y,2}}$ (%)	$\frac{n_{3,4}}{n_{x,4}}$ (%)	P_{evap} (bar)	P_{cond} (bar)	η_{cycle} (%)
Benzene	0.0	60.0	0.0	-47.1	0.2	12.9	0.098	1.254	0.123	46.3	88.0	14.4	0.3	21.2
	80.0	60.0	4.8	-46.1	0.2	14.0	0.106	1.254	0.133	50.1	97.2	14.4	0.3	22.9
Butane	0.0	60.0	0.0	-50.5	0.7	10.0	0.095	0.144	0.014	16.4	65.1	35.0	3.8	15.5
	80.0	60.0	18.1	-47.6	0.9	13.0	0.124	0.144	0.018	21.4	89.9	35.0	3.8	20.2
Heptane	0.0	60.0	0.0	-49.2	0.2	11.0	0.093	1.503	0.140	34.1	67.1	9.8	0.2	18.1
	80.0	60.0	16.2	-46.2	0.2	14.0	0.118	1.503	0.177	43.3	90.7	9.8	0.2	23.0
Isobutane	0.0	60.0	0.0	-52.4	0.7	8.3	0.099	0.107	0.011	12.2	58.9	35.0	5.3	12.7
	80.0	60.0	0.0	-52.4	0.7	8.3	0.099	0.107	0.011	12.2	58.9	35.0	5.3	12.7
Toluene	0.0	60.0	0.0	-48.2	0.1	12.3	0.098	1.465	0.144	47.6	82.5	7.5	0.2	20.4
	80.0	60.0	7.2	-46.7	0.1	13.8	0.110	1.465	0.161	53.3	95.2	7.5	0.2	22.8
Water	0.0	60.0	0.0	-53.3	0.1	6.7	0.022	11.511	0.255	84.3	100.0	0.7	0.1	11.2

Results for $T_{\text{cond}} = 40 \text{ }^\circ\text{C}$ and $T_{\text{max}} = 250 \text{ }^\circ\text{C}$



(a) Th diagrams (b) Ts diagrams
Figure 16: ORC with $T_{\text{cond}} = 40 \text{ C}$ and $T_{\text{max}} = 250 \text{ C}$

Table 16: Results of the cycle for $T_{\text{cond}} = 40.0 \text{ C}$ and $T_{\text{max}} = 250.0 \text{ C}$

	ϵ_{reg} (%)	\dot{Q}_{hot} (kW)	\dot{Q}_{reg} (kW)	\dot{Q}_{cold} (kW)	\dot{W}_{p} (kW)	\dot{W}_{exp} (kW)	\dot{m}_{work} (kg/s)	v_3 (m ³ /kg)	V_3 (m ³ /s)	$\frac{n_{1,2}}{n_{y,2}}$ (%)	$\frac{n_{3,4}}{n_{x,4}}$ (%)	P_{evap} (bar)	P_{cond} (bar)	η_{cycle} (%)
Benzene	0.0	60.0	0.0	-45.9	0.4	14.3	0.091	1.321	0.120	30.9	83.6	29.9	0.3	23.2
	80.0	60.0	6.6	-44.4	0.4	15.9	0.101	1.321	0.133	34.3	96.0	29.9	0.3	25.8
Heptane	0.0	60.0	0.0	-48.2	0.3	11.9	0.083	1.596	0.132	16.9	61.2	21.5	0.2	19.2
	80.0	60.0	19.9	-44.2	0.4	15.8	0.110	1.596	0.176	22.5	88.7	21.5	0.2	25.6
Toluene	0.0	60.0	0.0	-46.5	0.2	13.8	0.088	1.565	0.138	34.3	76.7	16.7	0.2	22.7
	80.0	60.0	9.9	-44.3	0.2	16.1	0.103	1.565	0.161	39.9	93.8	16.7	0.2	26.4
Water	0.0	60.0	0.0	-51.5	0.1	8.5	0.021	6.572	0.141	79.4	100.0	1.5	0.1	14.2

Results for $T_{cond} = 40\text{ °C}$ and $T_{max} = 300\text{ °C}$

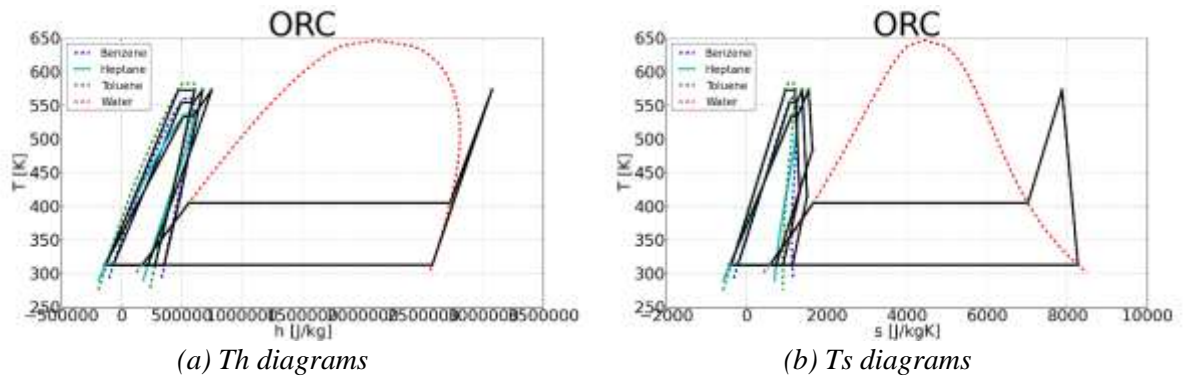


Figure 17: ORC with $T_{cond} = 40\text{ °C}$ and $T_{max} = 300\text{ °C}$

Table 17: Results of the cycle for $T_{cond} = 40.0\text{ °C}$ and $T_{max} = 300.0\text{ °C}$

	ϵ_{reg} (%)	\dot{Q}_{hot} (kW)	\dot{Q}_{reg} (kW)	\dot{Q}_{cold} (kW)	\dot{W}_p (kW)	\dot{W}_{exp} (kW)	\dot{m}_{work} (kg/s)	v_3 (m ³ /kg)	V_3 (m ³ /s)	$\frac{\dot{m}_{reg}}{\dot{m}_{y2}}$ (%)	$\frac{\dot{m}_{reg}}{\dot{m}_{x4}}$ (%)	P_{evap} (bar)	P_{cond} (bar)	η_{cycle} (%)
Benzene	0.0	60.0	0.0	-45.2	0.5	15.2	0.081	1.475	0.120	13.8	76.3	45.0	0.3	24.5
	80.0	60.0	9.8	-42.7	0.6	17.7	0.095	1.475	0.140	16.0	93.8	45.0	0.3	28.5
Heptane	0.0	60.0	0.0	-48.3	0.3	11.7	0.068	1.812	0.123	9.0	49.9	25.0	0.2	19.0
	80.0	60.0	28.6	-42.8	0.5	17.3	0.100	1.812	0.182	13.3	83.2	25.0	0.2	28.1
Toluene	0.0	60.0	0.0	-45.4	0.4	14.8	0.082	1.629	0.134	18.4	73.2	32.7	0.2	23.9
	80.0	60.0	11.5	-42.6	0.5	17.6	0.098	1.629	0.159	21.9	93.1	32.7	0.2	28.5
Water	0.0	60.0	0.0	-49.8	0.1	10.2	0.021	6.951	0.144	74.7	100.0	2.9	0.1	17.1

Results for $T_{cond} = 40\text{ °C}$ and $T_{max} = 350\text{ °C}$

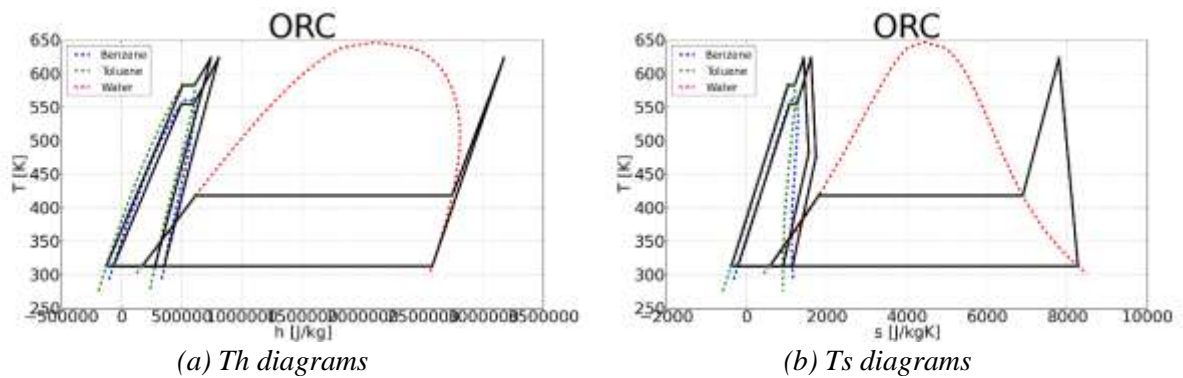


Figure 18: ORC with $T_{cond} = 40\text{ °C}$ and $T_{max} = 350\text{ °C}$

Table 18: Results of the cycle for $T_{cond} = 40.0\text{ °C}$ and $T_{max} = 350.0\text{ °C}$

	ϵ_{reg} (%)	\dot{Q}_{hot} (kW)	\dot{Q}_{reg} (kW)	\dot{Q}_{cold} (kW)	\dot{W}_p (kW)	\dot{W}_{exp} (kW)	\dot{m}_{work} (kg/s)	v_3 (m ³ /kg)	V_3 (m ³ /s)	$\frac{\dot{m}_{reg}}{\dot{m}_{y2}}$ (%)	$\frac{\dot{m}_{reg}}{\dot{m}_{x4}}$ (%)	P_{evap} (bar)	P_{cond} (bar)	η_{cycle} (%)
Benzene	0.0	60.0	0.0	-45.1	0.4	15.2	0.069	1.634	0.113	11.7	64.7	45.0	0.3	24.6
	80.0	60.0	16.0	-41.2	0.6	19.3	0.088	1.634	0.143	14.8	89.8	45.0	0.3	31.2
Toluene	0.0	60.0	0.0	-45.3	0.4	14.8	0.069	1.867	0.129	11.3	61.9	37.0	0.2	24.0
	80.0	60.0	17.9	-40.9	0.5	19.2	0.090	1.867	0.168	14.7	89.0	37.0	0.2	31.2
Water	0.0	60.0	0.0	-48.1	0.1	11.9	0.020	13.118	0.262	70.9	100.0	4.2	0.1	19.8

Results for $T_{cond} = 40\text{ }^{\circ}\text{C}$ and $T_{max} = 400\text{ }^{\circ}\text{C}$

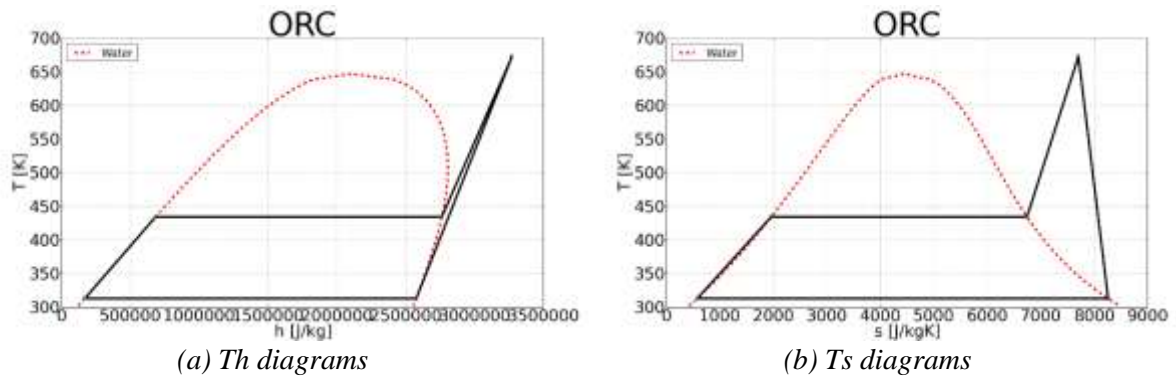


Figure 19: ORC with $T_{cond} = 40\text{ }^{\circ}\text{C}$ and $T_{max} = 400\text{ }^{\circ}\text{C}$

Table 19: Results of the cycle for $T_{cond} = 40.0\text{ }^{\circ}\text{C}$ and $T_{max} = 400.0\text{ }^{\circ}\text{C}$

	ϵ_{reg} (%)	\dot{Q}_{hot} (kW)	\dot{Q}_{reg} (kW)	\dot{Q}_{cond} (kW)	\dot{W}_p (kW)	\dot{W}_{exp} (kW)	$\dot{m}_{working}$ (kg/s)	v_1 (m ³ /kg)	V_3 (m ³ /s)	$\frac{\dot{m}_{reg}}{\dot{m}_{y2}}$ (%)	$\frac{\dot{m}_{reg}}{\dot{m}_{x4}}$ (%)	P_{evap} (bar)	P_{cond} (bar)	η_{cycle} (%)
Water	0.0	60.0	0.0	-46.6	0.1	13.5	0.019	6.871	0.133	67.0	100.0	6.4	0.1	22.4

Results for $T_{cond} = 80\text{ }^{\circ}\text{C}$ and $T_{max} = 150\text{ }^{\circ}\text{C}$

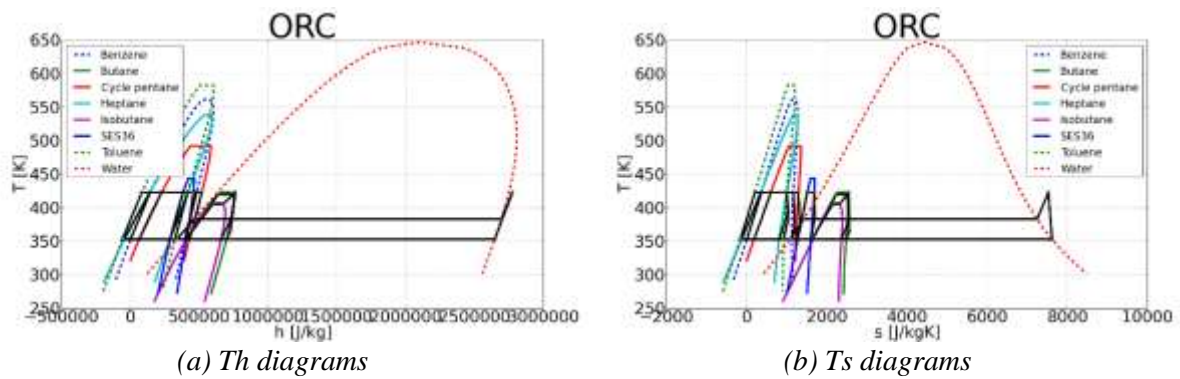
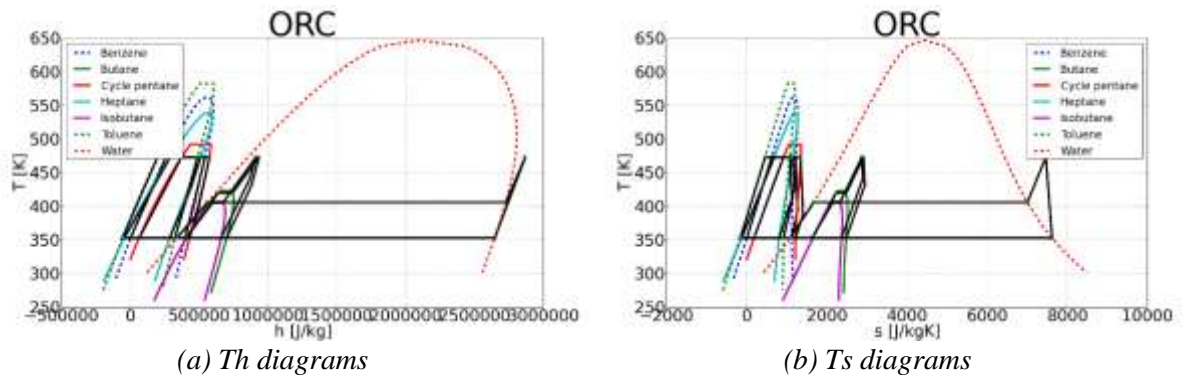


Figure 20: ORC with $T_{cond} = 80\text{ }^{\circ}\text{C}$ and $T_{max} = 150\text{ }^{\circ}\text{C}$

Table 20: Results of the cycle for $T_{cond} = 80.0\text{ }^{\circ}\text{C}$ and $T_{max} = 150.0\text{ }^{\circ}\text{C}$

	ϵ_{reg} (%)	\dot{Q}_{hot} (kW)	\dot{Q}_{reg} (kW)	\dot{Q}_{cond} (kW)	\dot{W}_p (kW)	\dot{W}_{exp} (kW)	$\dot{m}_{working}$ (kg/s)	v_1 (m ³ /kg)	V_3 (m ³ /s)	$\frac{\dot{m}_{reg}}{\dot{m}_{y2}}$ (%)	$\frac{\dot{m}_{reg}}{\dot{m}_{x4}}$ (%)	P_{evap} (bar)	P_{cond} (bar)	η_{cycle} (%)
Benzene	0.0	60.0	0.0	-53.1	0.1	7.0	0.126	0.378	0.047	70.4	93.1	5.8	1.0	11.5
	80.0	60.0	3.1	-52.8	0.1	7.3	0.132	0.378	0.050	74.0	98.5	5.8	1.0	12.1
Butane	0.0	60.0	0.0	-54.5	1.1	6.3	0.170	0.043	0.007	29.3	91.4	35.0	10.1	8.8
	80.0	60.0	3.3	-54.3	1.1	6.7	0.180	0.043	0.008	30.9	97.0	35.0	10.1	9.3
Cycle pentane	0.0	60.0	0.0	-52.1	0.2	8.0	0.132	0.159	0.021	64.1	92.6	11.8	2.6	12.9
	80.0	60.0	3.3	-51.7	0.2	8.4	0.139	0.159	0.022	67.6	98.4	11.8	2.6	13.6
Heptane	0.0	60.0	0.0	-53.9	0.1	6.1	0.131	0.540	0.071	59.9	79.8	3.8	0.6	10.1
	80.0	60.0	10.1	-52.9	0.1	7.2	0.153	0.540	0.082	70.0	95.1	3.8	0.6	11.8
Isobutane	0.0	60.0	0.0	-55.2	1.0	5.5	0.171	0.033	0.006	21.0	78.1	35.0	13.4	7.6
	80.0	60.0	10.7	-54.3	1.1	6.5	0.201	0.033	0.007	24.7	93.6	35.0	13.4	8.9
SES36	0.0	60.0	0.0	-54.2	0.5	6.3	0.359	0.041	0.015	44.2	76.5	17.6	3.8	9.6
	80.0	60.0	11.7	-53.1	0.6	7.5	0.429	0.041	0.018	52.9	93.5	17.6	3.8	11.5
Toluene	0.0	60.0	0.0	-53.5	0.1	6.7	0.127	0.740	0.094	70.5	90.3	2.8	0.5	11.2
	80.0	60.0	4.3	-53.0	0.1	7.2	0.136	0.740	0.101	75.5	97.6	2.8	0.5	12.0
Water	0.0	60.0	0.0	-56.8	0.1	3.2	0.025	2.500	0.062	91.5	100.0	1.4	0.5	5.3

Results for $T_{cond} = 80\text{ }^{\circ}\text{C}$ and $T_{max} = 200\text{ }^{\circ}\text{C}$

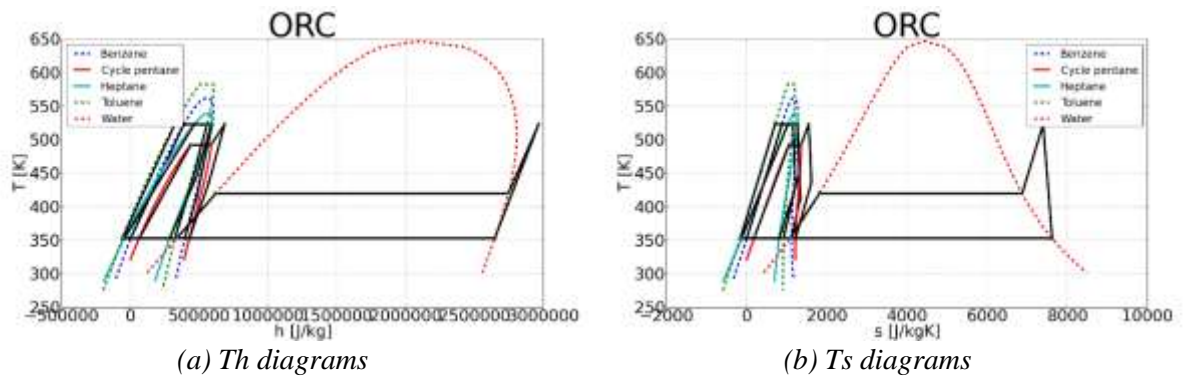


(a) Th diagrams (b) Ts diagrams
Figure 21: ORC with $T_{cond} = 80\text{ }^{\circ}\text{C}$ and $T_{max} = 200\text{ }^{\circ}\text{C}$

Table 21: Results of the cycle for $T_{cond} = 80.0\text{ }^{\circ}\text{C}$ and $T_{max} = 200.0\text{ }^{\circ}\text{C}$

	ϵ_{reg} (%)	\dot{Q}_{hot} (kW)	\dot{Q}_{reg} (kW)	\dot{Q}_{cold} (kW)	\dot{W}_p (kW)	\dot{W}_{exp} (kW)	\dot{m}_{work} (kg/s)	v_3 (m ³ /kg)	V_3 (m ³ /s)	$\frac{\dot{W}_{exp}}{\dot{Q}_{reg}}$ (%)	$\frac{\dot{W}_{exp}}{\dot{Q}_{hot}}$ (%)	P_{evap} (bar)	P_{cond} (bar)	η_{cycle} (%)
Benzene	0.0	60.0	0.0	-50.4	0.2	9.8	0.112	0.409	0.046	52.7	87.1	14.4	1.0	16.0
	80.0	60.0	5.6	-49.5	0.3	10.8	0.122	0.409	0.050	57.6	96.9	14.4	1.0	17.5
Butane	0.0	60.0	0.0	-54.5	0.7	6.1	0.115	0.056	0.006	19.8	61.7	35.0	10.1	9.0
	80.0	60.0	0.0	-54.5	0.7	6.1	0.115	0.056	0.006	19.8	61.7	35.0	10.1	9.0
Cycle pentane	0.0	60.0	0.0	-49.7	0.5	10.6	0.118	0.167	0.020	40.0	86.8	26.6	2.6	16.8
	80.0	60.0	5.7	-48.8	0.6	11.6	0.129	0.167	0.022	43.8	96.8	26.6	2.6	18.4
Heptane	0.0	60.0	0.0	-52.0	0.2	8.2	0.109	0.586	0.064	39.8	68.8	9.8	0.6	13.3
	80.0	60.0	16.4	-49.8	0.3	10.4	0.138	0.586	0.081	50.7	91.5	9.8	0.6	17.0
Isobutane	0.0	60.0	0.0	-55.4	0.7	5.1	0.120	0.042	0.005	14.8	54.7	35.0	13.4	7.4
	80.0	60.0	0.0	-55.4	0.7	5.1	0.120	0.042	0.005	14.8	54.7	35.0	13.4	7.4
Toluene	0.0	60.0	0.0	-50.6	0.1	9.5	0.110	0.792	0.087	53.5	82.9	7.5	0.5	15.7
	80.0	60.0	7.7	-49.4	0.1	10.8	0.125	0.792	0.099	60.3	95.9	7.5	0.5	17.7
Water	0.0	60.0	0.0	-54.7	0.1	5.3	0.024	2.755	0.065	85.6	100.0	3.0	0.5	8.8

Results for $T_{cond} = 80\text{ }^{\circ}\text{C}$ and $T_{max} = 250\text{ }^{\circ}\text{C}$



(a) Th diagrams (b) Ts diagrams
Figure 22: ORC with $T_{cond} = 80\text{ }^{\circ}\text{C}$ and $T_{max} = 250\text{ }^{\circ}\text{C}$

Table 22: Results of the cycle for $T_{cond} = 80.0\text{ }^{\circ}\text{C}$ and $T_{max} = 250.0\text{ }^{\circ}\text{C}$

	ϵ_{reg} (%)	\dot{Q}_{hot} (kW)	\dot{Q}_{reg} (kW)	\dot{Q}_{cold} (kW)	\dot{W}_p (kW)	\dot{W}_{exp} (kW)	\dot{m}_{work} (kg/s)	v_3 (m ³ /kg)	V_3 (m ³ /s)	$\frac{\dot{W}_{exp}}{\dot{Q}_{reg}}$ (%)	$\frac{\dot{W}_{exp}}{\dot{Q}_{hot}}$ (%)	P_{evap} (bar)	P_{cond} (bar)	η_{cycle} (%)
Benzene	0.0	60.0	0.0	-49.0	0.5	11.5	0.102	0.427	0.044	34.8	82.2	29.9	1.0	18.4
	80.0	60.0	7.7	-47.6	0.5	13.0	0.115	0.427	0.049	39.3	95.4	29.9	1.0	20.8
Cycle pentane	0.0	60.0	0.0	-49.5	0.6	11.0	0.097	0.192	0.019	24.0	71.8	35.0	2.6	17.4
	80.0	60.0	13.5	-47.1	0.7	13.5	0.119	0.192	0.023	29.4	92.4	35.0	2.6	21.3
Heptane	0.0	60.0	0.0	-51.1	0.4	9.3	0.096	0.621	0.059	19.5	61.8	21.5	0.6	14.9
	80.0	60.0	20.8	-48.0	0.5	12.6	0.129	0.621	0.080	26.2	88.6	21.5	0.6	20.1
Toluene	0.0	60.0	0.0	-48.8	0.2	11.3	0.098	0.842	0.082	38.1	76.3	16.7	0.5	18.4
	80.0	60.0	10.9	-46.7	0.3	13.3	0.116	0.842	0.097	45.0	94.1	16.7	0.5	21.7
Water	0.0	60.0	0.0	-52.7	0.1	7.3	0.023	3.397	0.078	80.8	100.0	4.4	0.5	12.1

Results for $T_{cond} = 80\text{ °C}$ and $T_{max} = 300\text{ °C}$

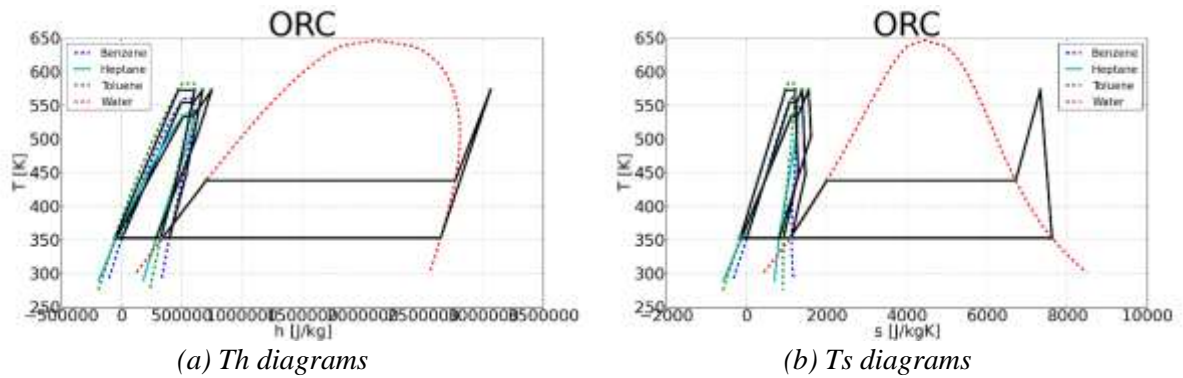


Figure 23: ORC with $T_{cond} = 80\text{ C}$ and $T_{max} = 300\text{ C}$

Table 23: Results of the cycle for $T_{cond} = 80.0\text{ C}$ and $T_{max} = 300.0\text{ C}$

	ϵ_{reg} (%)	\dot{Q}_{hot} (kW)	\dot{Q}_{reg} (kW)	\dot{Q}_{cold} (kW)	\dot{W}_p (kW)	\dot{W}_{exp} (kW)	\dot{m}_{work} (kg/s)	v_1 (m ³ /kg)	V_3 (m ³ /s)	$\frac{\dot{m}_{reg}}{\dot{m}_{y2}}$ (%)	$\frac{\dot{m}_{reg}}{\dot{m}_{x4}}$ (%)	P_{evap} (bar)	P_{cond} (bar)	η_{cycle} (%)
Benzene	0.0	60.0	0.0	-48.2	0.6	12.5	0.091	0.463	0.042	15.3	74.0	45.0	1.0	19.8
	80.0	60.0	11.7	-45.9	0.7	14.9	0.108	0.463	0.050	18.3	92.8	45.0	1.0	23.6
Heptane	0.0	60.0	0.0	-51.2	0.4	9.2	0.076	0.703	0.054	10.1	49.2	25.0	0.6	14.7
	80.0	60.0	31.5	-46.5	0.6	14.0	0.116	0.703	0.082	15.4	82.5	25.0	0.6	22.5
Toluene	0.0	60.0	0.0	-47.8	0.5	12.5	0.091	0.874	0.080	20.4	72.5	32.7	0.5	20.0
	80.0	60.0	12.7	-45.3	0.5	15.1	0.110	0.874	0.097	24.7	92.8	32.7	0.5	24.2
Water	0.0	60.0	0.0	-50.9	0.1	9.1	0.022	2.822	0.062	75.8	100.0	7.1	0.5	15.2

Results for $T_{cond} = 80\text{ °C}$ and $T_{max} = 350\text{ °C}$

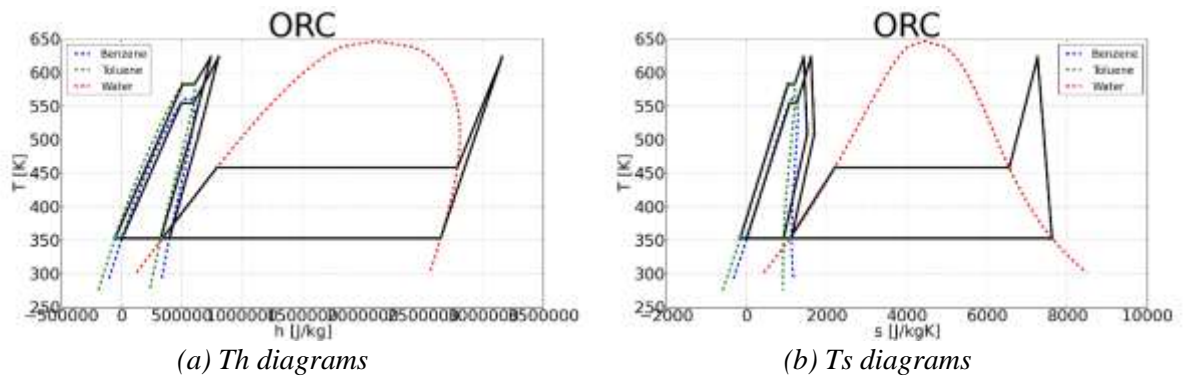


Figure 24: ORC with $T_{cond} = 80\text{ C}$ and $T_{max} = 350\text{ C}$

Table 24: Results of the cycle for $T_{cond} = 80.0\text{ C}$ and $T_{max} = 350.0\text{ C}$

	ϵ_{reg} (%)	\dot{Q}_{hot} (kW)	\dot{Q}_{reg} (kW)	\dot{Q}_{cold} (kW)	\dot{W}_p (kW)	\dot{W}_{exp} (kW)	\dot{m}_{work} (kg/s)	v_1 (m ³ /kg)	V_3 (m ³ /s)	$\frac{\dot{m}_{reg}}{\dot{m}_{y2}}$ (%)	$\frac{\dot{m}_{reg}}{\dot{m}_{x4}}$ (%)	P_{evap} (bar)	P_{cond} (bar)	η_{cycle} (%)
Benzene	0.0	60.0	0.0	-48.3	0.5	12.3	0.076	0.522	0.039	12.8	61.7	45.0	1.0	19.7
	80.0	60.0	19.3	-44.5	0.7	16.3	0.100	0.522	0.052	16.9	88.4	45.0	1.0	26.0
Toluene	0.0	60.0	0.0	-47.8	0.4	12.4	0.076	0.995	0.075	12.4	60.2	37.0	0.5	20.0
	80.0	60.0	20.3	-43.7	0.6	16.6	0.101	0.995	0.101	16.6	88.1	37.0	0.5	26.8
Water	0.0	60.0	0.0	-49.1	0.1	10.9	0.021	2.569	0.055	70.8	100.0	11.5	0.5	18.1

Results for $T_{cond} = 80 \text{ }^\circ\text{C}$ and $T_{max} = 400 \text{ }^\circ\text{C}$

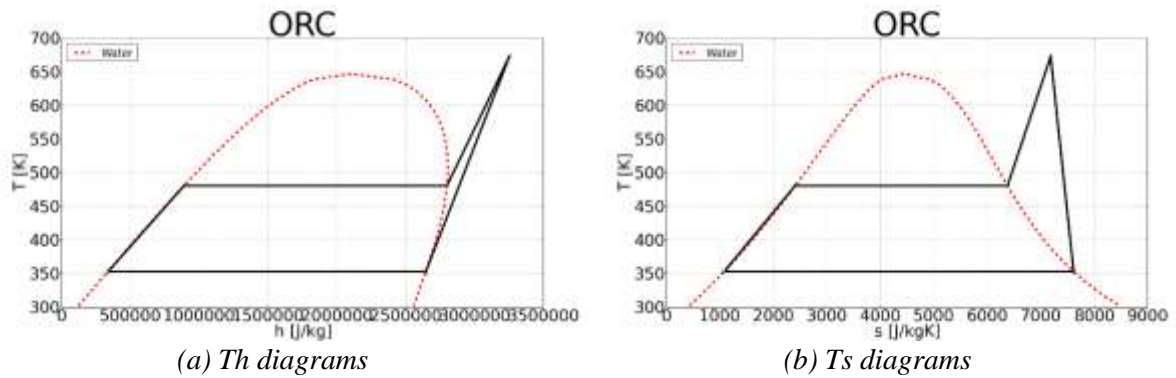


Figure 25: ORC with $T_{cond} = 80 \text{ C}$ and $T_{max} = 400 \text{ C}$

Table 25: Results of the cycle for $T_{cond} = 80.0 \text{ C}$ and $T_{max} = 400.0 \text{ C}$

	ϵ_{reg} (%)	\dot{Q}_{hot} (kW)	\dot{Q}_{reg} (kW)	\dot{Q}_{cool} (kW)	W_p (kW)	W_{exp} (kW)	\dot{m}_{work} (kg/s)	v_3 (m ³ /kg)	V_3 (m ³ /s)	$\frac{h_{12}}{h_{y2}}$ (%)	$\frac{h_{34}}{h_{y4}}$ (%)	P_{evap} (bar)	P_{cond} (bar)	η_{cycle} (%)
Water	0.0	60.0	0.0	-47.5	0.1	12.5	0.021	2.649	0.055	65.5	100.0	18.4	0.5	20.7

Results for $T_{cond} = 90 \text{ }^\circ\text{C}$ and $T_{max} = 150 \text{ }^\circ\text{C}$

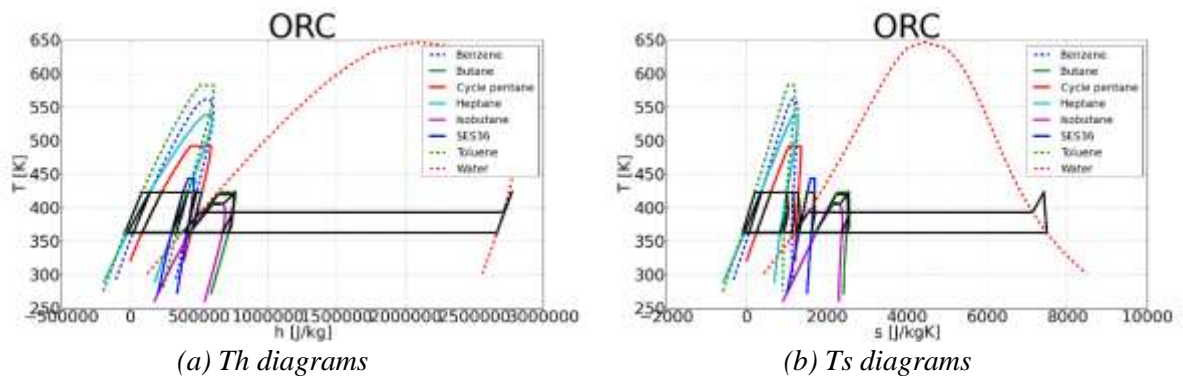


Figure 26: ORC with $T_{cond} = 90 \text{ C}$ and $T_{max} = 150 \text{ C}$

Table 26: Results of the cycle for $T_{cond} = 90.0 \text{ C}$ and $T_{max} = 150.0 \text{ C}$

	ϵ_{reg} (%)	\dot{Q}_{hot} (kW)	\dot{Q}_{reg} (kW)	\dot{Q}_{cool} (kW)	W_p (kW)	W_{exp} (kW)	\dot{m}_{work} (kg/s)	v_3 (m ³ /kg)	V_3 (m ³ /s)	$\frac{h_{12}}{h_{y2}}$ (%)	$\frac{h_{34}}{h_{y4}}$ (%)	P_{evap} (bar)	P_{cond} (bar)	η_{cycle} (%)
Benzene	0.0	60.0	0.0	-53.5	0.1	6.6	0.131	0.269	0.035	73.4	94.5	5.8	1.4	10.9
	80.0	60.0	2.4	-53.2	0.1	6.9	0.136	0.269	0.037	76.3	98.8	5.8	1.4	11.3
Butane	0.0	60.0	0.0	-55.1	1.1	5.7	0.186	0.033	0.006	31.9	93.0	35.0	12.5	7.8
	80.0	60.0	2.5	-55.0	1.1	6.0	0.193	0.033	0.006	33.3	97.1	35.0	12.5	8.1
Cycle pentane	0.0	60.0	0.0	-53.1	0.2	7.0	0.139	0.124	0.017	67.3	93.1	11.8	3.3	11.3
	80.0	60.0	3.0	-52.7	0.2	7.4	0.146	0.124	0.018	70.7	98.5	11.8	3.3	11.9
Heptane	0.0	60.0	0.0	-54.7	0.1	5.4	0.138	0.390	0.054	63.4	81.5	3.8	0.8	8.8
	80.0	60.0	9.3	-53.9	0.1	6.2	0.160	0.390	0.062	73.1	95.5	3.8	0.8	10.2
Isobutane	0.0	60.0	0.0	-56.3	1.0	4.7	0.187	0.027	0.005	23.0	77.6	35.0	16.4	6.2
	80.0	60.0	10.9	-55.6	1.1	5.5	0.221	0.027	0.006	27.2	92.8	35.0	16.4	7.3
SES36	0.0	60.0	0.0	-55.0	0.5	5.5	0.387	0.031	0.012	47.7	78.6	17.6	5.0	8.3
	80.0	60.0	10.7	-54.1	0.6	6.5	0.456	0.031	0.014	56.1	94.1	17.6	5.0	9.8
Toluene	0.0	60.0	0.0	-54.2	0.1	5.8	0.132	0.618	0.081	73.1	90.8	2.8	0.6	9.6
	80.0	60.0	4.2	-53.8	0.1	6.2	0.141	0.618	0.087	78.3	98.0	2.8	0.6	10.3
Water	0.0	60.0	0.0	-57.3	0.1	2.7	0.025	2.115	0.053	92.1	100.0	2.0	0.7	4.5

Results for $T_{cond} = 90\text{ }^{\circ}\text{C}$ and $T_{max} = 200\text{ }^{\circ}\text{C}$

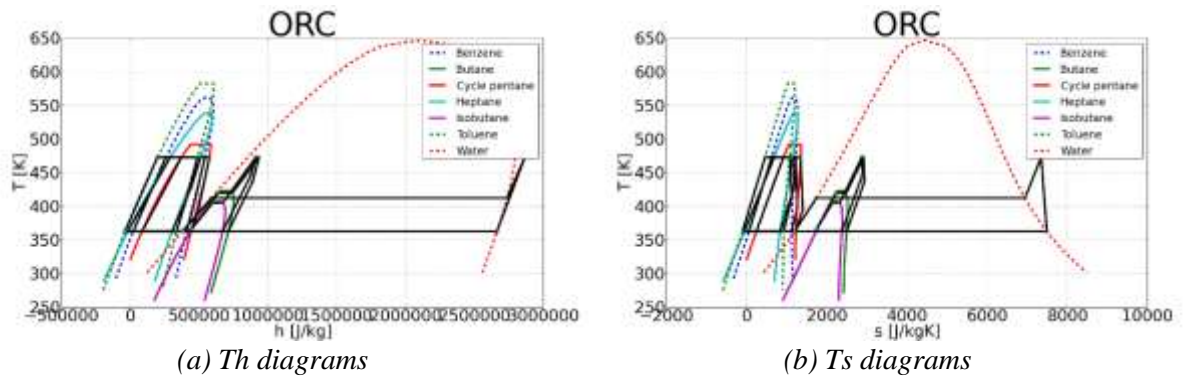


Figure 27: ORC with $T_{cond} = 90\text{ }^{\circ}\text{C}$ and $T_{max} = 200\text{ }^{\circ}\text{C}$

Table 27: Results of the cycle for $T_{cond} = 90.0\text{ }^{\circ}\text{C}$ and $T_{max} = 200.0\text{ }^{\circ}\text{C}$

	ϵ_{reg} (%)	\dot{Q}_{hot} (kW)	\dot{Q}_{reg} (kW)	\dot{Q}_{cold} (kW)	\dot{W}_p (kW)	\dot{W}_{exp} (kW)	\dot{m}_{work} (kg/s)	v_3 (m ³ /kg)	V_3 (m ³ /s)	$\frac{h_{12}}{h_{y2}}$ (%)	$\frac{h_{34}}{h_{x4}}$ (%)	P_{evap} (bar)	P_{cond} (bar)	η_{cycle} (%)
Benzene	0.0	60.0	0.0	-50.7	0.2	9.6	0.116	0.285	0.033	54.7	88.2	14.4	1.4	15.6
	80.0	60.0	5.1	-49.9	0.3	10.4	0.126	0.285	0.036	59.3	97.2	14.4	1.4	16.9
Butane	0.0	60.0	0.0	-55.2	0.7	5.4	0.122	0.044	0.005	20.9	60.9	35.0	12.5	7.9
	80.0	60.0	0.0	-55.2	0.7	5.4	0.122	0.044	0.005	20.9	60.9	35.0	12.5	7.9
Cycle pentane	0.0	60.0	0.0	-50.5	0.5	9.9	0.124	0.131	0.016	41.8	87.0	26.6	3.3	15.5
	80.0	60.0	5.6	-49.7	0.6	10.8	0.135	0.131	0.018	45.7	96.8	26.6	3.3	17.0
Heptane	0.0	60.0	0.0	-52.6	0.2	7.6	0.114	0.423	0.048	41.8	69.8	9.8	0.8	12.3
	80.0	60.0	15.9	-50.7	0.3	9.6	0.144	0.423	0.061	52.9	91.7	9.8	0.8	15.6
Isobutane	0.0	60.0	0.0	-56.4	0.7	4.3	0.128	0.034	0.004	15.7	52.9	35.0	16.4	6.0
	80.0	60.0	0.0	-56.4	0.7	4.3	0.128	0.034	0.004	15.7	52.9	35.0	16.4	6.0
Toluene	0.0	60.0	0.0	-51.4	0.1	8.8	0.114	0.660	0.075	55.3	83.1	7.5	0.6	14.4
	80.0	60.0	7.8	-50.3	0.1	9.9	0.129	0.660	0.085	62.5	96.0	7.5	0.6	16.3
Water	0.0	60.0	0.0	-55.1	0.1	4.9	0.024	2.361	0.057	86.4	100.0	3.6	0.7	8.1

Results for $T_{cond} = 90\text{ }^{\circ}\text{C}$ and $T_{max} = 250\text{ }^{\circ}\text{C}$

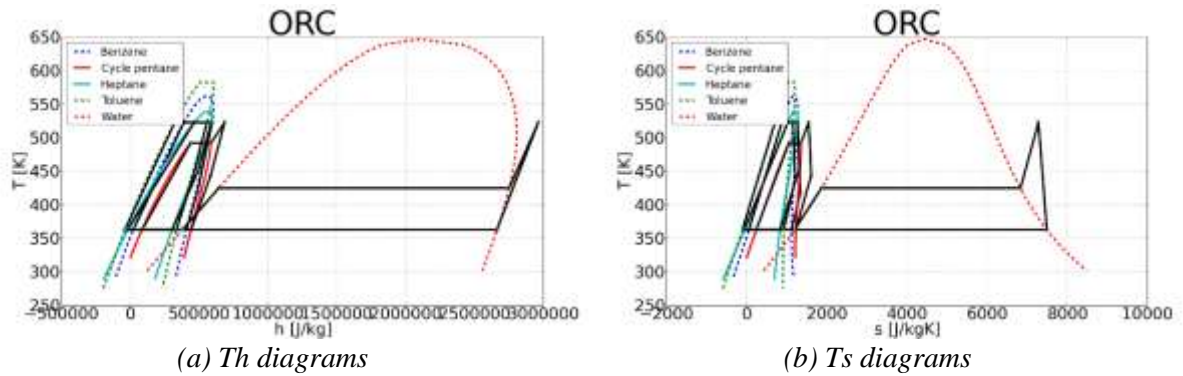


Figure 28: ORC with $T_{cond} = 90\text{ }^{\circ}\text{C}$ and $T_{max} = 250\text{ }^{\circ}\text{C}$

Table 28: Results of the cycle for $T_{cond} = 90.0\text{ }^{\circ}\text{C}$ and $T_{max} = 250.0\text{ }^{\circ}\text{C}$

	ϵ_{reg} (%)	\dot{Q}_{hot} (kW)	\dot{Q}_{reg} (kW)	\dot{Q}_{cold} (kW)	\dot{W}_p (kW)	\dot{W}_{exp} (kW)	\dot{m}_{work} (kg/s)	v_3 (m ³ /kg)	V_3 (m ³ /s)	$\frac{h_{12}}{h_{y2}}$ (%)	$\frac{h_{34}}{h_{x4}}$ (%)	P_{evap} (bar)	P_{cond} (bar)	η_{cycle} (%)
Benzene	0.0	60.0	0.0	-49.2	0.5	11.3	0.106	0.298	0.031	36.0	83.0	29.9	1.4	18.0
	80.0	60.0	7.3	-47.9	0.5	12.7	0.119	0.298	0.035	40.4	95.6	29.9	1.4	20.2
Cycle pentane	0.0	60.0	0.0	-50.3	0.6	10.2	0.101	0.151	0.015	24.9	71.5	35.0	3.3	16.1
	80.0	60.0	13.9	-48.0	0.7	12.6	0.124	0.151	0.019	30.6	92.2	35.0	3.3	19.8
Heptane	0.0	60.0	0.0	-51.6	0.4	8.8	0.100	0.449	0.045	20.3	62.4	21.5	0.8	14.0
	80.0	60.0	20.6	-48.8	0.6	11.9	0.134	0.449	0.060	27.3	88.7	21.5	0.8	18.8
Toluene	0.0	60.0	0.0	-49.6	0.3	10.6	0.101	0.701	0.071	39.4	76.3	16.7	0.6	17.3
	80.0	60.0	11.0	-47.7	0.3	12.6	0.120	0.701	0.084	46.6	93.9	16.7	0.6	20.5
Water	0.0	60.0	0.0	-53.0	0.1	7.0	0.023	2.361	0.055	81.7	100.0	5.0	0.7	11.6

Results for $T_{cond} = 90\text{ }^{\circ}\text{C}$ and $T_{max} = 300\text{ }^{\circ}\text{C}$

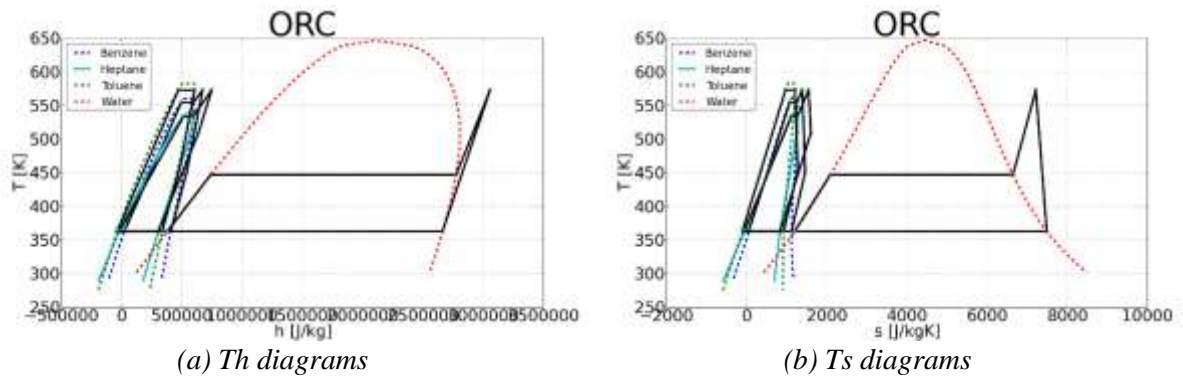


Figure 29: ORC with $T_{cond} = 90\text{ }^{\circ}\text{C}$ and $T_{max} = 300\text{ }^{\circ}\text{C}$

Table 29: Results of the cycle for $T_{cond} = 90.0\text{ }^{\circ}\text{C}$ and $T_{max} = 300.0\text{ }^{\circ}\text{C}$

	ϵ_{reg} (%)	\dot{Q}_{hot} (kW)	\dot{Q}_{reg} (kW)	\dot{Q}_{cold} (kW)	\dot{W}_p (kW)	\dot{W}_{exp} (kW)	\dot{m}_{work} (kg/s)	v_3 (m ³ /kg)	V_3 (m ³ /s)	$\frac{\dot{m}_{reg}}{\dot{m}_{y2}}$ (%)	$\frac{\dot{m}_{reg}}{\dot{m}_{x4}}$ (%)	P_{evap} (bar)	P_{cond} (bar)	η_{cycle} (%)
Benzene	0.0	60.0	0.0	-48.4	0.6	12.3	0.093	0.326	0.030	15.8	74.5	45.0	1.4	19.4
	80.0	60.0	11.5	-46.2	0.8	14.6	0.111	0.326	0.036	18.8	93.0	45.0	1.4	23.1
Heptane	0.0	60.0	0.0	-51.7	0.4	8.7	0.079	0.509	0.040	10.4	49.2	25.0	0.8	13.9
	80.0	60.0	31.9	-47.3	0.6	13.3	0.121	0.509	0.061	16.0	82.4	25.0	0.8	21.2
Toluene	0.0	60.0	0.0	-48.6	0.5	11.9	0.094	0.728	0.069	21.1	72.4	32.7	0.6	19.0
	80.0	60.0	12.8	-46.2	0.6	14.4	0.114	0.728	0.083	25.6	92.5	32.7	0.6	23.0
Water	0.0	60.0	0.0	-51.2	0.1	8.8	0.022	2.079	0.047	76.1	100.0	8.7	0.7	14.7

Results for $T_{cond} = 90\text{ }^{\circ}\text{C}$ and $T_{max} = 350\text{ }^{\circ}\text{C}$

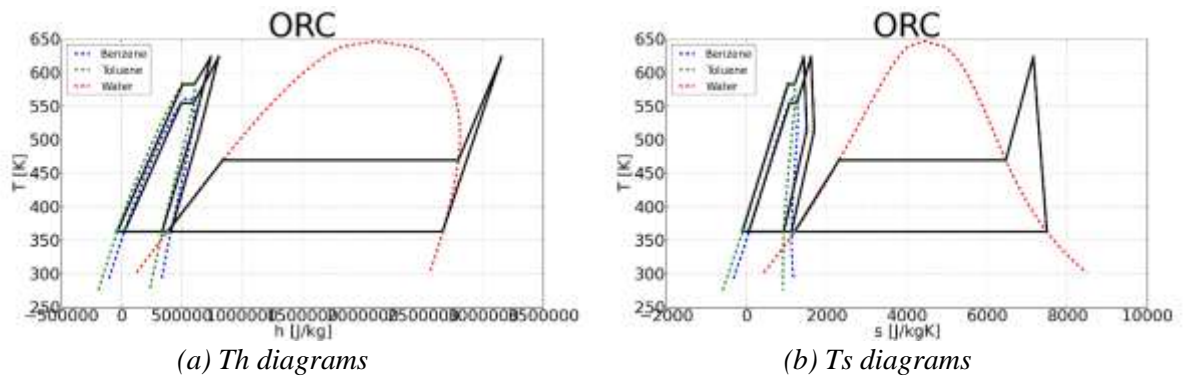


Figure 30: ORC with $T_{cond} = 90\text{ }^{\circ}\text{C}$ and $T_{max} = 350\text{ }^{\circ}\text{C}$

Table 30: Results of the cycle for $T_{cond} = 90.0\text{ }^{\circ}\text{C}$ and $T_{max} = 350.0\text{ }^{\circ}\text{C}$

	ϵ_{reg} (%)	\dot{Q}_{hot} (kW)	\dot{Q}_{reg} (kW)	\dot{Q}_{cold} (kW)	\dot{W}_p (kW)	\dot{W}_{exp} (kW)	\dot{m}_{work} (kg/s)	v_3 (m ³ /kg)	V_3 (m ³ /s)	$\frac{\dot{m}_{reg}}{\dot{m}_{y2}}$ (%)	$\frac{\dot{m}_{reg}}{\dot{m}_{x4}}$ (%)	P_{evap} (bar)	P_{cond} (bar)	η_{cycle} (%)
Benzene	0.0	60.0	0.0	-48.5	0.5	12.1	0.077	0.380	0.029	13.1	61.7	45.0	1.4	19.3
	80.0	60.0	19.4	-44.8	0.7	16.0	0.103	0.380	0.039	17.3	88.4	45.0	1.4	25.5
Toluene	0.0	60.0	0.0	-48.6	0.4	11.8	0.078	0.827	0.064	12.7	59.8	37.0	0.6	19.0
	80.0	60.0	20.9	-44.7	0.6	15.9	0.105	0.827	0.087	17.2	87.7	37.0	0.6	25.6
Water	0.0	60.0	0.0	-49.5	0.1	10.6	0.022	2.361	0.051	70.6	100.0	14.5	0.7	17.6

Results for $T_{cond} = 90\text{ }^{\circ}\text{C}$ and $T_{max} = 400\text{ }^{\circ}\text{C}$

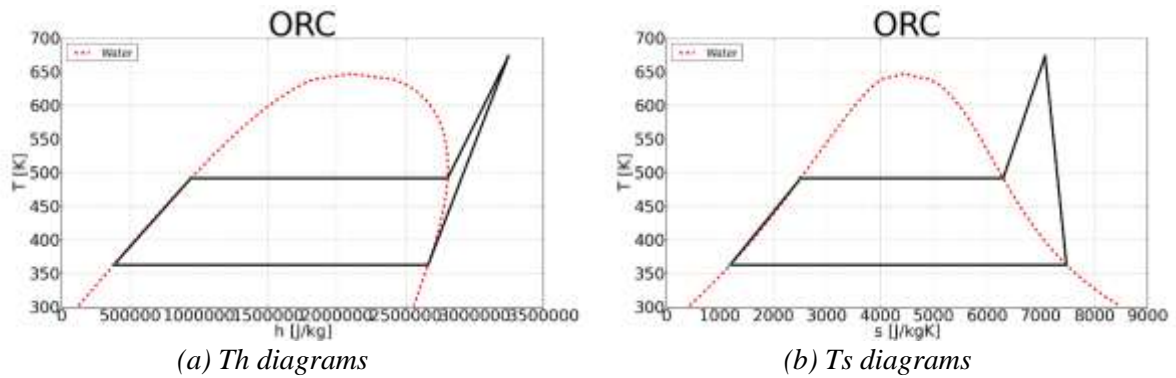


Figure 31: ORC with $T_{cond} = 90\text{ }^{\circ}\text{C}$ and $T_{max} = 400\text{ }^{\circ}\text{C}$

Table 31: Results of the cycle for $T_{cond} = 90.0\text{ }^{\circ}\text{C}$ and $T_{max} = 400.0\text{ }^{\circ}\text{C}$

	ϵ_{reg} (%)	\dot{Q}_{hot} (kW)	\dot{Q}_{reg} (kW)	\dot{Q}_{cold} (kW)	W_p (kW)	W_{exp} (kW)	\dot{m}_{work} (kg/s)	v_3 (m ³ /kg)	\dot{V}_3 (m ³ /s)	$\frac{h_{12}}{h_{y2}}$ (%)	$\frac{h_{34}}{h_{y4}}$ (%)	P_{evap} (bar)	P_{cond} (bar)	η_{cycle} (%)
Water	0.0	60.0	0.0	-47.9	0.1	12.2	0.021	1.901	0.040	65.1	100.0	22.8	0.7	20.3

Results for $T_{cond} = 100\text{ }^{\circ}\text{C}$ and $T_{max} = 150\text{ }^{\circ}\text{C}$

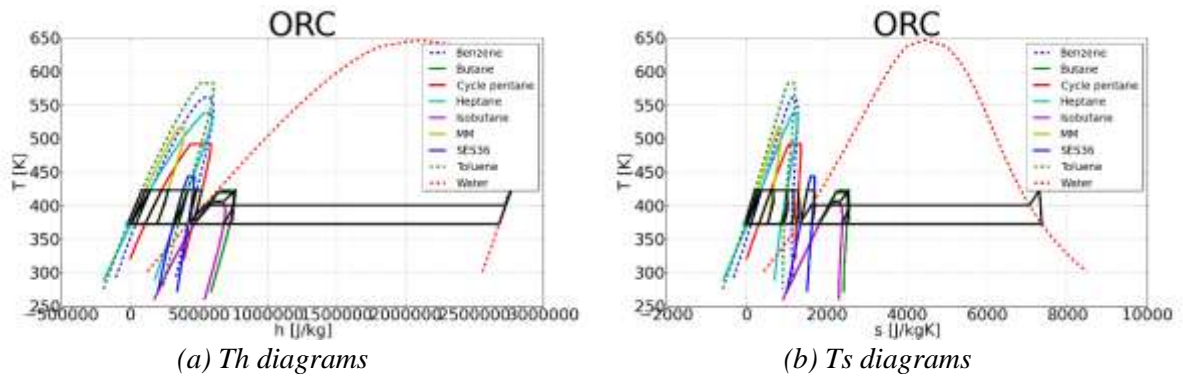


Figure 32: ORC with $T_{cond} = 100\text{ }^{\circ}\text{C}$ and $T_{max} = 150\text{ }^{\circ}\text{C}$

Table 32: Results of the cycle for $T_{cond} = 100.0\text{ }^{\circ}\text{C}$ and $T_{max} = 150.0\text{ }^{\circ}\text{C}$

	ϵ_{reg} (%)	\dot{Q}_{hot} (kW)	\dot{Q}_{reg} (kW)	\dot{Q}_{cold} (kW)	W_p (kW)	W_{exp} (kW)	\dot{m}_{work} (kg/s)	v_3 (m ³ /kg)	\dot{V}_3 (m ³ /s)	$\frac{h_{12}}{h_{y2}}$ (%)	$\frac{h_{34}}{h_{y4}}$ (%)	P_{evap} (bar)	P_{cond} (bar)	η_{cycle} (%)
Benzene	0.0	60.0	0.0	-53.9	0.1	6.2	0.137	0.211	0.029	76.6	95.9	5.8	1.8	10.2
	80.0	60.0	1.8	-53.7	0.1	6.4	0.141	0.211	0.030	78.9	99.1	5.8	1.8	10.5
Butane	0.0	60.0	0.0	-56.3	1.1	4.9	0.205	0.027	0.005	35.3	94.0	35.0	15.3	6.3
	80.0	60.0	1.7	-56.2	1.1	5.0	0.211	0.027	0.006	36.3	96.8	35.0	15.3	6.5
Cycle pentane	0.0	60.0	0.0	-54.4	0.2	5.7	0.146	0.100	0.015	71.0	93.2	11.8	4.2	9.1
	80.0	60.0	3.0	-54.2	0.2	6.0	0.154	0.100	0.015	74.6	98.4	11.8	4.2	9.6
Heptane	0.0	60.0	0.0	-55.5	0.1	4.7	0.147	0.295	0.043	67.4	83.5	3.8	1.1	7.6
	80.0	60.0	8.2	-54.9	0.1	5.3	0.167	0.295	0.049	76.6	96.0	3.8	1.1	8.7
Isobutane	0.0	60.0	0.0	-56.9	0.9	3.7	0.206	0.022	0.004	25.3	76.3	35.0	19.9	4.7
	80.0	60.0	11.9	-56.3	1.1	4.5	0.246	0.022	0.005	30.3	92.3	35.0	19.9	5.6
MM	0.0	60.0	0.0	-55.8	0.1	4.3	0.221	0.197	0.043	60.1	76.5	3.6	1.0	7.1
	80.0	60.0	12.6	-54.9	0.1	5.3	0.267	0.197	0.053	72.7	94.1	3.6	1.0	8.6
SES36	0.0	60.0	0.0	-55.8	0.5	4.8	0.420	0.024	0.010	51.8	80.9	17.6	6.3	7.1
	80.0	60.0	9.4	-55.1	0.6	5.5	0.486	0.024	0.012	59.9	94.8	17.6	6.3	8.2
Toluene	0.0	60.0	0.0	-55.2	0.1	4.9	0.138	0.446	0.061	76.5	91.8	2.8	0.8	8.1
	80.0	60.0	3.8	-54.9	0.1	5.2	0.147	0.446	0.065	81.3	98.1	2.8	0.8	8.6
Water	0.0	60.0	0.0	-57.7	0.1	2.3	0.026	1.477	0.038	93.0	100.0	2.5	1.0	3.8

Results for $T_{cond} = 100\text{ }^{\circ}\text{C}$ and $T_{max} = 200\text{ }^{\circ}\text{C}$

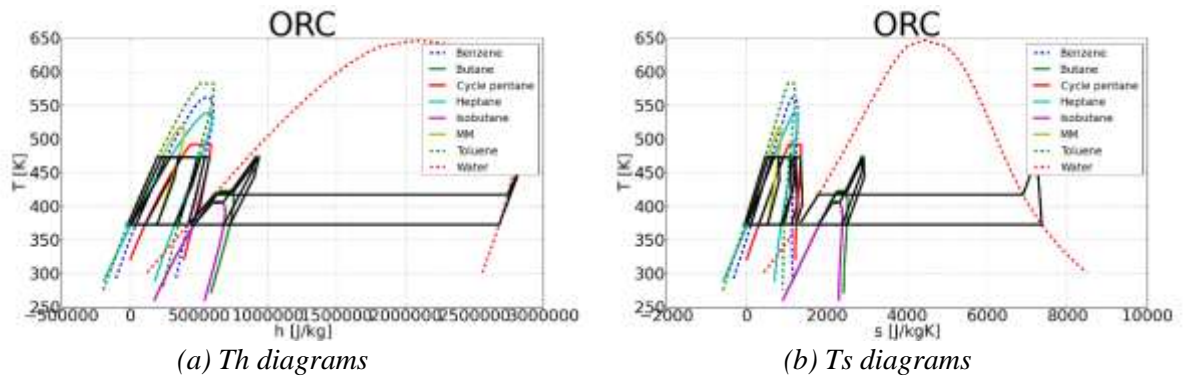


Figure 33: ORC with $T_{cond} = 100\text{ }^{\circ}\text{C}$ and $T_{max} = 200\text{ }^{\circ}\text{C}$

Table 33: Results of the cycle for $T_{cond} = 100.0\text{ }^{\circ}\text{C}$ and $T_{max} = 200.0\text{ }^{\circ}\text{C}$

	ϵ_{reg} (%)	\dot{Q}_{hot} (kW)	\dot{Q}_{reg} (kW)	\dot{Q}_{cold} (kW)	W_p (kW)	W_{exp} (kW)	\dot{m}_{work} (kg/s)	v_1 (m ³ /kg)	V_1 (m ³ /s)	$\frac{h_{1,g}}{h_{1,l}}$ (%)	$\frac{h_{2,g}}{h_{2,l}}$ (%)	P_{evap} (bar)	P_{cond} (bar)	η_{cycle} (%)
Benzene	0.0	60.0	0.0	-51.0	0.2	9.3	0.120	0.219	0.026	56.8	89.3	14.4	1.8	15.1
	80.0	60.0	4.6	-50.3	0.3	10.0	0.129	0.219	0.028	61.1	97.4	14.4	1.8	16.3
Butane	0.0	60.0	0.0	-56.2	0.7	4.6	0.130	0.036	0.005	22.3	59.6	35.0	15.3	6.5
	80.0	60.0	0.0	-56.2	0.7	4.6	0.130	0.036	0.005	22.3	59.6	35.0	15.3	6.5
Cycle pentane	0.0	60.0	0.0	-51.8	0.6	8.7	0.130	0.105	0.014	43.9	86.9	26.6	4.2	13.7
	80.0	60.0	5.7	-51.0	0.6	9.6	0.142	0.105	0.015	48.1	96.6	26.6	4.2	15.0
Heptane	0.0	60.0	0.0	-53.3	0.2	7.1	0.120	0.318	0.038	43.9	71.0	9.8	1.1	11.4
	80.0	60.0	15.3	-51.5	0.3	8.9	0.150	0.318	0.048	55.1	92.0	9.8	1.1	14.4
Isobutane	0.0	60.0	0.0	-57.1	0.6	3.3	0.136	0.028	0.004	16.8	50.4	35.0	19.9	4.6
	80.0	60.0	0.0	-57.1	0.6	3.3	0.136	0.028	0.004	16.8	50.4	35.0	19.9	4.6
MM	0.0	60.0	0.0	-54.2	0.3	6.1	0.173	0.216	0.037	35.1	61.6	9.4	1.0	9.8
	80.0	60.0	22.7	-52.0	0.4	8.4	0.238	0.216	0.051	48.4	88.6	9.4	1.0	13.5
Toluene	0.0	60.0	0.0	-52.1	0.1	8.1	0.119	0.478	0.057	57.5	83.7	7.5	0.8	13.2
	80.0	60.0	7.6	-51.1	0.1	9.1	0.134	0.478	0.064	64.8	96.1	7.5	0.8	14.9
Water	0.0	60.0	0.0	-55.5	0.1	4.5	0.025	1.629	0.040	87.3	100.0	4.1	1.0	7.5

Results for $T_{cond} = 100\text{ }^{\circ}\text{C}$ and $T_{max} = 250\text{ }^{\circ}\text{C}$

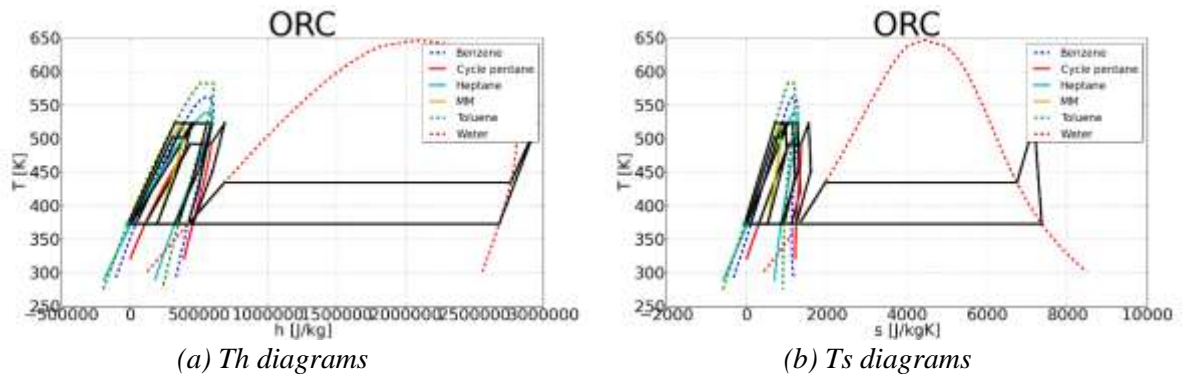


Figure 34: ORC with $T_{cond} = 100\text{ }^{\circ}\text{C}$ and $T_{max} = 250\text{ }^{\circ}\text{C}$

Table 34: Results of the cycle for $T_{cond} = 100.0\text{ }^{\circ}\text{C}$ and $T_{max} = 250.0\text{ }^{\circ}\text{C}$

	ϵ_{reg} (%)	\dot{Q}_{hot} (kW)	\dot{Q}_{reg} (kW)	\dot{Q}_{cold} (kW)	W_p (kW)	W_{exp} (kW)	\dot{m}_{work} (kg/s)	v_1 (m ³ /kg)	V_1 (m ³ /s)	$\frac{h_{1,g}}{h_{1,l}}$ (%)	$\frac{h_{2,g}}{h_{2,l}}$ (%)	P_{evap} (bar)	P_{cond} (bar)	η_{cycle} (%)
Benzene	0.0	60.0	0.0	-49.5	0.5	11.1	0.110	0.230	0.025	37.3	83.8	29.9	1.8	17.6
	80.0	60.0	6.9	-48.3	0.5	12.3	0.122	0.230	0.028	41.6	95.8	29.9	1.8	19.7
Cycle pentane	0.0	60.0	0.0	-51.4	0.6	9.2	0.105	0.121	0.013	25.9	70.8	35.0	4.2	14.3
	80.0	60.0	14.6	-49.3	0.8	11.4	0.131	0.121	0.016	32.2	91.8	35.0	4.2	17.7
Heptane	0.0	60.0	0.0	-52.2	0.4	8.4	0.104	0.339	0.035	21.2	63.1	21.5	1.1	13.2
	80.0	60.0	20.2	-49.5	0.6	11.2	0.140	0.339	0.047	28.4	88.9	21.5	1.1	17.7
MM	0.0	60.0	0.0	-53.8	0.3	6.7	0.136	0.239	0.033	18.6	48.9	15.0	1.0	10.5
	80.0	60.0	34.2	-50.2	0.5	10.4	0.213	0.239	0.051	29.2	82.2	15.0	1.0	16.5
Toluene	0.0	60.0	0.0	-50.3	0.3	10.0	0.105	0.505	0.053	40.8	76.7	16.7	0.8	16.3
	80.0	60.0	10.9	-48.5	0.3	11.9	0.124	0.505	0.063	48.2	93.9	16.7	0.8	19.3
Water	0.0	60.0	0.0	-53.4	0.1	6.6	0.024	1.506	0.036	81.9	100.0	6.5	1.0	11.0

Results for $T_{\text{cond}} = 100\text{ }^{\circ}\text{C}$ and $T_{\text{max}} = 300\text{ }^{\circ}\text{C}$

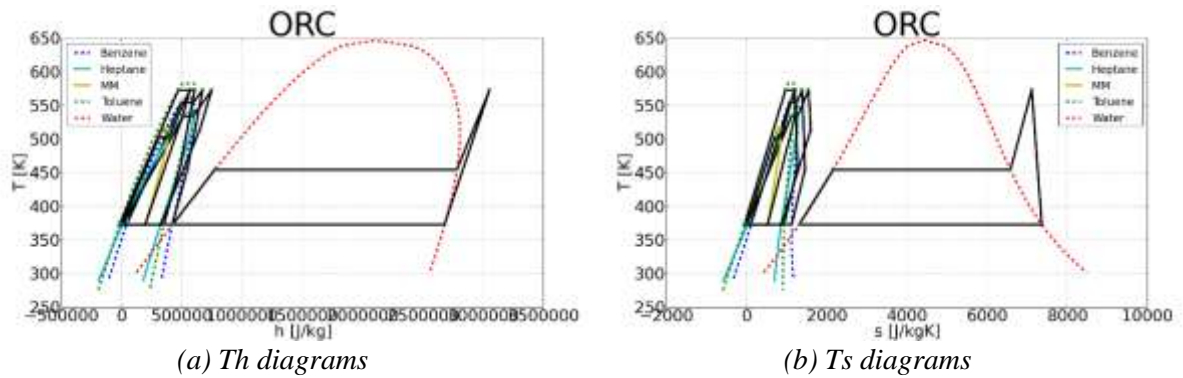


Figure 35: ORC with $T_{\text{cond}} = 100\text{ C}$ and $T_{\text{max}} = 300\text{ C}$

Table 35: Results of the cycle for $T_{\text{cond}} = 100.0\text{ C}$ and $T_{\text{max}} = 300.0\text{ C}$

	ϵ_{reg} (%)	\dot{Q}_{hot} (kW)	\dot{Q}_{reg} (kW)	\dot{Q}_{cold} (kW)	\dot{W}_p (kW)	\dot{W}_{exp} (kW)	\dot{m}_{work} (kg/s)	v_3 (m ³ /kg)	V_3 (m ³ /s)	$\frac{\dot{W}_{\text{reg}}}{\dot{Q}_{\text{hot}}}$ (%)	$\frac{\dot{W}_{\text{exp}}}{\dot{Q}_{\text{hot}}}$ (%)	P_{evap} (bar)	P_{cond} (bar)	η_{cycle} (%)
Benzene	0.0	60.0	0.0	-48.7	0.7	12.1	0.096	0.252	0.024	16.3	74.9	45.0	1.8	19.0
	80.0	60.0	11.2	-46.6	0.8	14.3	0.114	0.252	0.029	19.4	93.0	45.0	1.8	22.6
Heptane	0.0	60.0	0.0	-52.2	0.4	8.3	0.082	0.385	0.031	10.8	49.4	25.0	1.1	13.1
	80.0	60.0	32.1	-48.1	0.6	12.7	0.125	0.385	0.048	16.6	82.4	25.0	1.1	20.1
MM	0.0	60.0	0.0	-54.2	0.3	6.1	0.107	0.268	0.029	14.7	38.2	15.0	1.0	9.7
	80.0	60.0	0.0	-54.2	0.3	6.1	0.107	0.268	0.029	14.7	38.2	15.0	1.0	9.7
Toluene	0.0	60.0	0.0	-49.2	0.5	11.3	0.097	0.527	0.051	21.8	72.6	32.7	0.8	18.0
	80.0	60.0	12.9	-46.9	0.6	13.7	0.118	0.527	0.062	26.5	92.5	32.7	0.8	21.9
Water	0.0	60.0	0.0	-51.5	0.1	8.5	0.023	1.481	0.034	76.4	100.0	10.5	1.0	14.2

Results for $T_{\text{cond}} = 100\text{ }^{\circ}\text{C}$ and $T_{\text{max}} = 350\text{ }^{\circ}\text{C}$

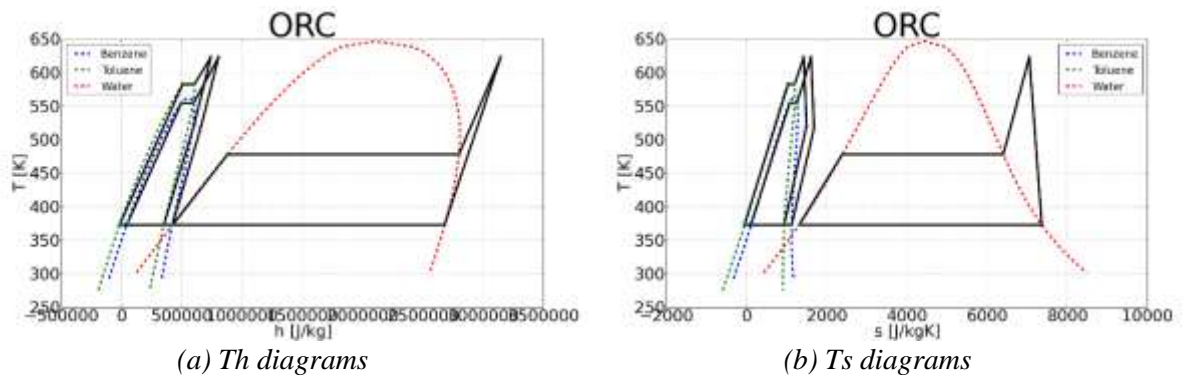


Figure 36: ORC with $T_{\text{cond}} = 100\text{ C}$ and $T_{\text{max}} = 350\text{ C}$

Table 36: Results of the cycle for $T_{\text{cond}} = 100.0\text{ C}$ and $T_{\text{max}} = 350.0\text{ C}$

	ϵ_{reg} (%)	\dot{Q}_{hot} (kW)	\dot{Q}_{reg} (kW)	\dot{Q}_{cold} (kW)	\dot{W}_p (kW)	\dot{W}_{exp} (kW)	\dot{m}_{work} (kg/s)	v_3 (m ³ /kg)	V_3 (m ³ /s)	$\frac{\dot{W}_{\text{reg}}}{\dot{Q}_{\text{hot}}}$ (%)	$\frac{\dot{W}_{\text{exp}}}{\dot{Q}_{\text{hot}}}$ (%)	P_{evap} (bar)	P_{cond} (bar)	η_{cycle} (%)
Benzene	0.0	60.0	0.0	-48.8	0.5	11.8	0.080	0.294	0.023	13.5	61.7	45.0	1.8	18.8
	80.0	60.0	19.5	-45.1	0.7	15.7	0.105	0.294	0.031	17.8	88.3	45.0	1.8	24.9
Toluene	0.0	60.0	0.0	-49.2	0.5	11.3	0.080	0.600	0.048	13.1	59.6	37.0	0.8	18.0
	80.0	60.0	21.3	-45.4	0.6	15.3	0.108	0.600	0.065	17.7	87.5	37.0	0.8	24.4
Water	0.0	60.0	0.0	-49.8	0.1	10.3	0.022	1.670	0.037	70.5	100.0	17.4	1.0	17.0

Results for $T_{\text{cond}} = 100 \text{ }^\circ\text{C}$ and $T_{\text{max}} = 400 \text{ }^\circ\text{C}$

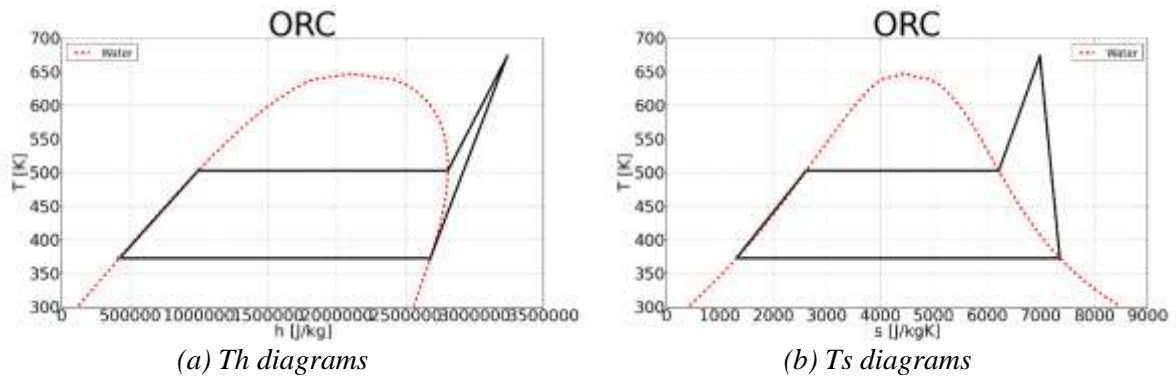


Figure 37: ORC with $T_{\text{cond}} = 100 \text{ C}$ and $T_{\text{max}} = 400 \text{ C}$

Table 37: Results of the cycle for $T_{\text{cond}} = 100.0 \text{ C}$ and $T_{\text{max}} = 400.0 \text{ C}$

	ϵ_{reg} (%)	\dot{Q}_{hot} (kW)	\dot{Q}_{reg} (kW)	\dot{Q}_{cold} (kW)	W_{p} (kW)	W_{exp} (kW)	\dot{m}_{work} (kg/s)	v_3 (m ³ /kg)	\dot{V}_3 (m ³ /s)	$\frac{h_{12}}{h_{y2}}$ (%)	$\frac{h_{34}}{h_{x4}}$ (%)	P_{evap} (bar)	P_{cond} (bar)	η_{cycle} (%)
Water	0.0	60.0	0.0	-48.2	0.1	11.9	0.021	1.473	0.031	64.5	100.0	28.2	1.0	19.7

Results for $T_{\text{cond}} = 150 \text{ }^\circ\text{C}$ and $T_{\text{max}} = 200 \text{ }^\circ\text{C}$

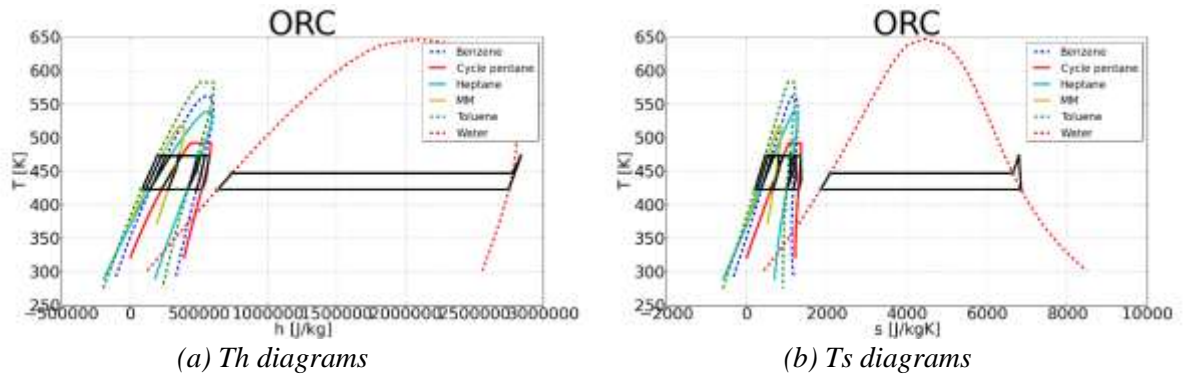


Figure 38: ORC with $T_{\text{cond}} = 150 \text{ C}$ and $T_{\text{max}} = 200 \text{ C}$

Table 38: Results of the cycle for $T_{\text{cond}} = 150.0 \text{ C}$ and $T_{\text{max}} = 200.0 \text{ C}$

	ϵ_{reg} (%)	\dot{Q}_{hot} (kW)	\dot{Q}_{reg} (kW)	\dot{Q}_{cold} (kW)	W_{p} (kW)	W_{exp} (kW)	\dot{m}_{work} (kg/s)	v_3 (m ³ /kg)	\dot{V}_3 (m ³ /s)	$\frac{h_{12}}{h_{y2}}$ (%)	$\frac{h_{34}}{h_{x4}}$ (%)	P_{evap} (bar)	P_{cond} (bar)	η_{cycle} (%)
Benzene	0.0	60.0	0.0	-55.3	0.2	4.8	0.151	0.072	0.011	71.5	92.0	14.4	5.8	7.7
	80.0	60.0	3.7	-55.1	0.2	5.1	0.161	0.072	0.012	75.8	98.1	14.4	5.8	8.2
Cycle pentane	0.0	60.0	0.0	-55.9	0.5	4.8	0.175	0.036	0.006	59.3	91.2	26.6	11.8	7.1
	80.0	60.0	3.7	-55.7	0.6	5.1	0.186	0.036	0.007	62.9	97.2	26.6	11.8	7.6
Heptane	0.0	60.0	0.0	-55.3	0.2	4.9	0.163	0.087	0.014	59.8	81.1	9.8	3.8	7.7
	80.0	60.0	9.7	-54.5	0.3	5.6	0.189	0.087	0.016	69.4	95.4	9.8	3.8	9.0
MM	0.0	60.0	0.0	-55.7	0.3	4.5	0.251	0.055	0.014	51.0	73.7	9.4	3.6	7.0
	80.0	60.0	14.4	-54.7	0.4	5.6	0.311	0.055	0.017	63.2	93.0	9.4	3.6	8.7
Toluene	0.0	60.0	0.0	-54.5	0.1	5.6	0.149	0.130	0.019	72.0	90.9	7.5	2.8	9.1
	80.0	60.0	4.2	-54.1	0.1	6.0	0.159	0.130	0.021	77.1	98.0	7.5	2.8	9.8
Water	0.0	60.0	0.0	-57.6	0.1	2.4	0.027	0.384	0.010	92.5	100.0	8.7	4.8	4.0

Results for $T_{cond} = 150\text{ }^{\circ}\text{C}$ and $T_{max} = 250\text{ }^{\circ}\text{C}$

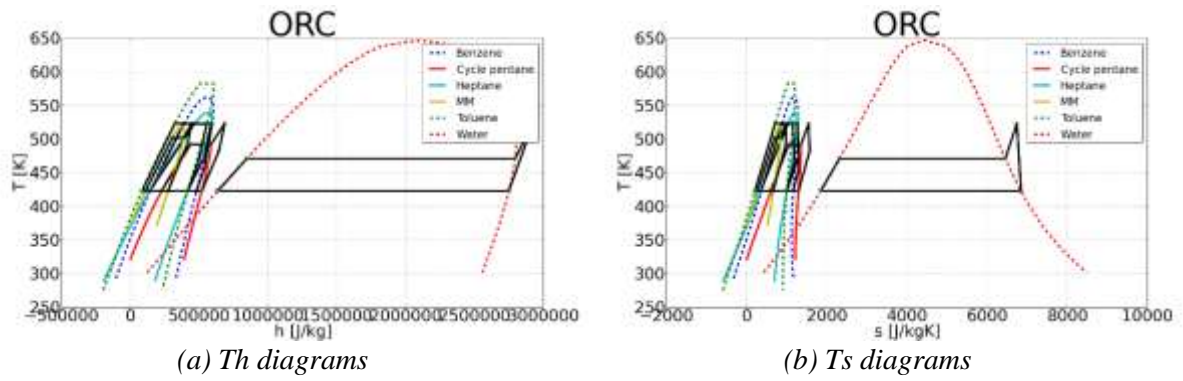


Figure 39: ORC with $T_{cond} = 150\text{ }^{\circ}\text{C}$ and $T_{max} = 250\text{ }^{\circ}\text{C}$

Table 39: Results of the cycle for $T_{cond} = 150.0\text{ }^{\circ}\text{C}$ and $T_{max} = 250.0\text{ }^{\circ}\text{C}$

	ϵ_{reg} (%)	\dot{Q}_{hot} (kW)	\dot{Q}_{reg} (kW)	\dot{Q}_{cold} (kW)	\dot{W}_p (kW)	\dot{W}_{exp} (kW)	\dot{m}_{work} (kg/s)	v_3 (m ³ /kg)	V_3 (m ³ /s)	$\frac{\dot{W}_{reg}}{\dot{W}_{p2}}$ (%)	$\frac{\dot{W}_{reg}}{\dot{W}_{e4}}$ (%)	P_{evap} (bar)	P_{cond} (bar)	η_{cycle} (%)
Benzene	0.0	60.0	0.0	-53.2	0.6	7.2	0.135	0.076	0.010	45.8	85.0	29.9	5.8	11.1
	80.0	60.0	6.9	-52.5	0.6	8.0	0.150	0.076	0.011	51.1	96.2	29.9	5.8	12.4
Cycle pentane	0.0	60.0	0.0	-55.3	0.6	5.5	0.133	0.042	0.006	32.8	69.9	35.0	11.8	8.1
	80.0	60.0	16.2	-54.0	0.8	7.0	0.169	0.042	0.007	41.6	91.0	35.0	11.8	10.3
Heptane	0.0	60.0	0.0	-53.8	0.5	6.7	0.136	0.094	0.013	27.6	69.4	21.5	3.8	10.2
	80.0	60.0	16.5	-52.1	0.7	8.5	0.173	0.094	0.016	35.2	91.3	21.5	3.8	13.0
MM	0.0	60.0	0.0	-55.1	0.4	5.3	0.180	0.064	0.011	24.7	53.5	15.0	3.6	8.1
	80.0	60.0	30.6	-52.5	0.6	8.0	0.272	0.064	0.017	37.3	84.7	15.0	3.6	12.3
Toluene	0.0	60.0	0.0	-52.0	0.3	8.1	0.127	0.140	0.018	49.5	81.6	16.7	2.8	13.1
	80.0	60.0	8.8	-50.8	0.3	9.3	0.146	0.140	0.020	56.7	95.6	16.7	2.8	15.0
Water	0.0	60.0	0.0	-55.5	0.1	4.6	0.026	0.383	0.010	85.2	100.0	15.0	4.8	7.6

Results for $T_{cond} = 150\text{ }^{\circ}\text{C}$ and $T_{max} = 300\text{ }^{\circ}\text{C}$

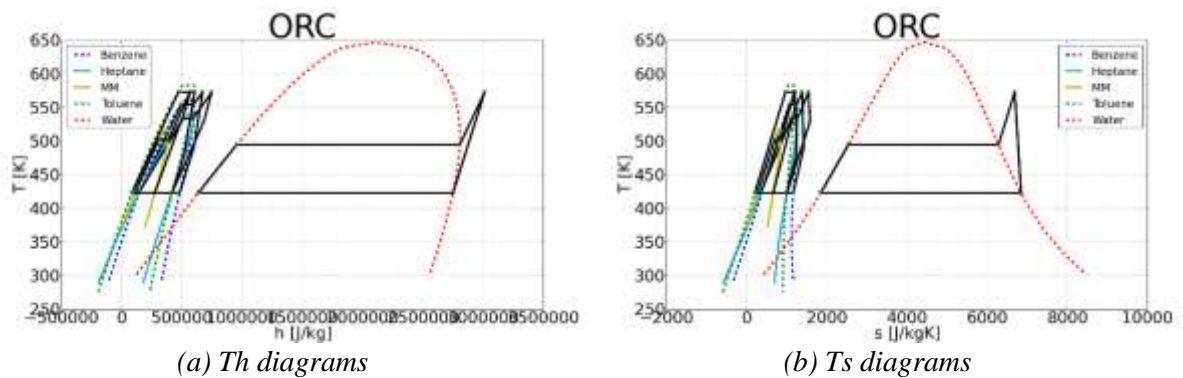


Figure 40: ORC with $T_{cond} = 150\text{ }^{\circ}\text{C}$ and $T_{max} = 300\text{ }^{\circ}\text{C}$

Table 40: Results of the cycle for $T_{cond} = 150.0\text{ }^{\circ}\text{C}$ and $T_{max} = 300.0\text{ }^{\circ}\text{C}$

	ϵ_{reg} (%)	\dot{Q}_{hot} (kW)	\dot{Q}_{reg} (kW)	\dot{Q}_{cold} (kW)	\dot{W}_p (kW)	\dot{W}_{exp} (kW)	\dot{m}_{work} (kg/s)	v_3 (m ³ /kg)	V_3 (m ³ /s)	$\frac{\dot{W}_{reg}}{\dot{W}_{p2}}$ (%)	$\frac{\dot{W}_{reg}}{\dot{W}_{e4}}$ (%)	P_{evap} (bar)	P_{cond} (bar)	η_{cycle} (%)
Benzene	0.0	60.0	0.0	-52.1	0.8	8.5	0.115	0.083	0.010	19.5	74.3	45.0	5.8	12.9
	80.0	60.0	12.6	-50.5	0.9	10.3	0.139	0.083	0.012	23.6	92.9	45.0	5.8	15.6
Heptane	0.0	60.0	0.0	-53.9	0.5	6.5	0.100	0.109	0.011	13.2	50.9	25.0	3.8	10.1
	80.0	60.0	32.2	-50.6	0.7	10.0	0.153	0.109	0.017	20.3	83.3	25.0	3.8	15.5
MM	0.0	60.0	0.0	-55.7	0.3	4.6	0.133	0.074	0.010	18.2	38.9	15.0	3.6	7.1
	80.0	60.0	0.0	-55.7	0.3	4.6	0.133	0.074	0.010	18.2	38.9	15.0	3.6	7.1
Toluene	0.0	60.0	0.0	-50.7	0.6	9.7	0.116	0.144	0.017	26.0	76.3	32.7	2.8	15.2
	80.0	60.0	11.2	-49.0	0.7	11.5	0.138	0.144	0.020	30.9	93.8	32.7	2.8	18.0
Water	0.0	60.0	0.0	-53.4	0.1	6.7	0.025	0.384	0.010	78.0	100.0	24.0	4.8	11.0

Results for $T_{cond} = 150\text{ °C}$ and $T_{max} = 350\text{ °C}$

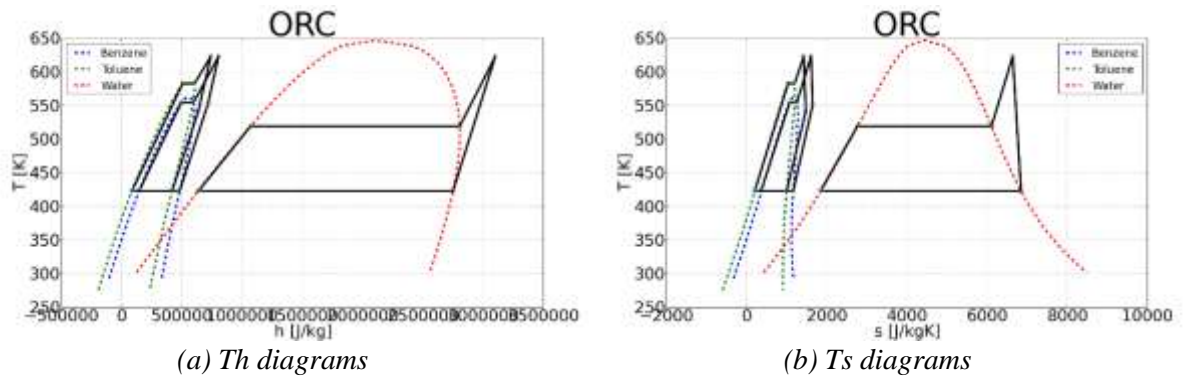


Figure 41: ORC with $T_{cond} = 150\text{ C}$ and $T_{max} = 350\text{ C}$

Table 41: Results of the cycle for $T_{cond} = 150.0\text{ C}$ and $T_{max} = 350.0\text{ C}$

	ϵ_{reg} (%)	\dot{Q}_{hot} (kW)	\dot{Q}_{reg} (kW)	\dot{Q}_{cold} (kW)	\dot{W}_p (kW)	\dot{W}_{exp} (kW)	\dot{m}_{work} (kg/s)	v_3 (m ³ /kg)	\dot{V}_3 (m ³ /s)	$\frac{h_{1,2}}{h_{y,2}}$ (%)	$\frac{h_{3,4}}{h_{x,4}}$ (%)	P_{evap} (bar)	P_{cond} (bar)	η_{cycle} (%)
Benzene	0.0	60.0	0.0	-52.3	0.6	8.2	0.092	0.096	0.009	15.5	59.1	45.0	5.8	12.7
	80.0	60.0	23.5	-49.3	0.9	11.4	0.128	0.096	0.012	21.6	87.3	45.0	5.8	17.7
Toluene	0.0	60.0	0.0	-50.9	0.5	9.5	0.092	0.166	0.015	15.1	60.4	37.0	2.8	15.0
	80.0	60.0	21.7	-47.5	0.7	13.0	0.126	0.166	0.021	20.6	88.0	37.0	2.8	20.5
Water	0.0	60.0	0.0	-51.6	0.1	8.6	0.024	0.388	0.009	70.6	100.0	37.3	4.8	14.1

Results for $T_{cond} = 150\text{ °C}$ and $T_{max} = 400\text{ °C}$

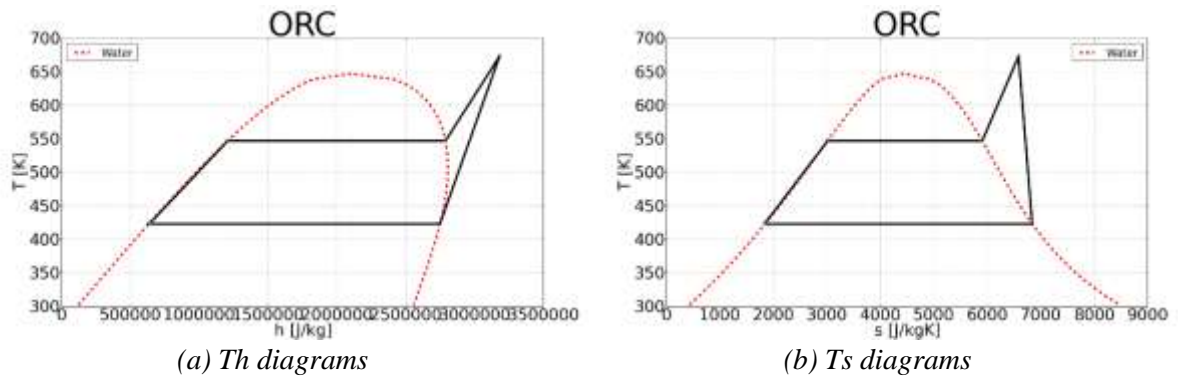


Figure 42: ORC with $T_{cond} = 150\text{ C}$ and $T_{max} = 400\text{ C}$

Table 42: Results of the cycle for $T_{cond} = 150.0\text{ C}$ and $T_{max} = 400.0\text{ C}$

	ϵ_{reg} (%)	\dot{Q}_{hot} (kW)	\dot{Q}_{reg} (kW)	\dot{Q}_{cold} (kW)	\dot{W}_p (kW)	\dot{W}_{exp} (kW)	\dot{m}_{work} (kg/s)	v_3 (m ³ /kg)	\dot{V}_3 (m ³ /s)	$\frac{h_{1,2}}{h_{y,2}}$ (%)	$\frac{h_{3,4}}{h_{x,4}}$ (%)	P_{evap} (bar)	P_{cond} (bar)	η_{cycle} (%)
Water	0.0	60.0	0.0	-50.0	0.2	10.2	0.024	0.377	0.009	62.4	100.0	58.5	4.8	16.8